THE ROLE OF DORSAL ROOT GANGLION GLUTAMINASE IN NOCICEPTION – A NOVEL THERAPEUTIC TARGET FOR INFLAMMATORY PAIN

By

ERNEST MATTHEW HOFFMAN

Bachelor of Science in Biology
The University of Tulsa
Tulsa, Oklahoma
2004

Submitted to the Faculty of the
Graduate College of the
Oklahoma State University
Center for Health Sciences
in partial fulfillment of
the requirements for
the Degree of
DOCTOR OF PHILOSOPHY
May, 2009

THE ROLE OF DORSAL ROOT GANGLION

GLUTAMINASE IN NOCICEPTION – A

NOVEL THERAPEUTIC TARGET

FOR INFLAMMATORY PAIN

Dissertation Approved:

Kenneth E. Miller

Dissertation Adviser

William D. Meek

Randy S. Wymore

Robert D. Foreman

A. Gordon Emslie

Dean of the Graduate College

ACKNOWLEDGMENTS

Significant scientific endeavors cannot be completed without the help of many individuals. This is particularly true when the undertaking is being carried out by a student, as in the case of a dissertation research project. I am deeply indebted to those who gave their time, encouragement, and guidance. Foremost is my advisor and friend Dr. Kenneth Miller, who was willing to listen to my ideas, troubleshoot technical problems, and redirect my efforts, often at short notice, during the course of my research project. He also provided invaluable editorial services for all of my writing, including this dissertation. Dr. Ruben Schechter, a pediatrician and scientist, was instrumental in discussing many of the implications of my results and contributed advice on how the results should be presented in writing. My other committee members, Drs. Bill Meek, Randy Wymore, and Bob Foreman, have provided constructive feedback on the content of this dissertation. I am grateful to Kristy Edwards, Zijia Zhang, and Michael Anderson, who helped with labor intensive laboratory procedures and made the hours in the laboratory more enjoyable. Most of all, I would like to thank my wife, Mandy, who encouraged me when I needed it the most and stood by me even when I erroneously put my research and studies as first priority. I will be forever appreciative of her sacrifices.

TABLE OF CONTENTS

Chapter Page

LIST OF TABLES

LIST OF FIGURES

Figure Page

NOMENCLATURE

ALS – anterolateral system
CFA – complete Freund's adjuvant
CGRP – calcitonin gene-related peptide
CIPA – congenital insensitivity to pain with anhidrosis
CNS – central nervous system
COX – cyclooxygenase
CSF – cerebrospinal fluid
cytC – cytochrome C
DAPI – 4',6-diamino-2-phenylindole; binds to DNA and emits blue fluorescence
DRG – dorsal root ganglion
DON – 6-diazo-5-oxo-L-norleucine; irreversible glutaminase inhibitor
EAATs – excitatory amino acid transporters
EAAT1 – glial glutamate transporter
EAAT3 – neuronal glutamate transporter
ELISA – enzyme-linked immunosorbant assay
FITC – fluorescein isothiocyanate; emits green fluorescence
Fos – protein product of proto-oncogene *c-fos*; nuclear marker of neuronal activation
GDNF – glial-derived neurotrophic factor
GLS – glutaminase
GS – glutamine synthetase
IB4 – isolectin B4; labels non-peptidergic dorsal root ganglion neurons
IR - immunoreactivity
Na_vs – voltage-gated sodium channel isoforms
NGF – nerve growth factor
NMDA – N-methyl-D-aspartic acid; agonist of NMDA ionotropic glutamate receptors
NSAIDs – non-steroidal anti-inflammatory drugs
OPD – *o*-phenylenediamine
PBS – phosphate buffered saline
PBS-T – phosphate buffered saline with Triton X-100
PCML – posterior column medial lemniscal
PVP – polyvinylpyrollidone
ROIs – regions of interest
SCBS – sodium carbonate buffered saline
SCG – superior cervical ganglion
SNATs – sodium-coupled neutral amino acid transporters
SNAT1 – neuronal glutamine transporter
SP – substance P
TCAs – tricyclic antidepressants
TG – trigeminal ganglion

TH – tyrosine hydroxylase
trkA – high affinity nerve growth factor receptor
TRPs – transient receptor potential receptor members
TRPV1 – transient receptor potential vanilloid receptor 1; capsaicin receptor
VGLUTs – vesicular glutamate transporters
VPL – ventral posterior lateral

CHAPTER 1

Introduction

The two primary somatosensory pathways for the body (Martin 2003)

Somatic sensory information from the body is conveyed to the cerebral cortex primarily via one of two pathways: the posterior column-medial lemniscal (PCML) pathway and the anterolateral system (ALS). These pathways have several things in common: they each have primary sensory neurons located in the dorsal root ganglia (DRG), second order neurons located in the ipsilateral central nervous system, and third order neurons in the contralateral ventral posterior lateral (VPL) nucleus of the thalamus which project to the cortex. The second order neurons of both pathways cross the midline so that sensory perception occurs in cortex contralateral to the side of stimulation. The commonalities end here. The central axons of ALS DRG neurons enter the spinal cord and synapse in the ipsilateral dorsal horn, whereas the central axons of PCML neurons enter the spinal cord, ascend in the dorsal columns, and synapse in the medullary dorsal column nuclei (Figure 1.1). The second order neurons for both pathways then cross the midline (decussate) and ascend to the VPL nucleus in the thalamus.

In addition to differing anatomically, these two pathways differ in the modalities that they convey. The ALS pathway primarily conveys the sensory modalities of pain, temperature, and crude touch, while the PCML pathway primarily conveys the sensory

modalities of fine touch, proprioception, and vibration. ALS DRG neurons generally have bare nerve endings that act as the sensory receptors themselves, whereas PCML pathway DRG neurons generally have encapsulated nerve endings. Peripheral axons of ALS DRG neurons are endowed with specific sets of proteins that allow them to transduce thermal, noxious, or mechanical sensory stimuli into action potentials. The encapsulated nerve endings act as sensory end organs specific to certain mechanical stimuli (i.e., stretch, vibration, proprioception, light touch).

Sensitization and hyperalgesia

Acute pain occurs in response to potentially damaging stimuli, and its duration and intensity correlate with the stimulus. This makes acute pain adaptive. Tissue damage, inflammation, and nerve damage alter the response properties of primary afferent neurons via a process called sensitization, which can lead to chronic maladaptive pain that requires clinical treatment. Sensitization is characterized by decreased firing threshold, increased response to suprathreshold stimuli, and spontaneous activity in primary afferents. These are the physiological correlates of hyperalgesia as defined by decreased pain threshold, increased pain to noxious stimuli, and spontaneous pain, respectively (Meyer, M. et al. 2005).

The process of sensitization involves post-translational modification as well as expression dependent changes within primary afferent neurons (Woolf and Costigan 1999; Costigan and Woolf 2000; Woolf and Salter 2000; Woolf and Ma 2007). Post-translational modification can be mediated by sensitizers (i.e., bradykinin, prostaglandins, interleukins, protons, ATP, glutamate and nerve growth factor [NGF]) interacting with receptors on the membrane of peripheral terminals. Subsequently, via second messenger

and other signaling cascades, proteins such as transient receptor potential receptors (TRPs) and voltage-gated sodium channels (Na_vs) are modified by phosphorylation or allosteric modulation (Woolf and Ma 2007). These alterations increase nerve terminal excitability and reduce the activation threshold.

Increased electrical activity entering the cell body can initiate alterations in gene expression. Furthermore, some signaling molecules, e.g., NGF, can be retrogradely transported from the peripheral terminal back to the cell body where they can regulate gene expression (Woolf and Ma 2007). Post-translational modifications of proteins already at the peripheral terminal can result in hyperalgesia within seconds to minutes, whereas expression-dependent changes take longer to develop and may last for hours, days, or longer (Woolf and Costigan 1999). Expression-dependent changes are thought to be necessary for maintaining chronic pain (Bolay and Moskowitz 2002).

Dorsal root ganglion neuron populations

DRG neurons can be classified by cell body size, axon diameter, conduction velocity, sensory modality, and molecular markers. The most widely established subdivision of DRG neurons is by the size of their cell bodies (Willis and Coggeshall 1991). Studies that are concerned with DRG neurons typically divide cells into two populations: large and small. The evidence that there are at least two populations of DRG neurons based on cell body size comes from histograms that relate cell body size (diameter or area) with cell number. A bimodal distribution is often apparent (Figure 1.2) with a tall, but narrow small cell peak and a short, but broad large cell peak (Lawson, Harper et al. 1984; Harper and Lawson 1985).

In addition to two populations of DRG neurons based on size of the cell body, there are also two populations based on axon diameter: small and large. The small neurons typically have unmyelinated small diameter axons and the large neurons have myelinated large diameter axons (Yoshida and Matsuda 1979; Lee, Chung et al. 1986). Cell body size can, therefore, be used as a predictor of axon diameter. Axon diameter correlates well with conduction velocity as a general physiological principle, and it has been shown that large cells with large axons conduct at velocities greater than 2.5 m/s (A fibers) while small cells with small axons conduct at velocities less than 2.5 m/s (C fibers) (Lee, Chung et al. 1986). The A fibers can be divided further into Aα/Aβ and Aδ fibers, whereby Aα/Aβ fibers conduct faster than Aδ fibers. The Aα/Aβ fibers belong to the large cell population while the Aδ and C fibers appear to belong to the small cell population (Harper and Lawson 1985).

Receptive fields of primary sensory neurons can be tested with various stimuli, both noxious and non-noxious, concurrent with electrophysiological recording of the cell body to determine the sensory threshold for individual neurons. Most neurons with conduction velocities in the Aα/Aβ range respond to non-noxious stimuli, while most neurons in the Aδ and C range respond to noxious and thermal stimuli (Fang, McMullan et al. 2005). However, some neurons in the Aα/Aβ range also are nociceptors (Lawson 2002), and some unmyelinated fibers signal touch (Douglas and Ritchie 1957). The anatomical and physiological correlations combined with modality specific information can be summarized as follows: DRG neurons are roughly divided into large and small cell populations that correspond with peripheral terminals that sense non-noxious and noxious stimuli, respectively. There are, of course, many exceptions to this oversimplification,

but dividing DRG neurons in this way provides a useful terminology to discuss experimental results and is commonly used in contemporary research.

The reported distributions for most molecular markers of DRG subpopulations vary from study to study, but some generalizations can be made. Large diameter non-nociceptors typically label for specific, high molecular weight, neurofilament proteins (Lawson, Harper et al. 1984). Small diameter nociceptive neurons, which label for the neurofilament, peripherin (Goldstein, House et al. 1991), can be roughly divided into peptidergic and nonpeptidergic subpopulations. Peptidergic neurons characteristically contain the peptides substance P (SP) and calcitonin gene-related peptide (CGRP), whereas nonpeptidergic small diameter neurons do not. The former population is thought to express the high affinity NGF receptor, trkA. The latter population often is identified by labeling with isolectin-B4 (IB4) from the plant *Griffonia simplicifolia*, which binds to α-D-galactosyl residues on proteins or lipids made in these cells (Averill, McMahon et al. 1995; Priestley, Michael et al. 2002; Fang, Djouhri et al. 2006). Both types of small diameter neurons are considered to be nociceptors (Fang, Djouhri et al. 2006), but they have different termination patterns in the periphery and the spinal cord dorsal horn (Zylka, Rice et al. 2005). It has been noted that there is considerable overlap of these two populations (Kashiba, Uchida et al. 2001), but these distinctions are still useful.

The aforementioned classification by molecular markers is the most prevalent used, but there are many other proteins that may indicate unique populations of DRG neurons. These include the Na_v isoforms (Fukuoka, Kobayashi et al. 2008) and TRP receptors (Tominaga and Caterina 2004). There are constantly more markers being proposed to identify specific populations of DRG neurons, but as with the established markers, there

are often discrepancies as to their exact distribution. For instance, within a single study, the estimated percentages of the TRPV1, a receptor that responds to painful heat (Caterina, Schumacher et al. 1997), were staggeringly different between an anatomical assay and a functional assay (Bautista, Jordt et al. 2006). The immunofluorescence experiment showed that approximately 25% of mouse DRG neurons immunolabel for TRPV1, whereas approximately 75% of neurons responded with calcium imaging after capsaicin stimulation (capsaicin is a TRPV1 agonist). Similarly, estimates of $Na_v1.8$, which is thought to be expressed exclusively in nociceptors, were very different between two studies. Immunofluorescence indicated that approximately 50% of adult rat DRG neurons express $Na_v1.8$ (Benn, Costigan et al. 2001), whereas in-situ hybridization has shown that 66.5-68.9% of DRG neurons express $Na_v1.8$ (Fukuoka, Kobayashi et al. 2008). It would be beneficial to standardize how the distributions of new molecular markers are determined by thoroughly optimizing experimental conditions. This is not just a goal for those studying DRG neuron subpopulations, but for any investigations, clinical or scientific, where accurate determination of antigen distribution is desired (Taylor and Levenson 2006; Walker 2006).

Glutamate as a neurotransmitter for dorsal root ganglion neurons

The amino acid glutamate is widely accepted as the primary excitatory neurotransmitter for the central nervous system (CNS), and glutamate metabolism and compartmentalization have been well characterized in the CNS (Hertz 2004). Glutamate released from CNS neurons is transported back into neurons, but also into glial cells by excitatory amino acid transporters (EAATs). Glia convert glutamate to glutamine with the enzyme glutamine synthetase (GS). Glutamine is released into the extracellular space

where it is taken up by neurons via sodium-coupled neutral amino acid transporters (SNATs). Neurons convert glutamine to glutamate with the enzyme glutaminase (GLS). Newly synthesized glutamate can be packaged into vesicles by vesicular glutamate transporters (VGLUTs) to await synaptic release.

Many of the proteins involved in this "glutamate-glutamine cycle" have been localized to the DRG, indicating that glutamate metabolism in the peripheral nervous system has similarities with that in the CNS (Figure 1.3). The neuronal glutamate transporter EAAT3 localizes to DRG neurons (Tao, Liaw et al. 2004), while the glial glutamate transporter EAAT1 localizes to satellite glial cells (Berger and Hediger 2000). GS is found in satellite glial cells of the DRG (Miller, Richards et al. 2002) and trigeminal ganglia (TG) (Hanani 2005). SNAT1 (Miller, Kriebel et al. 2005) and GLS (Miller, Douglas et al. 1993) have been detected in DRG neurons. Presence of the abovementioned proteins, in their respective locations within the DRG, suggests that glutamate and glutamine exchange and metabolism can occur between peripheral neurons and glia. This notion is supported by the *in vitro* observation that [^{3}H]glutamate is transported into satellite glial cells (Roberts and Keen 1974; Duce and Keen 1983) while [^{3}H]glutamine is transported into DRG neurons and quickly converted to glutamate (Duce and Keen 1983). These findings, however, do not necessarily implicate glutamate as a neurotransmitter of DRG neurons since glutamate can also be used as an energy substrate for the TCA cycle (McKenna 2007).

Presence of VGLUTs in neurons is, in contrast, an extremely specific indicator of glutamatergic neurons, because they are necessary for filling synaptic vesicles with glutamate. VGLUTs have been localized to neuronal cell bodies of the DRG (Oliveira,

Hydling et al. 2003; Brumovsky, Watanabe et al. 2007) and TG (Li, Xiong et al. 2003). Furthermore, they have been localized to regions of the spinal and medullary dorsal horn where DRG and TG neurons synapse, respectively (Li, Fujiyama et al. 2003). In addition, it has been suggested that certain populations of primary afferents release glutamate as neurotransmitter from their peripheral terminals (Carlton 2001), and localization of VGLUTs to peripheral terminals (Nunzi, Pisarek et al. 2004; Brumovsky, Watanabe et al. 2007) gives further support for this.

In addition to localizing glutamate-glutamine cycle components to DRG and VGLUTs at central and peripheral sites of glutamate release, glutamate concentrations in these areas also have been measured during various types of noxious stimulation. The concentration of extracellular glutamate increases in rat dorsal horn after pinching, carrageenan induced inflammation (Dmitrieva, Rodriguez-Malaver et al. 2004), plantar incision (Zahn, Sluka et al. 2002), formalin injection, and sodium channel activation (Skilling, Smullin et al. 1988). Formalin induced intraplantar inflammation and carrageenan induced intraarticular inflammation increase glutamate concentration in the subcutaneous tissue (Omote, Kawamata et al. 1998) and synovial fluid (Lawand, McNearney et al. 2000), respectively. Although non-neural sources may contribute to these glutamate increases, other studies show support for a neural source, specifically primary afferent nociceptors. Antidromic stimulation of the sciatic nerve results in increased extracellular glutamate concentrations in the subcutaneous intraplantar tissue (deGroot, Zhou et al. 2000; Jin, Nishioka et al. 2006). Peripheral inflammation also increases the glutamate content of peripheral nerve in monkeys (Westlund, Sun et al. 1992). Capsaicin, an agonist of the TRPV1 receptor located on nociceptive primary

afferents (Caterina, Schumacher et al. 1997), can selectively stimulate these peripheral terminals when applied topically. Subcutaneous glutamate concentrations increase in response to noxious thermal stimulation or capsaicin application, and such increases are attenuated with systemic or intraplantar morphine (Jin, Nishioka et al. 2006). These findings indicate that glutamate is released from nociceptor peripheral terminals in response to painful stimulation and that activation of opioid receptors on these peripheral endings can suppress noxious stimulus-induced glutamate release.

Glutamate appears to be involved in acute and tonic nociceptive transmission at both the central and peripheral terminals of DRG neurons in animal pain models. Evidence for involvement in chronic pain in humans comes from studies of patients with joint or skin inflammation. Patients with chronic arthritis and gold-induced dermatitis showed elevated levels of glutamate in the joint (McNearney, Speegle et al. 2000; McNearney, Baethge et al. 2004) and skin (Nordlind, Johansson et al. 1993), respectively. Antagonism of ionotropic and excitatory metabotropic glutamate receptors at the site of inflammation or injury has provided analgesia in many animal studies (Carlton, Hargett et al. 1995; Jackson, Graff et al. 1995; Davidson, Coggeshall et al. 1997; Lawand, Willis et al. 1997; Bhave, Karim et al. 2001; Leem, Hwang et al. 2001) and for human burn injury (Warncke, Jorum et al. 1997).

Glutamate also is implicated as an acute activator and sensitizer of nociceptive primary afferents as it appears to have this ability both *ex vivo* (Du, Koltzenburg et al. 2001) and *in vivo* (Follenfant and Nakamura-Craig 1992; Zhou, Bonasera et al. 1996; Du, Zhou et al. 2003). Primary afferent sensitization in response to glutamate also occurs in humans, because subcutaneous injection of glutamate elicits acute pain and subsequent

hyperalgesia (Gazerani, Wang et al. 2006). Presence of glutamate receptors on peripheral unmyelinated axons from animals (Carlton, Hargett et al. 1995; Coggeshall and Carlton 1998; Bhave, Karim et al. 2001) and humans (Kinkelin, Brocker et al. 2000) are further support that glutamate is acting directly on nociceptive peripheral terminals. The primary afferent may be, therefore, both the source and the target of peripheral glutamate release during noxious stimulation (Carlton 2001).

Glutamate release from central terminals of DRG neurons increases during inflammation (Skilling, Smullin et al. 1988; Dmitrieva, Rodriguez-Malaver et al. 2004), and this glutamate, in concert with substance P, is involved in sensitization of the second order neurons in the spinal cord dorsal horn (Dougherty and Willis 1991; Dougherty, Palecek et al. 1993). Despite much evidence for glutamate autostimulation and sensitization of peripheral primary afferent terminals and dorsal horn neurons during inflammation, very little is known about alterations in glutamate metabolism during such conditions. It would be beneficial to determine how constituents of the glutamate-glutamine cycle are regulated, either via post-translational modification or expression changes, during inflammation. Investigation of glutamate metabolism may reveal novel therapeutic targets for treatment of inflammatory pain. For this dissertation, it was hypothesized that GLS would be elevated in DRG neurons during chronic inflammation.

GLS is a logical constituent of the glutamate-glutamine cycle to examine when considering increased glutamate levels since it is the enzyme that synthesizes neurotransmitter glutamate. As mentioned previously for many other proteins expressed in the DRG, there is often disagreement among the reported distributions for a particular protein from different laboratories. Such is also the case for GLS. GLS activity was

identified in the DRG of rats and was shown to decrease by approximately 60% when 70% of the DRG neurons where killed during development (McDougal, Yu et al. 1981). When only capsaicin sensitive neurons were killed during development, GLS activity decreased by 26% (McDougal, Yuan et al. 1983). This indicated that the small diameter neurons expressed glutaminase, but were not the only DRG neurons to do so. The first reports of GLS distribution by histological means indicated that 30% of small DRG neurons and no large DRG neurons expressed GLS (Cangro, Sweetnam et al. 1984; Cangro, Sweetnam et al. 1985). A subsequent study determined that 40% of DRG neurons contained glutaminase, and they were all in the small cell population (Battaglia and Rustioni 1988). In 1993, Miller et al. demonstrated GLS immunoreactivity in more than 80% of DRG neurons, irrespective of cell body size. This was reiterated in another study where "almost all" DRG neurons were said to be immunoreactive for GLS (Li, Ohishi et al. 1996). The difference between the former two and latter two studies can be accounted by the different fixatives used for perfusion. The former studies, which reported lower estimates of GLS distribution, used a relatively high concentration (4% w/v) of the cross-linking fixative formaldehyde in their perfusates. The latter studies, which reported more ubiquitous GLS distributions, used a concentration that was 20-fold lower (0.2% w/v) and added 1% (w/v) picric acid. This phenomenon had been reported in a qualitative manner for neurons of the CNS (Kaneko, Itoh et al. 1989), although it has not been confirmed as to whether less formaldehyde or more picric acid is responsible for the increased sensitivity of GLS detection. Optimization of fixation methods needs to be performed for accurate determination of GLS distribution in the DRG. Such a protocol also should be applied for other proteins in the DRG for which there is no consensus on

the exact distribution. Optimization of fixation, therefore, is the first project of this dissertation, prior to evaluation of GLS during inflammation.

Nerve growth factor (NGF)

Another inflammatory mediator with the ability to sensitize primary afferents is NGF. Recently, NGF antagonism has been suggested as a therapeutic approach for inflammatory pain (Hefti, Rosenthal et al. 2006; Watson, Allen et al. 2008). Much of what is known about the effects of NGF on the peripheral nervous system comes from NGF deprivation studies. Once NGF had been isolated and purified (Bocchini and Angeletti 1969), it was used to raise heterologous antibodies that were subsequently injected into animals. Anti-NGF antibodies bind and prevent endogenous NGF from interacting with its targets. Such experiments revealed that NGF deprivation during development resulted in loss of peripheral autonomic and sensory neurons (Levi-Montalcini and Booker 1960). If NGF was deprived in mature animals, only peripheral autonomic neurons were lost. These experiments determined that all peripheral neurons rely on NGF for survival during development, but only peripheral autonomic neurons still have an NGF requirement for survival in adulthood. The question as to what role, if any, NGF had in postnatal sensory neurons remained unanswered. To help answer this question, a method of autoimmunization was developed wherein animals were actively immunized against NGF so that anti-NGF titers could be maintained chronically (Gorin and Johnson 1979). This method allowed further characterization of chronic NGF deprivation in mature animals and confirmed that DRG neurons do not die or atrophy even after long term NGF deprivation (Gorin and Johnson 1980; Johnson, Gorin et al. 1982; Schwartz, Pearson et al. 1982). However, NGF immunized rats had delayed

withdrawal responses to noxious stimuli as measured by the hot plate test (Chudler, Anderson et al. 1997), which indicated a functional alteration of the small cell population of DRG neurons. Injection of exogenous NGF can cause hyperalgesia in animals (Lewin, Ritter et al. 1993; Della Seta, de Acetis et al. 1994; Amann, Schuligoi et al. 1995) and humans (Dyck, Peroutka et al. 1997; Svensson, Cairns et al. 2003), and endogenous production of NGF increases during inflammation (Woolf, Safieh-Garabedian et al. 1994). Elevated levels of NGF sensitize primary afferents by both post-translational modification of pre-existing proteins and by increasing expression of proteins (Woolf, Safieh-Garabedian et al. 1994; Leslie, Emson et al. 1995; Schuligoi and Amann 1998; Gould, Gould et al. 2000; Ramer, Bradbury et al. 2001; Ji, Samad et al. 2002; Mamet, Lazdunski et al. 2003). For this dissertation, it was hypothesized that normal expression of proteins important for nociception are dependent on basal NGF levels present in non-inflamed tissue and depriving NGF would down-regulate expression of these proteins. $Na_v1.8$ current density and mRNA levels are decreased in IB4 negative rat DRG neurons after NGF deprivation (Fjell, Cummins et al. 1999). SP protein levels are decreased in the DRG, the dorsal horn of spinal cord and the skin after NGF deprivation (Schwartz, Pearson et al. 1982). These are the only studies that document a decreased expression of pain-related proteins after long term NGF deprivation, and leave down-regulation of $Na_v1.8$ and SP as the only explanation for hypoalgesia in NGF deprived animals.

Fos expression in spinal cord

Neuronal expression of the proto-oncogene *c-fos* is rapidly and transiently elevated in response to stimulation. Fos is the protein product of *c-fos*, and it forms heterodimeric complexes with other proteins in the Jun family that bind to the AP-1 target site on DNA

to regulate gene expression. The function of Fos is, therefore, to link extracellular events to long-term cellular responses. Noxious stimulation increases Fos expression in the dorsal horn of spinal cord where nociceptive DRG neurons of the ALS synapse (Hunt, Pini et al. 1987). Since this initial discovery, spinal Fos expression, as measured by counting Fos-immunoreactive nuclei, has been used extensively to study cellular activity during noxious stimulation and quantify effects of various analgesics (Coggeshall 2005). Fos expression increases in dorsal horn after most types of noxious stimulation, but with varying degrees, localizations, temporal profiles, and susceptibility to analgesic suppression.

One of the most commonly used and well characterized models is intraplantar injection of λ-carrageenan. In response to carrageenan inflammation of the hind paw, Fos expression is rapidly elevated in the lumbar spinal cord dorsal horn (especially L4-L5) in superficial (I-II) and deep laminae (V-VI), peaks at 3 hours post injection, and is susceptible to suppression by central and peripheral analgesics (Honore, Buritova et al. 1995; Coggeshall 2005). Peripheral inhibition of cyclooxygenase (COX), the enzyme that makes prostaglandins, reduces Fos expression in dorsal horn during inflammation (Buritova and Besson 1998). Since both prostaglandins and glutamate are implicated in nociceptor sensitization, measuring Fos expression in the dorsal horn would be a useful tool to study the analgesic potential of glutamate antagonism during inflammation. As mentioned above, peripheral glutamate receptor antagonism attenuates hyperalgesia during inflammation, and decreased dorsal horn Fos expression corroborates these findings (Wang, Liu et al. 1997). Since a previous study has shown that peripheral GLS inhibition has analgesic effects (Miller, Herzog et al. 2006), it would be interesting to

know if GLS inhibition can also reduce Fos expression during inflammation. This was the fourth project of the current dissertation.

Clinical problem of pain

Chronic pain is medically managed with anti-inflammatory drugs, opioids, tricyclic antidepressants (TCAs), anticonvulsants, or any combination of these (Miller 2005). While many patients obtain relief from these treatments, there are cases of intractable and refractory pain that require high-risk interventional procedures. In addition, there are many side effects of the aforementioned drugs because their molecular targets are widely expressed. For instance, high doses of anti-inflammatory drugs can reach very high levels of pain relief, but can also precipitate gastrointestinal bleeding, renal failure, and congestive heart failure (McQuay and Moore 2005). Another example would be the use of opioids for analgesia. Opioids offer analgesic control over the most severe pain by inhibiting release of neurotransmitter from nociceptors and hyperpolarizing spinal cord neurons, but at the cost of affecting many other neurons in the CNS. In addition to adverse effects of short-term opioid use such as constipation, nausea, and dysphoria, long-term adverse effects include psychological dependence, drug abuse, addiction, and physiological tolerance (Miller 2005). Tricyclic antidepressants and anticonvulsants also are used as treatments for intractable pain. The amine uptake inhibition of TCAs potentiates the effect of inhibitory neurotransmitters in the spinal cord and brain, but this most commonly leads to weakness and fatigue. TCAs also have relatively potent antimuscarinic effects that produce adverse autonomic disturbances. Anticonvulsants block sodium and calcium channels, thereby decreasing excitation in activated pain

pathways, but also throughout the nervous system. This widespread decreased excitation can lead to dizziness, somnolence, ataxia, headache, blurred vision, and tremor.

To avoid adverse side effects and provide treatment for problematic pain, novel analgesics should be directed at the neurons and sensitizing factors of the pain pathway. The TRPs (Patapoutian, Tate et al. 2009), Na_vs (Kort, Drizin et al. 2008), and NGF (Hefti, Rosenthal et al. 2006) have been suggested as targets for analgesic development since they have a somewhat limited distribution and have been shown to be integral to sensitization of nociceptors. Peripheral glutamate antagonism also has been suggested for analgesic development (Carlton 2001). While glutamate is the most common neurotransmitter used at CNS synapses, specific peripheral inhibition at the site of inflammation may provide a novel analgesic strategy that would have few central effects.

Summary

Current analgesics cannot provide adequate pain relief for all individuals with chronic pain, and they have many adverse effects that prohibit prescribing long-term high doses. New therapeutic options, therefore, are needed for management of chronic pain. Neurons in the DRG that are part of the "pain pathway" present a useful target for design of novel analgesics since they are at the beginning of the pathway. If their sensitization can be prevented or inhibited, then the burden of pain on the patient will be lessened. In order to identify potential molecular targets in these cells, more detailed characterization of nociceptive DRG neuron populations is necessary. In general, small diameter DRG neurons with thin, lightly myelinated or unmyelinated axons that synapse in the dorsal horn of spinal cord bring nociceptive information into the CNS. The two most widely accepted nociceptor populations are peptidergic and nonpeptidergic based on their ability

to release the peptides SP and CGRP. Identifying the exact distribution of molecular markers among DRG neurons is crucial for development of new analgesics. However, there are inconsistencies with current estimates of marker distribution among studies, ***indicating the need for optimization and standardization of the protocol for determining DRG neuron populations (Chapter 2)***.

Much evidence indicates that all DRG neurons use the neurotransmitter glutamate for release at synapses within the CNS, and it is strongly implicated in autostimulation of the peripheral terminal as well. However, ***the distribution of GLS, the glutamate synthesizing enzyme, is not clear and needs to be determined (Chapter 2)***. Glutamate is a sensitizer of both the peripheral terminal and dorsal horn neurons. Levels of glutamate increase in inflamed tissues and spinal cord dorsal horn, and the source may be primary afferent neurons in both cases. GLS is, therefore, a potential analgesic target. During sensitization, DRG neurons increase expression of proteins important for nociception, and ***it is important to know if GLS is among the proteins up-regulated during sensitization (Chapter 3)***.

Nerve growth factor, the inflammatory mediator and primary afferent sensitizer, is thought to be involved not only in the increased expression of proteins in DRG neurons during sensitization, but also in determining the basal expression of these proteins. Deprivation of NGF by autoimmunization has been used as a way to study the effects of NGF on DRG and peripheral autonomic neurons. Autoimmunization produces hypoalgesia in rats, but it is not known if decreased glutamate availability is included in the mechanism. ***It would be advantageous to know if basal expression of GLS is regulated by peripheral NGF levels (Chapter 4)***.

Antagonism of glutamate receptors at the periphery during inflammation provides analgesia. If GLS is responsible for elevated glutamate levels produced during inflammation, then peripheral GLS inhibition may be a viable pain therapy. Glutamate receptor antagonism (Wang, Liu et al. 1997) at the periphery can decrease expression of Fos in the spinal cord during inflammation, implicating suppression of sensitization and hyperalgesia. ***In order to substantiate GLS as a novel therapeutic target for inflammatory pain, the ability of peripheral GLS inhibition to suppress spinal Fos expression needs to be demonstrated (Chapter 5)***.

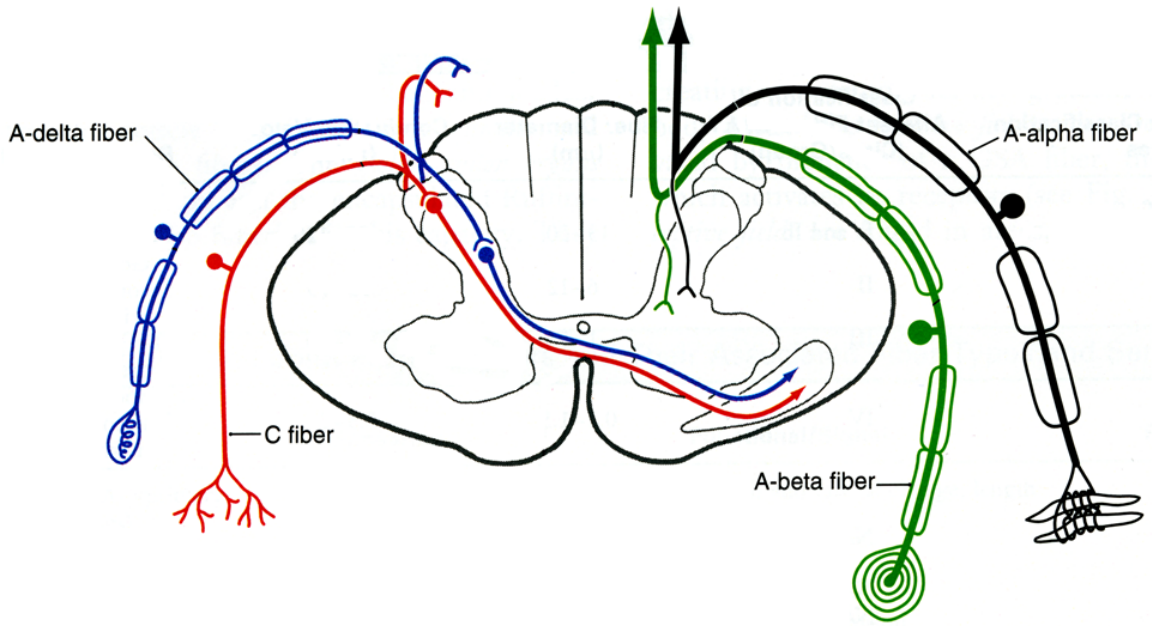

Figure 1.1. Schematic representation of the spinal circuitry for the two primary somatosensory systems modified from Haines 2005. The anterolateral system (ALS) is represented on the left and the posterior column-medial lemniscal (PCML) system is represented on the right. The ALS primarily conveys sensory information regarding pain, temperature and crude touch. The PCML pathway primarily conveys light touch, proprioception and vibration sensory information. C-fibers are unmyelinated, whereas A fibers are myelinated. However, the Aδ fibers are more lightly myelinated than Aα/β fibers. C-fibers terminate as bare nerve endings that have membrane proteins specific to nociceptive stimuli (Haines 2005).

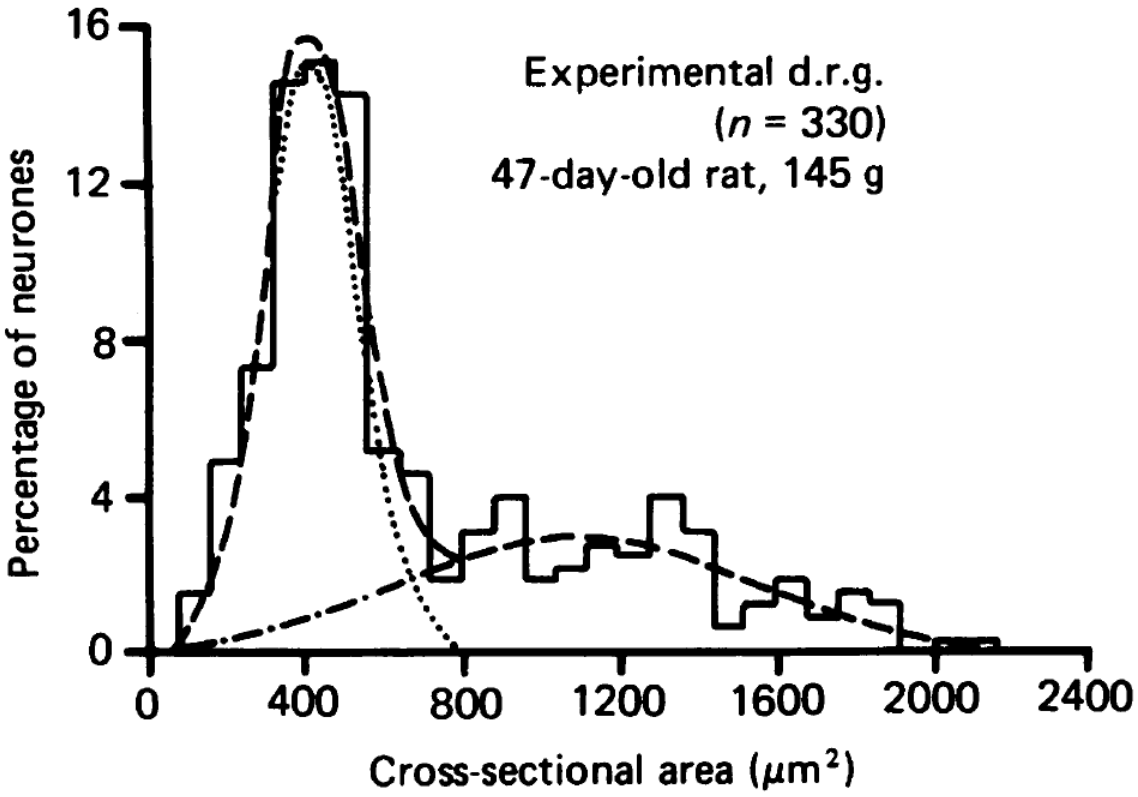

Figure 1.2. Frequency distribution relating cell size with cell number. Two populations are apparent as demonstrated by two computer-identified normal distributions. The small cell population (……) is tall and narrow, while the large cell population (·-·-·-·-·-) is short and broad. The summation of the two populations is shown as -------. (Harper and Lawson 1985)

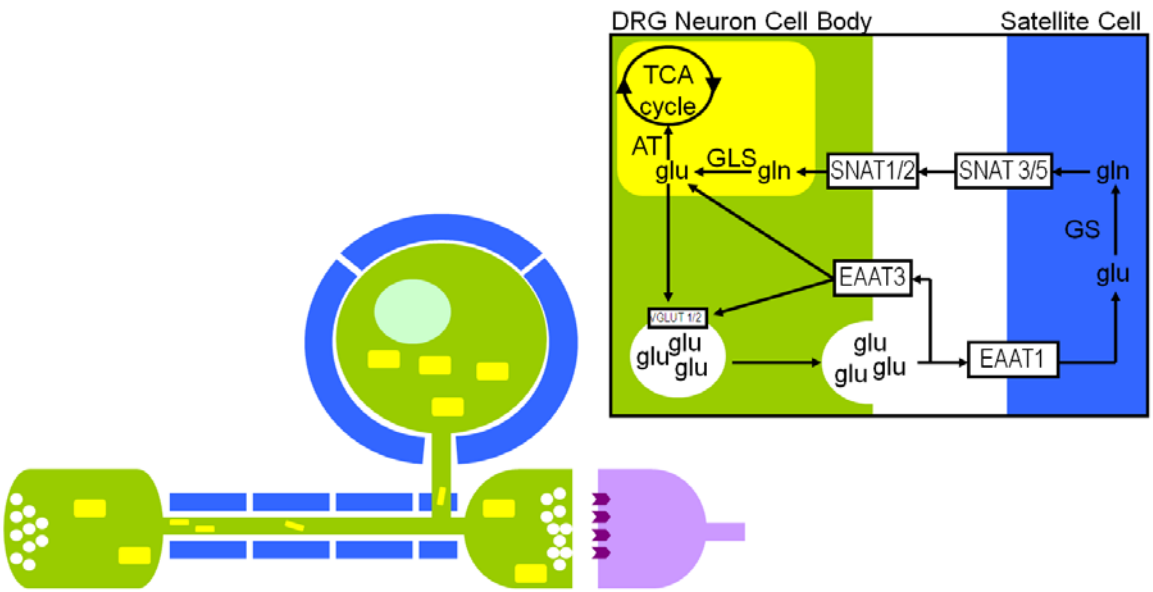

Figure 1.3. Schematic view of the glutamate-glutamine cycle between DRG neurons and their glia. Released glutamate (glu) is transported into neurons and glia by excitatory amino acid transporter 3 (EAAT3) and EAAT1, respectively. Satellite glial cells and Schwann cells convert glutamate to glutamine (gln) with the enzyme glutamine synthetase (GS). Glutamine is transported back to neurons by sodium-coupled neutral amino acid transporters (SNATs) where it is converted to glutamate by the enzyme glutaminase (GLS). Glutamate is packaged into synaptic vesicles by vesicular glutamate transporters (VGLUTs). A DRG neuron is represented in green, glia in blue, post-synaptic dorsal horn neuron in purple. Mitochondria are represented in yellow.

CHAPTER 2

Determination of glutaminase distribution in the rat dorsal root ganglion and optimization of immunofluorescence methods

Abstract

Identification of populations and subpopulations of dorsal root ganglion neurons is commonly accomplished with immunofluorescence and immunohistochemical techniques that rely on the specific interaction between antigen and antibody. In addition to the variable binding affinities and kinetics of certain antibodies and antisera raised against antigens, mode and length of fixation influences antigen-antibody interactions. Although antibody dilution and incubation length are routinely optimized during technique development, the results are rarely analyzed and discussed. Occasionally, different methods or lengths of fixation are examined, but the effect of individual fixative components on immunoreactivity has not been systematically examined with quantitative image analysis methods. Proper characterization of DRG neuron populations relies on robust detection of antigen. In this study, we compared five concentrations of formaldehyde (4%, 2%, 1%, 0.5%, and 0.25% w/v) and five concentrations of picric acid (0.8%, 0.4%, 0.2%, 0.1%, and 0.0%) on immunoreactivity (IR) for glutaminase, voltage gated sodium channel $Na_v1.8$, and the capsaicin receptor TRPV1. In addition, we demonstrated the effect of incubation length in primary antiserum on IR. Decreasing formaldehyde concentration led to an increase in glutaminase- and TRPV1-IR, while

increasing picric acid concentration led to an increase in $Na_v1.8$-IR. Increasing IR has the net effect of improving detection sensitivity and leads to wider definitions of DRG neuron populations. By selecting fixation conditions that optimize IR, our results for glutaminase, $Na_v1.8$, and TRPV1 concur with other methods of investigating these neuronal populations.

Introduction

Immunohistochemical and immunofluorescence methods have been essential in identifying putative neurotransmitters for specific neurons throughout the central and peripheral nervous systems. Glutamate is widely accepted as the major excitatory neurotransmitter of the central nervous system and is a candidate for use by pseudounipolar primary sensory neurons at all central terminals (Skilling, Smullin et al. 1988; De Biasi and Rustioni 1990; Zahn, Sluka et al. 2002; Li, Fujiyama et al. 2003; Dmitrieva, Rodriguez-Malaver et al. 2004; Brumovsky, Watanabe et al. 2007) and at some peripheral terminals (deGroot, Zhou et al. 2000; Jin, Nishioka et al. 2006; Brumovsky, Watanabe et al. 2007). One marker of glutamatergic function is the enzyme glutaminase (GLS; EC 3.5.1.2), which synthesizes glutamate from glutamine. However, based on GLS-immunoreactivity (IR), there is inconsistency between the estimated percentages of glutamatergic peripheral sensory neurons ranging from approximately 30%-40% of the small cell population in the rat dorsal root ganglion (DRG) (Cangro, Sweetnam et al. 1984; Cangro, Sweetnam et al. 1985; Battaglia and Rustioni 1988) to greater than 80% of all DRG cells (Miller, Douglas et al. 1993; Li, Ohishi et al. 1996). One difference between these DRG studies is the fixative used for tissue preservation. GLS-IR in brain neurons diminishes as formaldehyde concentration in the fixative

increases from 0.2% to 4% (w/v) (Kaneko, Itoh et al. 1989); therefore, a similar phenomenon may occur in the DRG. Picric acid concentration in the fixative also differed among studies of GLS-IR as well as length of incubation in the primary antiserum.

In the present study, we compared the effects of formaldehyde and picric acid concentrations in the fixative as well as length of incubation in primary antiserum for immunofluorescence studies of GLS, voltage-gated sodium channel 1.8 ($Na_v1.8$), and transient receptor potential vanilloid receptor 1 (TRPV1) in rat DRG. Electrophysiological properties, axon diameters, and cell body sizes have been used in attempts to classify populations of DRG neurons (Yoshida and Matsuda 1979; Lee, Chung et al. 1986; Fang, McMullan et al. 2005). More recently, protein markers have been used to identify subpopulations of some modalities, like TRPV1 for painful heat (Caterina, Schumacher et al. 1997). However, as with GLS, the reported percentages of DRG neurons expressing specific markers have varied, thus hindering a firm classification schema from being adopted. We propose that rigorous optimization of tissue preparation, including fixation, for each antigen should take place to determine its true distribution and relative abundance in DRG neurons.

Methods

Sprague-Dawley rats (n = 13; 200-300 g) were housed on a 12 hour light: 12 hour dark cycle and given free access to food and water. Procedures were conducted according to guidelines from the National Institutes of Health (NIH 2003) and were approved by the Oklahoma State University Center for Health Sciences Institutional

Animal Care and Use Committee. All appropriate efforts were made to minimize the number of animals used in this study.

Rats were anesthetized with Avertin (2.5% w/v) and xylazine and then perfused through the ascending aorta with 75 mL calcium-free Tyrode's solution, pH 7.3 followed by 300 mL fixative. Five rats were used for the formaldehyde comparison. The fixative used for each rat contained 0.2% (w/v) picric acid, 0.1 M sodium phosphate buffer, and was adjusted to pH 7.3. Formaldehyde concentration was varied among the five fixatives to contain 4%, 2%, 1%, 0.5%, or 0.25% (w/v). Five rats were used for the picric acid comparison. The fixative used for each rat contained 1.0% (w/v) formaldehyde, 0.1 M sodium phosphate buffer, and was adjusted to pH 7.3. Picric acid concentration was varied among the five fixatives to contain 0.8%, 0.4%, 0.2%, 0.1%, or 0.0% (w/v). Two additional rats were used for the primary antisera incubation time comparison. The fixative used for both animals was 0.2% picric acid and 1.0% formaldehyde in 0.1 M sodium phosphate buffer adjusted to pH 7.3. Left and right L4 DRG were dissected from perfused rats. DRG from each rat were post-fixed for four hours at 4°C in the same fixative used for perfusion and then were cryoprotected overnight at 4°C in phosphate buffered saline, pH 7.3 (PBS) containing 10% (w/v) sucrose.

All DRG for a given comparison (i.e., formaldehyde, picric acid, primary incubation time) were embedded into one frozen block and cut in 8 μm serial sections on a Microm HM 550 OMVP cryostat (Richard Allan Scientific; Kalamazoo, MI). To prevent recounting of neurons for a given primary antiserum, sections were allotted in order to one of the three antisera and the fourth section was discarded each time, making the minimum approximate distance between two analyzed sections 24 μm. Sections were

thaw-mounted to gelatin-coated SuperFrost slides (Fisher Scientific; Pittsburg, PA, USA) and dried for two hours at 37°C. Dried sections were rinsed three times in PBS before blocking for one hour at room temperature in 5% (v/v) normal goat serum, 1% (w/v) bovine serum albumin, and 1% (w/v) polyvinylpyrollidone (PVP) in PBS with 0.2% (v/v) Triton X-100 (PBS-T). Sections for the formaldehyde and picric acid comparisons were incubated in primary antisera diluted with PBS-T for four days at 4°C. Sections for the primary incubation time comparison were incubated at room temperature for two hours or at 4°C for 20, 48, 96, or 192 hours. For GLS detection, polyclonal rabbit antiserum against whole GLS made by N.P. Curthoys (Colorado State University; Ft. Collins, CO) was used at 1:10,000. For $Na_v1.8$ detection, polyclonal rabbit antiserum (Sigma; St.Louis, MO) against a 15 amino acid peptide corresponding to the C-terminal residues (EDEVAAKEGNSPGPQ) of rat $Na_v1.8$ was used at 1:2,000. For TRPV1 detection, polyclonal guinea pig antiserum (Neuromics; Edina, MN) against a 22 amino acid peptide corresponding to the C-terminal residues (YTGSLKPEDAEVFKDSMVPGEK) of rat TRPV1 was used at 1:2,000. Following incubation in primary antiserum, sections were rinsed three times in PBS and incubated in secondary antibody diluted in PBS-T at 1.0 μg/mL for one hour at room temperature. For detection of rabbit anti-GLS antiserum or rabbit anti-$Na_v1.8$ antiserum, biotinylated goat anti-rabbit (Vector Laboratories; Burlingame, CA) antiserum was used. For detection of guinea pig anti-TRPV1 antiserum, AlexaFluor 488 conjugated goat anti-guinea pig (Molecular Probes; Carlsbad, CA) antiserum was used. GLS and $Na_v1.8$ sections were rinsed two more times in PBS, once in sodium carbonate buffered saline, pH 9.0 (SCBS), and then incubated for one hour at room temperature in 1.0 μg/mL fluorescein-conjugated avidin D (Vector

Laboratories) diluted in SCBS. All sections were rinsed three more times in PBS and coverslipped with ProLong Gold (Molecular Probes).

Primary antiserum absorption control and secondary antiserum control experiments were performed for the three primary antisera and two secondary antisera, respectively. An additional rat was perfused with 0.8% picric acid and 0.25% formaldehyde, concentrations that gave the highest immunofluorescence. For primary absorption controls, each diluted antiserum was incubated for 24 hours at 4°C with the respective antigen at 10-40 μg/mL. Adjacent sections were incubated for four days at 4°C in either absorbed diluted antisera or non-absorbed antisera. The secondary controls sections were incubated in antiserum diluents only for four days at 4°C prior to routine processing.

Images were acquired using the 20X objective on an Olympus BX51 epifluorescence microscope (Olympus; Center Valley, PA, USA) equipped with a SPOT RT740 monochrome camera (Diagnostic Instruments; Sterling Heights, MI, USA). To ensure proper quantitation, all images were captured at a bit-depth of 8 using a 300 millisecond exposure with the gain set at 1. Captured images were 1600 × 1200 pixels with 2.69 pixels per micrometer. For the formaldehyde and picric acid comparisons, three slides for each antiserum were used and three images from each of the five treatments were captured, making 45 images per antiserum and 135 images per fixative comparison. For the primary antibody incubation comparison, two slides for each antiserum for each of the five time points were used and four images from each slide, making 40 images per antiserum. All neuron profiles with a visible nucleus that were not touching the edge of the image were traced on a Cintiq 21UX interactive pen display (Wacom; Kita Saitama-Gun, Saitama, Japan) using the freehand selections tool in ImageJ (NIH). Nuclei were

excluded from the regions of interest (ROIs), making each ROI correspond to the cytoplasmic profile of a single DRG neuron. Pixel intensities could range from 0 (darkest) to 255 (lightest) on a grayscale. The mean gray value and area in μm^2 for each cytoplasmic profile was measured and copied to a spreadsheet.

Data were analyzed with Prism v5.01 (GraphPad Software; San Diego, CA). The mean gray values for each cell were converted to Relative Immunoreactivity by using the following formula [(MAX – mean gray value)/(MAX – MIN)] × 100, where MAX and MIN are the maximum and minimum mean gray values for cytoplasmic profiles in a given comparison of experimental conditions with one of the three antisera. Scatter plots were made where the cytoplasmic profile area was plotted as cell size (μm^2) on the x-axis and the relative immunoreactivity (ranging from 0 to 100) was plotted on the y-axis. For subsequent calculations, the values for area (μm^2) of the cytoplasmic profile were binned into small (<600 μm^2) and large (>600 μm^2) size categories to indicate two broadly defined neuronal subpopulations. All data are represented as mean ± SD. Significant differences in mean relative immunoreactivities for small and large cells among different experimental conditions were determined by two-way ANOVA with Bonferroni post-tests. Correlation and linear regression analyses were done by plotting the experimental condition that was varied on the x-axis and the relative immunoreactivity on the y-axis with small and large cell values representing separate data sets. Results were considered significant when $P < 0.05$.

Results

A total of 3115 cytoplasmic profiles were traced and analyzed for the formaldehyde comparison. The number of cytoplasmic profiles analyzed per condition (three antisera ×

five formaldehyde concentrations = 15 conditions) was 208 ± 43. The numbers of cytoplasmic profiles traced and analyzed for GLS, $Na_v1.8$, and TRPV1 were 1103, 1232, and 780, respectively.

The effect of formaldehyde on GLS-IR was qualitatively apparent from images (Figure 2.1A-E) or the scatter plot (Figure 2.2A) and is reminiscent of the effects noted in brain neurons (Kaneko, Itoh et al. 1989). Decreasing the fixative formaldehyde concentration from 4% (commonly used) to 2% or lower significantly increased GLS-IR for both small and large cells (Figure 2.3A). There was a significant negative correlation between formaldehyde concentration and GLS-IR (Figure 2.4A) between both small ($P < 0.0001$) and large cells ($P < 0.0001$). Linear regression analyses determined the slopes and y-intercepts of the lines to be -9.794 ± 0.2905 and 58.47 ± 0.6289 ($r^2 = 0.6159$) for the small cells and -10.88 ± 0.4045 and 51.64 ± 0.8149 ($r^2 = 0.6498$) for the large cells (Figure 2.4A). Therefore, as formaldehyde concentration increased, GLS-IR decreased, and 62-65% of the variation in GLS-IR can be explained by variation in formaldehyde concentration. The magnitude of this effect on small and large cells was estimated by the slope of the linear regression lines, which showed that the effect was significantly greater on large cells ($P = 0.034$). Also, as seen in the images (Figure 2.1A), scatter plots (Figure 2.2A), and means plots (Figure 2.3A), small cells consistently have higher GLS-IR than large cells. This is recapitulated by the y-intercept values from the regression lines (Figure 2.4A). It is not possible to test whether the y-intercepts differ significantly, because the slopes are significantly different.

To see if the effects of formaldehyde concentration in the fixative were specific to GLS-IR, we examined $Na_v1.8$-IR and TRPV1-IR in DRG sections from the same rats.

Qualitatively, the effect of formaldehyde on IR for these two proteins (Figure 2.1F-J and 2.1K-O) was not as apparent as it was for GLS (Figure 2.1A-E). Quantitative image analysis, however, revealed that lowering the formaldehyde concentration to 2% and lower led to significant increase in $Na_v1.8$-IR of small cells, whereas it had to be lowered all the way to 0.25% in order to show a significant increase in $Na_v1.8$-IR of large cells (Figure 2.3B). Similarly, lowering the formaldehyde concentration to 1% and lower led to a significant increase in TRPV1-IR of small cells, whereas it had to be lowered to 0.5% in order to show a significant increase in TRPV1-IR of large cells (Figure 2.3C). Negative correlations between formaldehyde concentration and $Na_v1.8$-IR (Figure 2.4B) were significant for small ($P < 0.0001$) and large cells ($P = 0.0142$). The slopes and y-intercepts were -2.342 ± 0.3510 and 36.57 ± 0.6792 ($r^2 = 0.05166$) for small cells and -1.204 ± 0.4890 and 21.46 ± 1.082 ($r^2 = 0.1454$) for large cells (Figure 2.4B). Negative correlations between formaldehyde and TRPV1-IR (Figure 2.4C) were significant for small ($P < 0.0001$) and large cells ($P < 0.0001$). The slopes and y-intercepts were -4.250 ± 0.4322 and 29.77 ± 0.8025 ($r^2 = 0.1496$) for small cells and -1.747 ± 0.2705 and 15.83 ± 0.6168 ($r^2 = 0.1558$) for large cells (Figure 2.4C). Therefore, the magnitude of the effect of formaldehyde concentration on $Na_v1.8$-IR and TRPV1-IR is less than on GLS-IR, as evidenced by the slopes. Moreover, the effect on $Na_v1.8$-IR is not significantly different between small and large cells while it is significantly different ($P < 0.001$) for TRPV1-IR. Since the slopes did not differ for $Na_v1.8$, it was possible to determine that the difference was significantly different ($P < 0.0001$) between the y-intercepts, indicating that small cells consistently had higher $Na_v1.8$-IR. Even though it could not be determined statistically in the linear regression model, qualitative assessment of

images (Figure 2.1C) in addition to evaluation of the means indicated that small cells had higher TRPV1-IR than large cells.

A total of 2955 cytoplasmic profiles were traced and analyzed for the picric acid comparison. The number of cytoplasmic profiles analyzed per condition (three antisera × five picric acid concentrations = 15 conditions) was 197 ± 41. The numbers of cytoplasmic profiles traced and analyzed for GLS, $Na_v1.8$, and TRPV1 were 935, 993, and 1027, respectively.

The effect of picric acid on GLS-IR was not qualitatively apparent from images (Figure 2.5A-E) or the scatter plot (Figure 2.2B). Adding any amount of picric acid in the fixative did not significantly increase the mean immunoreactivity for either small or large cells (Figure 2.6A). There was no significant correlation between picric acid concentration and GLS-IR (Figure 2.7A) between either small ($P = 0.8306$) or large cells ($P = 0.5251$). Linear regression analyses determined the slopes and y-intercepts of the lines to be 0.5816 ± 2.717 and 45.14 ± 1.163 ($r^2 = 0.00008392$) for the small cells and 2.184 ± 3.434 and 31.31 ± 1.355 ($r^2 = 0.001050$) for the large cells (Figure 2.8A). Therefore, picric acid concentration did not affect GLS-IR because only 0.008% to 0.1% of the variation in GLS-IR can be explained by variation in picric acid concentration. Even though there was no picric acid effect on GLS-IR, there was still a cell size effect on GLS-IR as seen in the images (Figure 2.5A-E), scatter plot (Figure 2.2B), and means plots (Figure 2.6A) where small cells consistently had higher GLS-IR than large cells. This is recapitulated by the y-intercept values from the regression lines (Figure 2.7A). Since the slopes for the small and large cells were not significantly different ($P = 0.71$), it was possible to show that the y-intercepts differed significantly ($P < 0.0001$).

To determine if the picric acid concentration in the fixative had effects on IR for proteins other than GLS, we examined $Na_v1.8$-IR and TRPV1-IR in DRG sections from the same rats. Qualitatively, the effect of picric acid on IR for these two proteins was more apparent than it was for GLS (Figure 2.5F-O). Quantitative image analysis revealed that raising the picric acid concentration to 0.2% and higher led to significant increase in $Na_v1.8$-IR of small cells, whereas adding any amount of picric acid did not show a significant increase in $Na_v1.8$-IR of large cells (Figure 2.6B). The only significant difference in $Na_v1.8$-IR among large cells was a slight decrease when 0.4% was used. Adding any amount of picric acid led to a significant increase in TRPV1-IR of small cells, whereas it had to be increased to 0.8% (w/v) in order to show a significant increase in TRPV1-IR of large cells (Figure 2.6C). Positive correlations between picric acid concentration and $Na_v1.8$-IR (Figure 2.7B) were significant for small ($P < 0.0001$) but not large cells ($P = 0.9198$). The slopes and y-intercepts were 25.40 ± 2.237 and 27.70 ± 0.9834 ($r^2 = 0.1939$) for small cells and 0.3161 ± 3.139 and 23.87 ± 1.182 ($r^2 = 0.00002238$) for large cells (Figure 2.7B). Positive correlations between picric acid and TRPV1-IR (Figure 2.7C) were significant for small ($P < 0.0001$) and large cells ($P < 0.0001$). The slopes and y-intercepts were 10.10 ± 2.015 and 24.33 ± 0.9458 ($r^2 = 0.03821$) for small cells and 7.151 ± 1.441 and 12.48 ± 0.5939 ($r^2 = 0.05921$) for large cells (Figure 2.7C). There was, therefore, an effect of picric acid concentration on $Na_v1.8$-IR in small cells but not on large cells and the magnitude of the effect of picric acid concentration on TRPV1-IR was not significantly different on small and large cells ($P = 0.31$). Since the slopes did not differ for TRPV1-IR, it was possible to determine that the difference was significant ($P < 0.0001$) between the y-intercepts, indicating that

small cells consistently had higher TRPV1-IR. Even though it could not be determined statistically in the linear regression model, qualitative assessment of images (Figure 2.5F-J), in addition to evaluation of the means (Figure 2.6B), indicated that small cells had higher $Na_v1.8$-IR than large cells.

A total of 2838 cytoplasmic profiles were traced and analyzed for the incubation length comparison. The number of cytoplasmic profiles analyzed per condition (three antisera × five incubation lengths = 15 conditions) was 189 ± 35. The numbers of cytoplasmic profiles traced and analyzed for GLS, $Na_v1.8$, and TRPV1 were 1012, 1002, and 824, respectively.

The effect of incubation length on GLS-IR was qualitatively apparent from images (Figure 2.8A-E) and the scatter plot (Figure 2.2C). Quantitative analysis (Figure 2.9A) revealed that incubating for 20-48 hours increased GLS-IR significantly compared to just two hours of incubation ($P < 0.0001$); however, there was no significant difference between incubating for 24 versus 48 hours. Moreover, incubating for 96 to 192 hours further increased GLS-IR above 24-48 hours of incubation ($P < 0.0001$). The longest incubation of 192 hours did not yield higher GLS-IR than 96 hours. Significant differences among incubation lengths, or lack thereof, were similar between small and large cells. There was significant correlation between primary antiserum incubation length and GLS-IR (Figure 2.10A) between both small ($P < 0.0001$) and large cells ($P < 0.0001$). Linear regression analyses determined the slopes and y-intercepts of the lines to be 0.1588 ± 0.8251 and 25.11 ± 0.8251 ($r^2 = 0.3661$) for the small cells and 0.1760 ± 0.01005 and 17.46 ± 0.9370 ($r^2 = 0.4454$) for the large cells (Figure 2.10A). Therefore, increasing incubation length increased GLS-IR, and approximately 37 to 45% of the

variation in GLS-IR can be explained by variation in incubation length. The magnitude of this effect on small and large cells was estimated by the slope of the linear regression lines, which showed that the effect was not significantly different between cell sizes ($P = 0.21$; Figure 2.10A). Also, as seen in the images (Figure 2.8A-E), scatter plots (Figure 2.2C), and means plots (Figure 2.9A), small cells consistently have higher GLS-IR than large cells. This is recapitulated by the y-intercept values from the regression lines (Figure 2.10A). Since the slopes were not significantly different, it was possible to show that the y-intercepts differed significantly ($P < 0.0001$).

To see if the effects of incubation length in primary antiserum were specific to GLS-IR, we examined $Na_v1.8$-IR and TRPV1-IR in DRG sections from the same rats. Qualitatively, the effect of incubation length on IR for these two proteins (Figure 2.8F-O) was apparent after at least 48 hours of incubation. However, quantitative image analysis (Figure 2.9B) revealed that a significant increase in $Na_v1.8$-IR of small cells occurred between 2 and 20 hours ($P < 0.0001$). Increasing incubation length continued to increase $Na_v1.8$-IR up to 192 hours, with the exception that there was no significant difference between 48 and 96 hours of incubation. For large cells, $Na_v1.8$-IR was not significantly different between 48, 96, and 192 hours of incubation. Results were similar for TRPV1-IR (Figure 2.9C) in that quantitative differences were noted as early as 20 hours of incubation, while there were no significant differences between 96 and 192 hours of incubation for either small or large cells. Positive correlations between incubation length and $Na_v1.8$-IR (Figure 2.10B) were significant for small ($P < 0.0001$) and large cells ($P < 0.0001$). The slopes and y-intercepts were 0.1673 ± 0.009206 and 27.23 ± 0.8734 ($r^2 = 0.3397$) for small cells and 0.08559 ± 0.01290 and 19.49 ± 1.296 ($r^2 = 0.1100$) for large

cells (Figure 2.10B). Positive correlations between incubation length and TRPV1-IR (Figure 2.10C) were significant for small ($P < 0.0001$) and large cells ($P < 0.0001$). The slopes and y-intercepts were 0.09434 ± 0.006352 and 19.11 ± 0.6532 ($r^2 = 0.2735$) for small cells and 0.07518 ± 0.008109 and 13.74 ± 0.6708 ($r^2 = 0.2686$) for large cells (Figure 2.10C). The magnitude of the effect of incubation length on $Na_v1.8$-IR was significantly different ($P < 0.0001$) between small and large cells, whereas it was not for TRPV1-IR ($P = 0.13$). Since the slopes were not different for TRPV1-IR between small and large cells, it was possible to show that the y-intercept was significantly higher for small cells ($P < 0.0001$), which is consistent with previous comparisons.

Absorbing each of the three antisera with antigen diminished IR to near background levels (Figure 2.12, top three rows). In addition, omitting primary antisera resulted in no IR (Figure 2.12, bottom row). Control experiments indicate that the primary antisera used were specific for their respective antigens and the secondary antisera used produced little to no nonspecific labeling. These control experiments were effective at optimal or near optimal fixative concentrations and incubation lengths.

Discussion

In the present study, we sought to clarify the extent of GLS expression among rat DRG neurons and determine the effects of fixative composition and incubation length on IR for GLS, $Na_v1.8$, and TRPV1. Previous studies showed a broad range in the percentage of rat DRG neurons exhibiting GLS-IR (Cangro, Sweetnam et al. 1984; Cangro, Sweetnam et al. 1985; Miller, Douglas et al. 1993; Li, Ohishi et al. 1996), which we attributed to the difference in formaldehyde concentration in the fixative used for tissue preservation (Kaneko, Itoh et al. 1989). We therefore hypothesized a negative

correlation between GLS-IR and formaldehyde concentration. By performing a two-fold dilution curve of formaldehyde concentration in fixative, we were able show this correlation qualitatively (Figure 2.1A-E). In addition, we obtained quantitative measures of GLS-IR of the cytoplasm in combination with size measurements for each neuron (Figure 2.2A). Statistical analysis of these data revealed significant elevations in GLS-IR as formaldehyde concentration decreased (Figure 2.3A). Furthermore, a statistically significant negative correlation was found to be present in the quantitative data, as hypothesized (Figure 2.4A). Picric acid is another fixative component used in the studies that reported higher estimates of GLS expression in the rat DRG, so we also compared the effects of five concentrations of picric acid on GLS-IR. Our results indicate that picric acid has no effect on GLS-IR (for the polyclonal anti-GLS used in this study), and we presume the reported differences in GLS expression were primarily due to effects of formaldehyde concentration in the fixative.

Estimating percentages of DRG neurons labeling for a specific antigen is typically performed by qualitatively scoring images to obtain counts of labeled and unlabeled neurons. The qualitative score is assigned based on the investigator's opinion of the staining intensity/quality relative to background IR levels. The simplest and closest way to quantitatively approximate this type of scoring is to set an intensity threshold, above which neurons are considered labeled, and below which they are considered unlabeled. The threshold must be set by the investigator in a manner similar to qualitative scoring by viewing many images from a data set and determining an intensity that best distinguishes labeled from unlabeled neurons. When such a practice was carried out for GLS-IR in our formaldehyde comparison, we estimated that 38% of all neurons had GLS-IR above the

chosen threshold when using 4% formaldehyde in the fixative (Figure 2.11A). Using the same threshold, this estimate changed to 100% when 1% or less formaldehyde was used (Figure 2.11B). The quality of GLS-IR (i.e. punctuate "mitochondrial" staining) indicated that the IR most likely was specific for GLS and, therefore, sensitivity was increasing as formaldehyde concentration decreased. Background fluorescence did not increase appreciably, indicating that loss of specificity did not account for the higher estimates of GLS expression. Expression of GLS in all DRG neurons is consistent with the need of all DRG neurons to have a means to synthesize neurotransmitter glutamate at their central terminals (Skilling, Smullin et al. 1988; De Biasi and Rustioni 1990; Zahn, Sluka et al. 2002; Li, Xiong et al. 2003; Dmitrieva, Rodriguez-Malaver et al. 2004; Brumovsky, Watanabe et al. 2007). The higher GLS-IR of small DRG neurons may correspond to the added ability of small diameter nociceptive DRG neurons to release glutamate from their peripheral terminals (deGroot, Zhou et al. 2000; Jin, Nishioka et al. 2006; Brumovsky, Watanabe et al. 2007).

Similar, albeit less pronounced, effects were seen for $Na_v1.8$ and TRPV1, indicating that the effect of fixation on IR is not specific to GLS. For $Na_v1.8$, however, picric acid had the largest effect on IR. As higher concentrations of picric acid were used in the fixative, $Na_v1.8$-IR increased. The percentages of DRG neurons labeling for $Na_v1.8$ were 53% and 69% using 0% and 0.8% picric acid, respectively (Figure 2.11C and D). Interestingly, the effect of picric acid seemed to be specific for DRG neurons under 600 μm^2 (Figure 2.6B and 2.7B) since $Na_v1.8$-IR of larger neurons was not consistently increased by picric acid concentration (Figure 2.6B and 2.7B). According to another study using immunofluorescence that fixed with 4% formaldehyde and 0.0% picric acid,

approximately 50% of adult rat DRG neurons express $Na_v1.8$ (Benn, Costigan et al. 2001). Although there have been no studies of $Na_v1.8$-IR where 0.8% picric acid has been used to fix rat DRG, in-situ hybridization for $Na_v1.8$ has shown that 66.5-68.9% of DRG neurons express $Na_v1.8$ mRNA (Fukuoka, Kobayashi et al. 2008).

TRPV1-IR was affected by both formaldehyde and picric acid concentration. Decreasing formaldehyde and increasing picric acid elevated TRPV1-IR. The effect of formaldehyde was greater in this study than that of picric acid. The effect of picric acid, however, may have been greater if the formaldehyde concentration used for the picric acid comparison was lower than 1%. To prevent morphological changes to the tissue caused by inadequate fixation, we chose to include 1% formaldehyde in all of the picric acid comparisons. The percentages of DRG neurons labeling for TRPV1 were 25% and 70% using 4% and 0.25% formaldehyde, respectively (Figure 2.11E and F). Background IR levels were not appreciably different when using different concentrations of formaldehyde and picric acid suggesting that lowering formaldehyde or increasing picric acid is not resulting in a sacrifice in specificity. We suggest that TRPV1 expression has been underestimated previously by using a high concentration (4%) of formaldehyde in the fixative. One study noted that 25% of primary sensory neurons had TRPV1-IR, however, in the same study 65% of DRG neurons responded to the TRPV1 agonist capsaicin with calcium imaging. These estimates are close to our results of 25% and 70% with 4% and 0.25% formaldehyde, respectively.

The antigen masking properties of formaldehyde have been well documented (Sompuram, Vani et al. 2004) and many antigen retrieval techniques have been developed in order to restore epitope-antibody interactions that are hindered by aldehyde

mediated changes of the tissue (Shi, Key et al. 1991; Shi, Cote et al. 2001; Shi, Liu et al. 2007). Antigen retrieval is empirical by nature. There is no guarantee that 100% retrieval will be accomplished even when all incubation solutions and temperatures have been attempted. For clinical pathology labs, antigen retrieval is sometimes the only option, as the standard fixative (formalin) is close to the 4% formaldehyde used in many research laboratories and taking another sample for the purpose of fixing it differently is not always an option. However, basic research is not limited by the same standard fixation protocol. The results of our study suggest optimizing the fixation step so that antigen retrieval is unnecessary.

In addition to fixation conditions, it is also necessary to optimize incubation length in immunoreagents to obtain a clear picture concerning the distribution and relative amount of antigen in DRG neurons. The incubation length comparison revealed increased IR with longer incubation periods for all three antigens tested. The presumed reason for a gradual increase in IR as incubation length increased in this study is that polyclonal antisera were used. Each polyclonal antiserum has a heterogeneous mixture of antibodies, some of which may bind more slowly than others. Only the antibodies with highest avidity for antigen will bind after short incubation periods. It should be expected that longer incubation lengths in polyclonal antisera will allow for lower avidity antibodies (which are no less specific) to bind antigen (Polak and Van Noorden 2003).

In this study, we showed that the sensitivity of immunofluorescence techniques can be affected by fixative composition and incubation length in primary antibody. We used quantitative image analysis to objectively measure IR for GLS, $Na_v1.8$, and TRPV1. Decreasing the formaldehyde concentration in the fixative from the commonly used

concentration of 4% led to an increase in IR for GLS and TRPV1, whereas adding picric acid, to the fixative led to an increase in IR for $Na_v1.8$. Determining the distribution of antigens in the DRG is of much importance for studying populations or subpopulations of DRG neurons. Antigen distribution is often determined by the intensity of staining, therefore, increasing the sensitivity of immunofluorescence techniques may allow for other markers of DRG neuron subpopulations to be more accurately characterized.

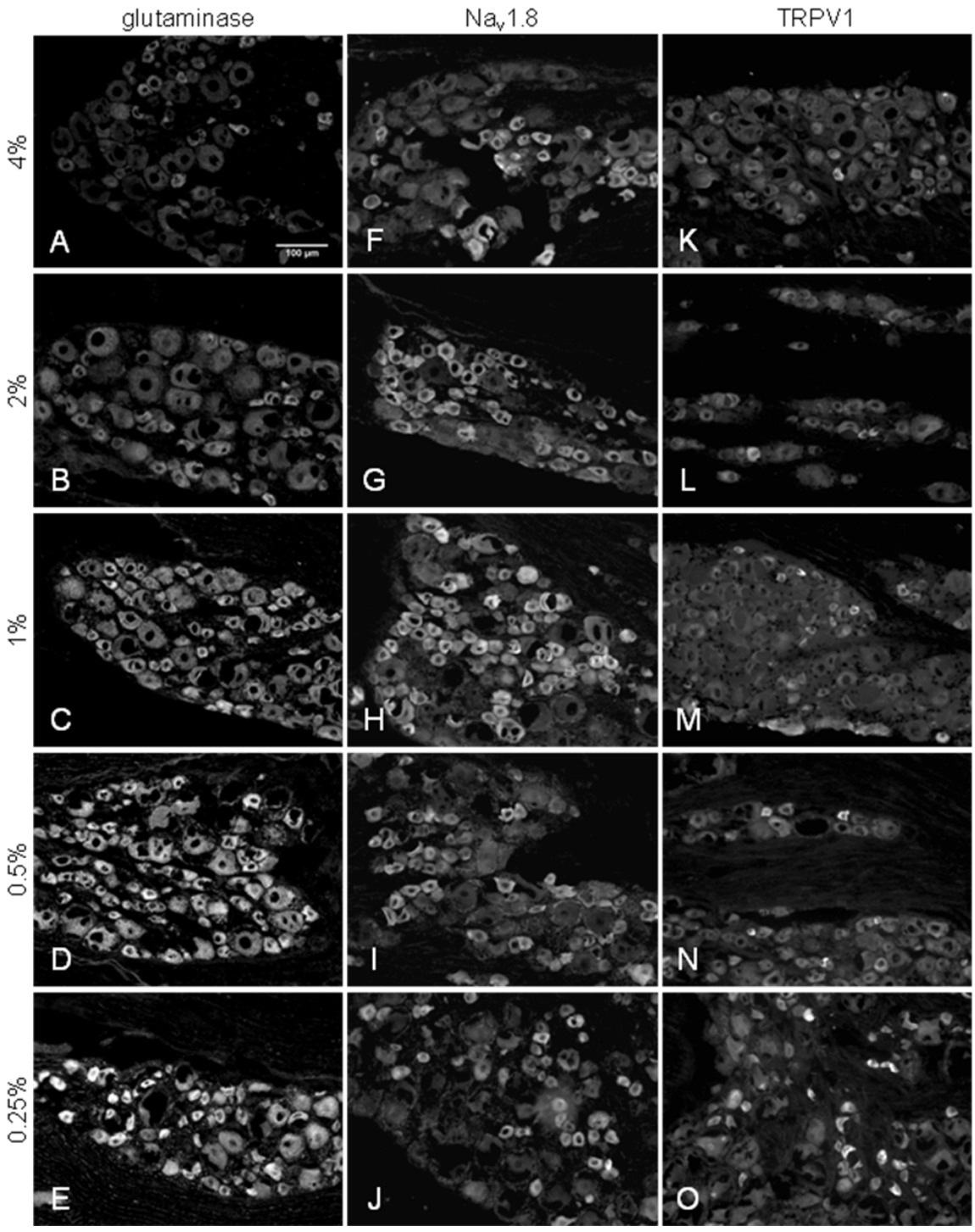

Figure 2.1. Representative images from the formaldehyde comparison for GLS, $Na_v1.8$, and TRPV1. As formaldehyde concentration decreases, GLS-IR increased (A-E) in both small and large diameter DRG neurons. Decreasing formaldehyde concentration did not

appear to have the same magnitude of effect on $Na_v1.8$- (F-J) or TRPV1-IR (K-O). At the highest concentration of formaldehyde (A), only small DRG neurons appear labeled for GLS, whereas with lower formaldehyde concentrations (C-E), all DRG neurons have GLS-IR. Large neurons do not appear labeled for $Na_v1.8$ or TRPV1, even at the lowest formaldehyde concentrations (J and O).

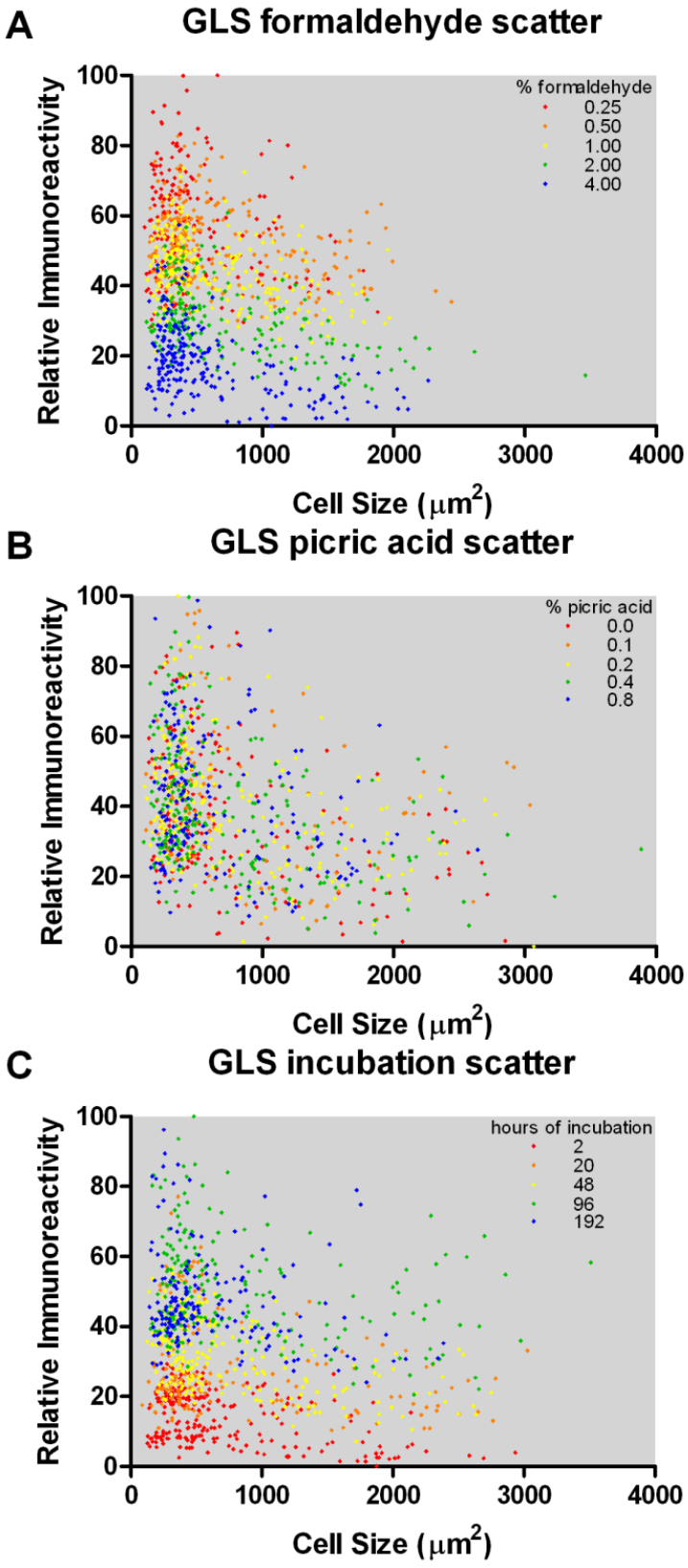
A
GLS formaldehyde scatter
Relative Immunoreactivity
Cell Size (μm²)
% formaldehyde
0.25
0.50
1.00
2.00
4.00
B
GLS picric acid scatter
Relative Immunoreactivity
Cell Size (μm²)
% picric acid
0.0
0.1
0.2
0.4
0.8
C
GLS incubation scatter
Relative Immunoreactivity
Cell Size (μm²)
hours of incubation
2
20
48
96
192

Figure 2.2. Scatter plots from the formaldehyde, picric acid, and primary incubation comparisons for GLS. (A) Decreasing formaldehyde concentration in the fixative increased the relative immunoreactivity for both small and large DRG neurons such that each decrease in formaldehyde concentration resulted in an increase in relative immunoreactivity over the previous level. (B) Changing the concentration of picric acid in the fixative did not have any effect on the relative immunoreactivity. (C) Increasing incubation time in primary antiserum increased relative immunoreactivity for both small and large DRG neurons such that each increase in incubation resulted in higher relative immunoreactivity until a plateau was reached at 96 hours.

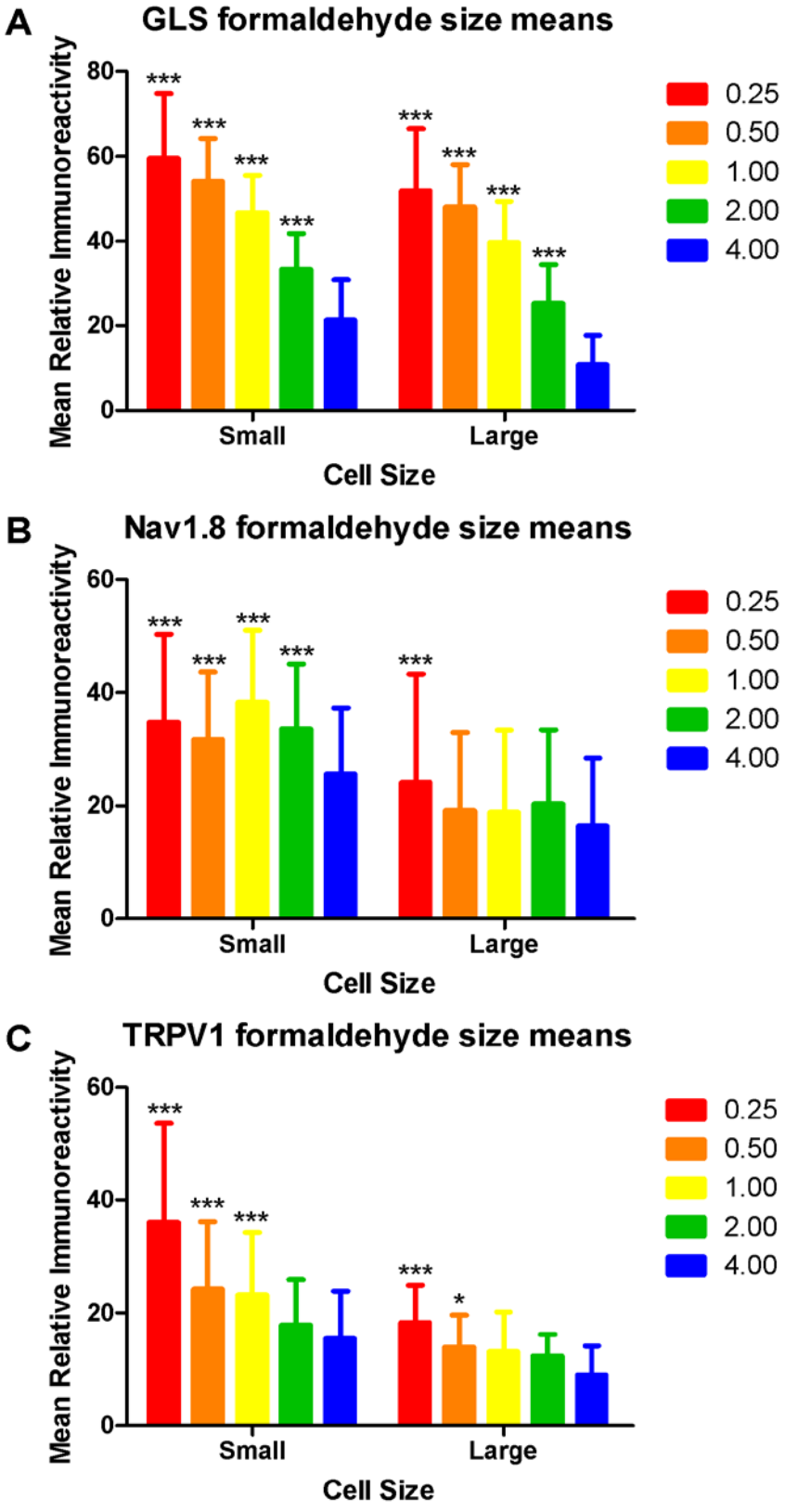
A
GLS formaldehyde size means
Mean Relative Immunoreactivity
80
60
40
20
0
***
Small
Large
Cell Size
0.25
0.50
1.00
2.00
4.00
B
Nav1.8 formaldehyde size means
Mean Relative Immunoreactivity
60
40
20
0
***
Small
Large
Cell Size
0.25
0.50
1.00
2.00
4.00
C
TRPV1 formaldehyde size means
Mean Relative Immunoreactivity
60
40
20
0
***
*
Small
Large
Cell Size
0.25
0.50
1.00
2.00
4.00

Figure 2.3. Effect of formaldehyde concentration in fixative on relative immunoreactivity means for small and large cells. (A) Decreasing formaldehyde from 4% had a concentration dependent effect, such that each decrease in concentration of formaldehyde resulted in GLS-IR being significantly ($P<0.05$ or better) higher than the previous concentration. The effect was similar for both small and large DRG neurons. (B) Decreasing formaldehyde from 4% slightly increased $Na_v1.8$-IR in small DRG neurons, however, there was no significant difference between 2%-0.25%, indicating a plateau of the effect. $Na_v1.8$-IR of large DRG neurons was only significantly elevated when 0.25% formaldehyde was used. (C) Decreasing formaldehyde from 4% began to significantly increase TRPV1-IR of small DRG neurons at 1% and continued to increase it at 0.25%. TRPV1-IR of large DRG neurons did not begin to significantly increase until 0.5% was used. (significance is indicated for comparisons against 4.00% formaldehyhde; *$P<0.05$, ***$P<0.001$)

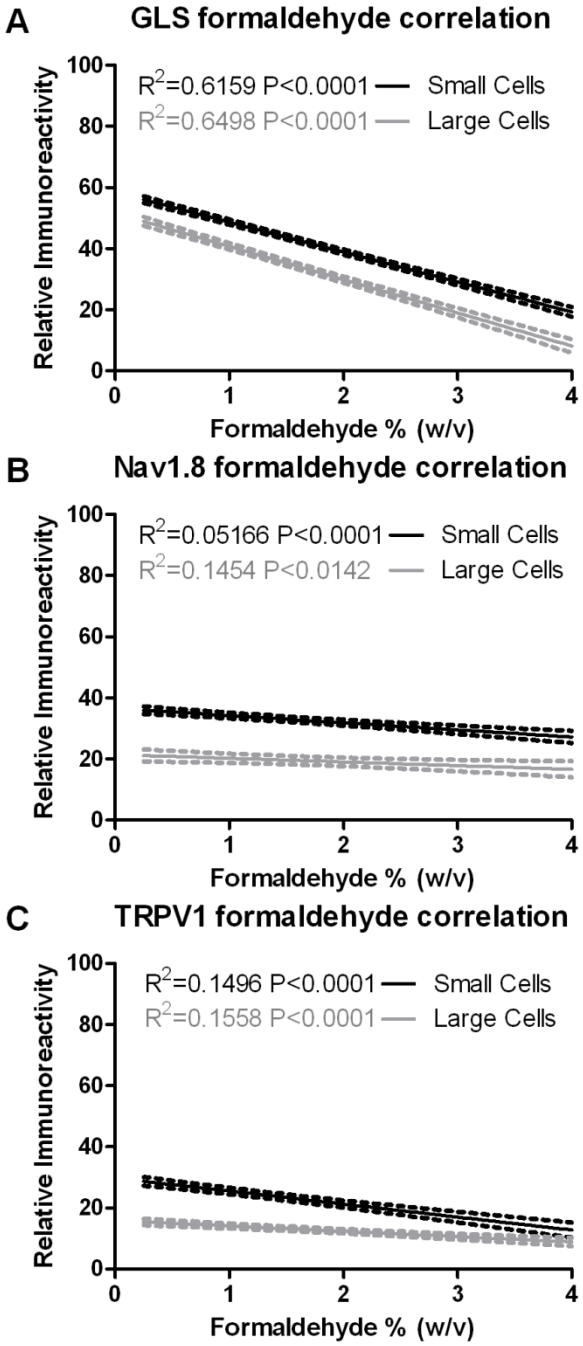

Figure 2.4. Correlations of formaldehyde concentration with IR for GLS, $Na_v1.8$, and TRPV1. (A) Formaldehyde concentration had a strong negative correlation with GLS-IR for both small and large cells, however, small cells maintained higher GLS-IR at all

formaldehyde concentrations. (B) $Na_v1.8$-IR did not have as strong of a negative correlation with formaldehyde concentration, albeit it was significant for both small and large cells. The magnitude of the effect (slope) was not a large as for GLS-IR, but the small cells again maintained higher $Na_v1.8$-IR at all formaldehyde concentrations. (C) The correlation between TRPV1-IR and formaldehyde was again negative for both small and large cells, but not as strong or of as great a magnitude as for GLS-IR.

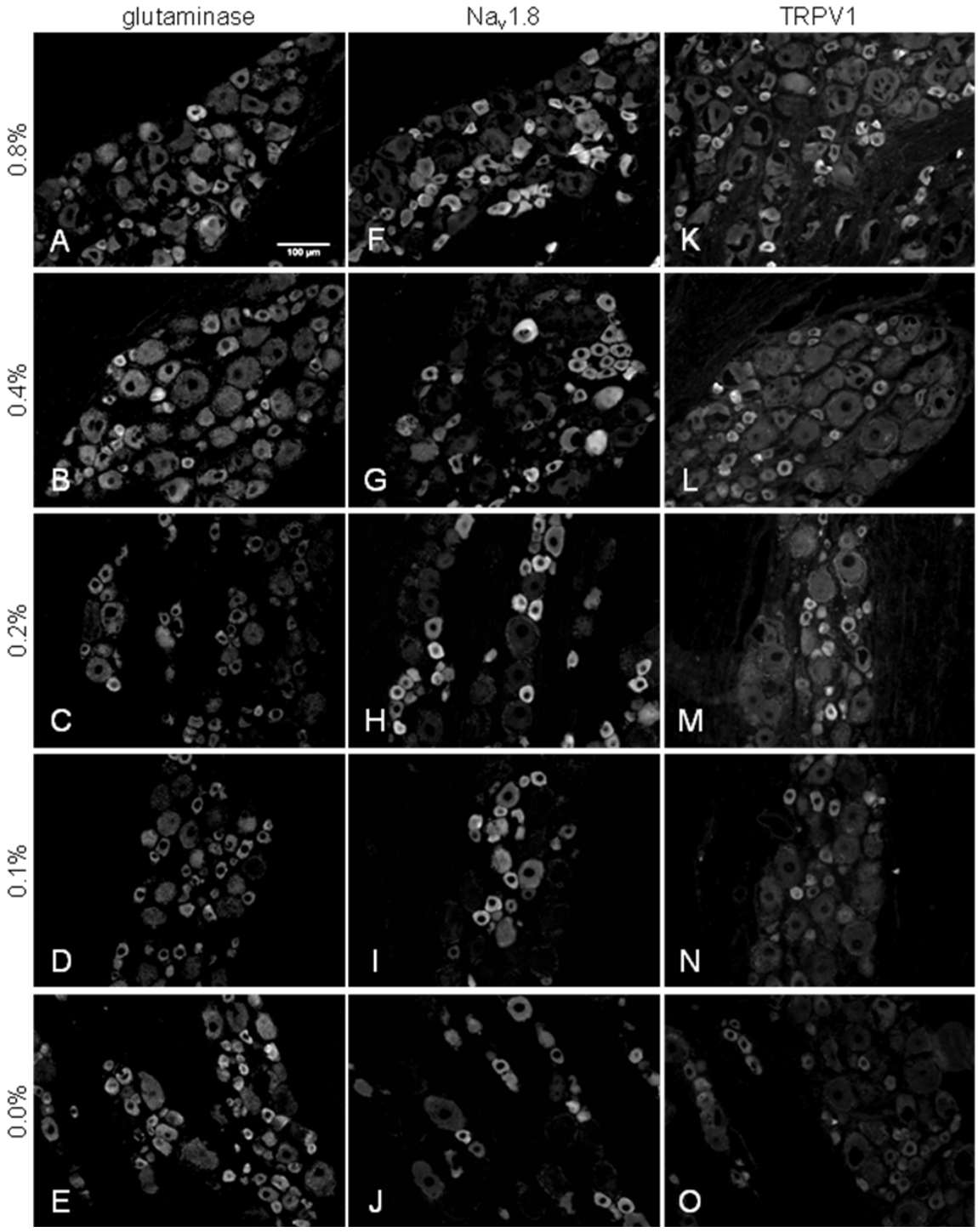

Figure 2.5. Representative images from the picric acid comparison for GLS, $Na_v1.8$, and TRPV1. No obvious qualitative change in GLS-IR was observed as picric acid concentration was increased (A-E). A slight increase in $Na_v1.8$-IR was noticed in small

DRG neurons as picric acid was added to the fixative in increasing amounts, but there was not a noticeable change in the IR of large DRG neurons or background staining (F-J). Increasing picric acid concentration in the fixative increased TRPV1-IR of small DRG neurons (K-O).

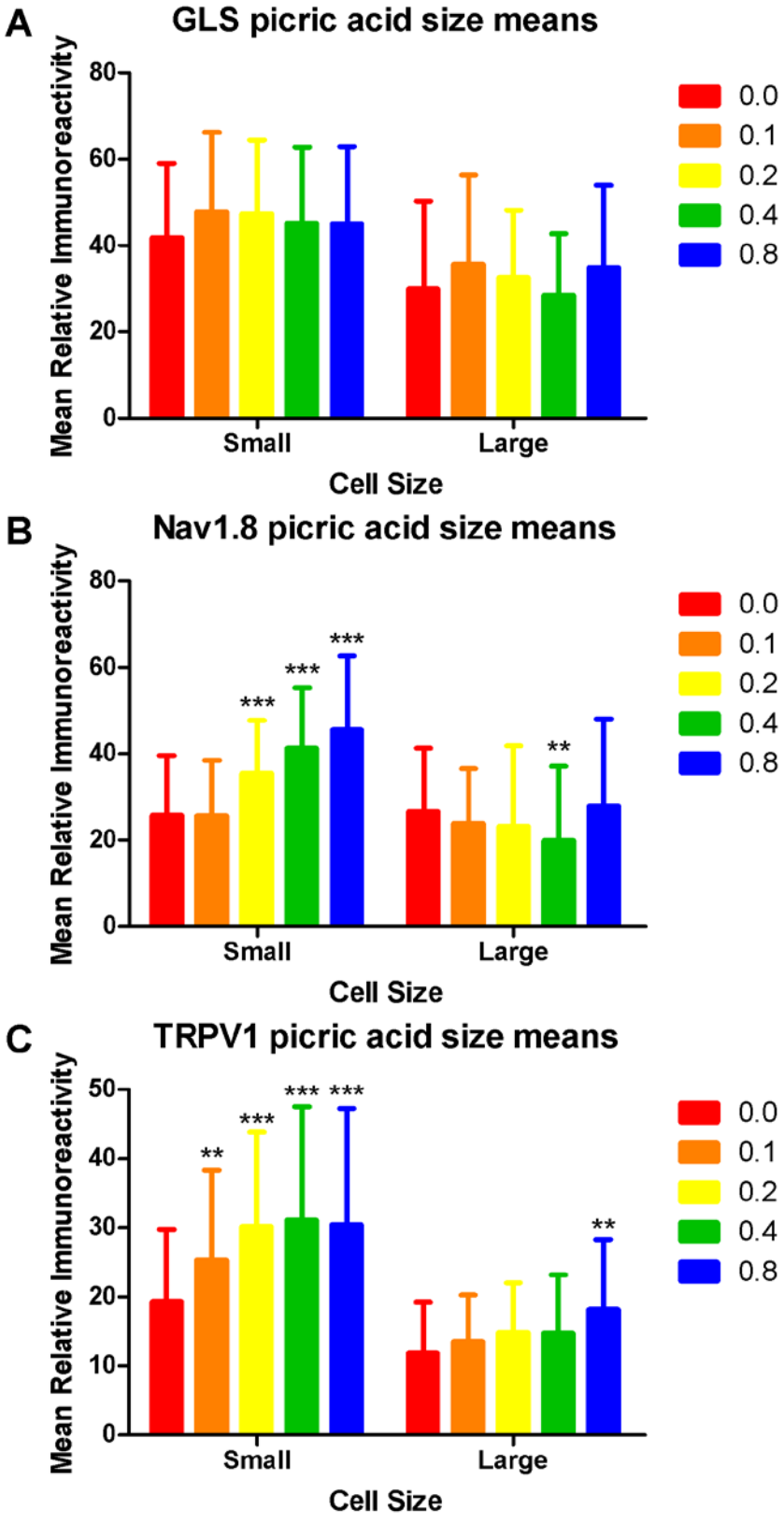
A
GLS picric acid size means
Mean Relative Immunoreactivity
80
60
40
20
0
Small
Large
Cell Size
0.0
0.1
0.2
0.4
0.8
B
Nav1.8 picric acid size means
Mean Relative Immunoreactivity
80
60
40
20
0
***
***
***
**
Small
Large
Cell Size
0.0
0.1
0.2
0.4
0.8
C
TRPV1 picric acid size means
Mean Relative Immunoreactivity
50
40
30
20
10
0
**
***
*** ***
**
Small
Large
Cell Size
0.0
0.1
0.2
0.4
0.8

Figure 2.6. Effect of picric acid concentration in fixative on relative immunoreactivity means for small and large cells. (A) Increasing picric acid in the fixative had no significant effect on GLS-IR for either small or large DRG neurons. (B) In contrast, increasing the picric acid to 0.2% and higher significantly raised the $Na_v1.8$-IR in small cells, but there was not a trend of significant elevation in IR for large DRG neurons as picric acid concentration was increased. (C) TRPV1-IR of small DRG neurons increased as picric acid was added, but the effect reached a plateau at 0.2%. Large DRG neurons only had significantly elevated IR at the highest concentration of picric acid. (significance is indicated for comparisons against 0.0% picric acid; **P<0.01, ***P<0.001)

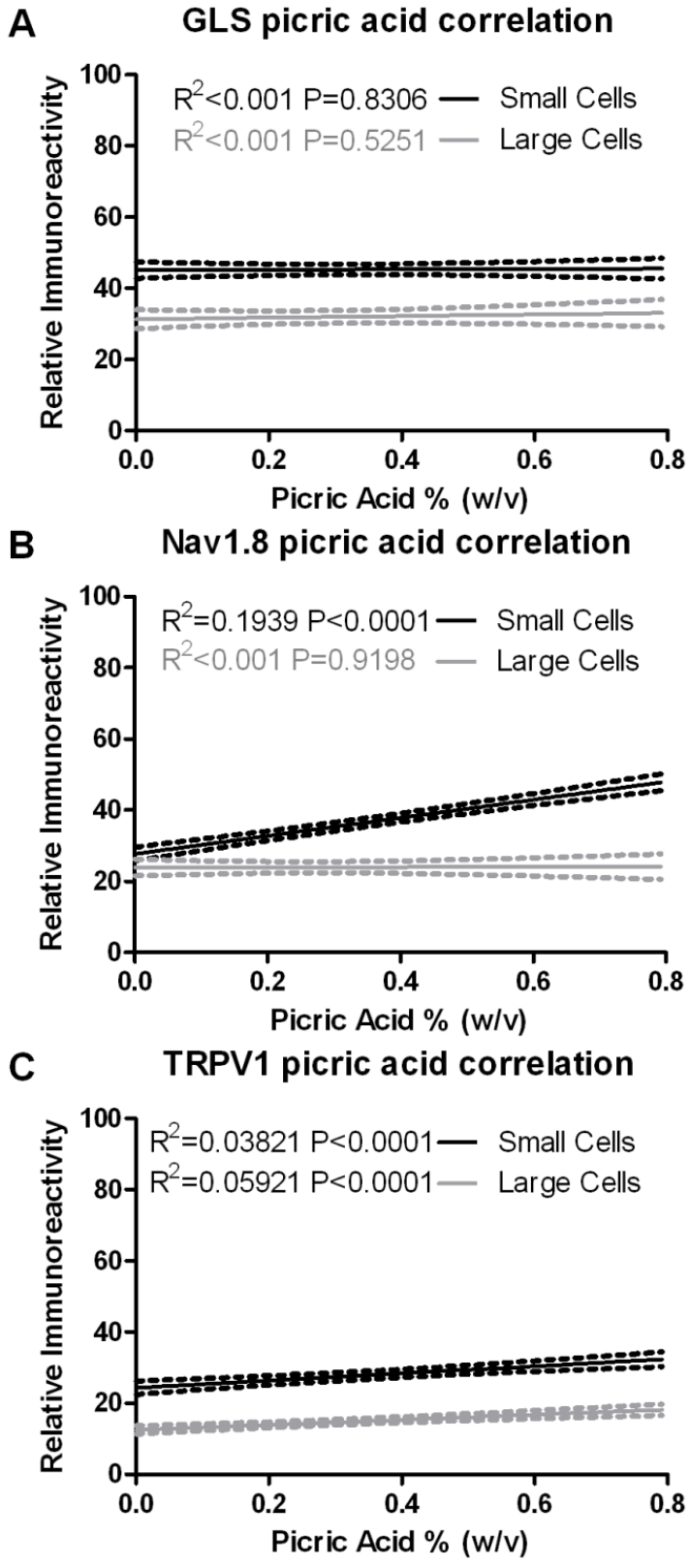
A
GLS picric acid correlation
R2<0.001 P=0.8306
Small Cells
R2<0.001 P=0.5251
Large Cells
Relative Immunoreactivity
Picric Acid % (w/v)
B
Nav1.8 picric acid correlation
R2=0.1939 P<0.0001
Small Cells
R2<0.001 P=0.9198
Large Cells
Relative Immunoreactivity
Picric Acid % (w/v)
C
TRPV1 picric acid correlation
R2=0.03821 P<0.0001
Small Cells
R2=0.05921 P<0.0001
Large Cells
Relative Immunoreactivity
Picric Acid % (w/v)

Figure 2.7. Correlations of picric acid concentration with IR for GLS, $Na_v1.8$, and TRPV1. (A) There was no significant correlation between the concentration of picric acid in the fixative and GLS-IR for either small or large DRG neurons. Small DRG neurons again had higher GLS-IR than large DRG neurons that was significant across all concentrations of picric acid (y-intercepts were significantly different). (B) There was a moderate but significant positive correlation between picric acid concentration and $Na_v1.8$-IR for small DRG neurons. The IR of large neurons did not correlate with picric acid concentration in the fixative. (C) TRPV1-IR of both small and large DRG neurons had a weak but significant positive correlation with picric acid concentration. The magnitude of the effect on small and large neurons was not significantly different (from comparing slopes), and the small neurons always had higher IR than large neurons over the entire range of picric acid concentrations tested (from comparing y-intercepts).

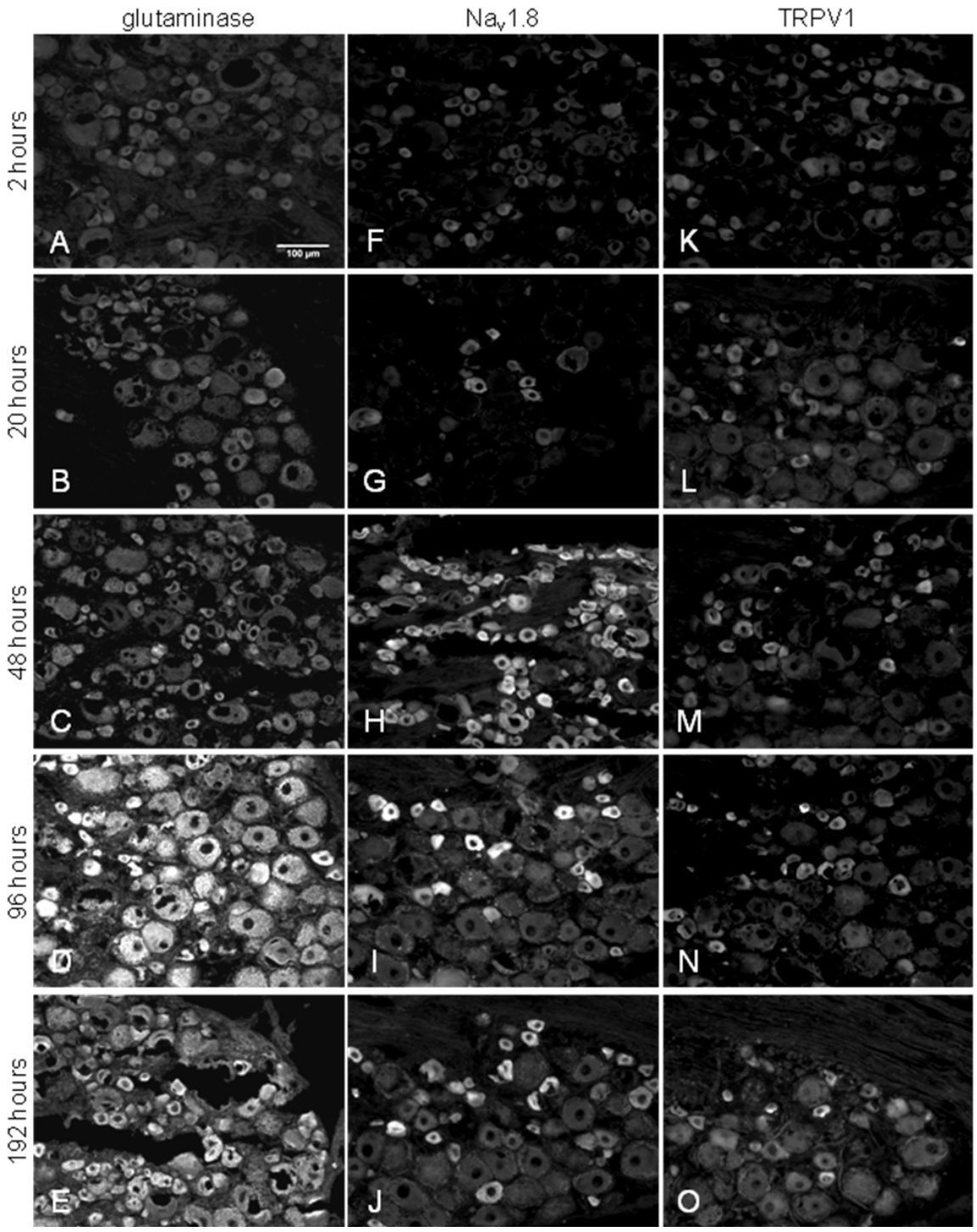

Figure 2.8. Representative images from the primary antisera incubation comparison for GLS, $Na_v1.8$, and TRPV1. Extending the length of incubation in primary antiserum always increased the IR for the antigen studied. Background levels of fluorescence also

increased at 96, 48, and 120 hours respectively for tissue processed for GLS (D), $Na_v1.8$ (H), and TRPV1 (O). Maximal specific (e.g. neuronal) labeling appeared to occur at 96 hours for all three antigens (D, I, & N).

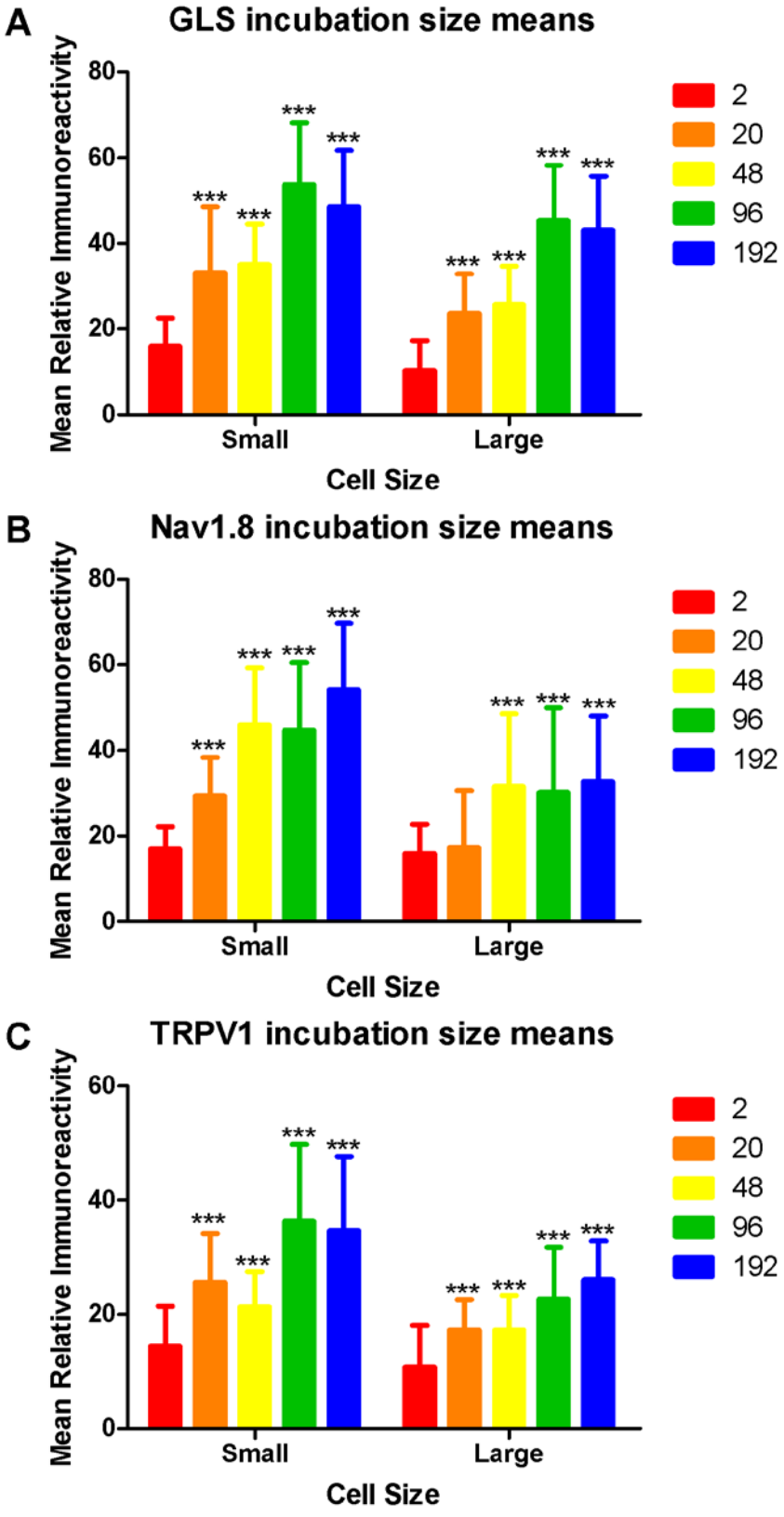
A
GLS incubation size means
Mean Relative Immunoreactivity
80
60
40
20
0
***
Small
Large
Cell Size
2
20
48
96
192
B
Nav1.8 incubation size means
C
TRPV1 incubation size means

Figure 2.9. Effect of incubation length in primary antiserum on relative immunoreactivity means for small and large cells. (A) Maximal GLS-IR was obtained after 96 hours of incubation for both small and large DRG neurons. (B) $Na_v1.8$-IR of small DRG neurons reached maximal levels after 192 hours of incubation, while large DRG neurons reached maximal IR at 48 hours. (C) Incubating for 96 hours resulted in maximal TRPV1-IR of small and large DRG neurons. (significance is indicated for comparisons against 2 hours; **P<0.01, ***P<0.001)

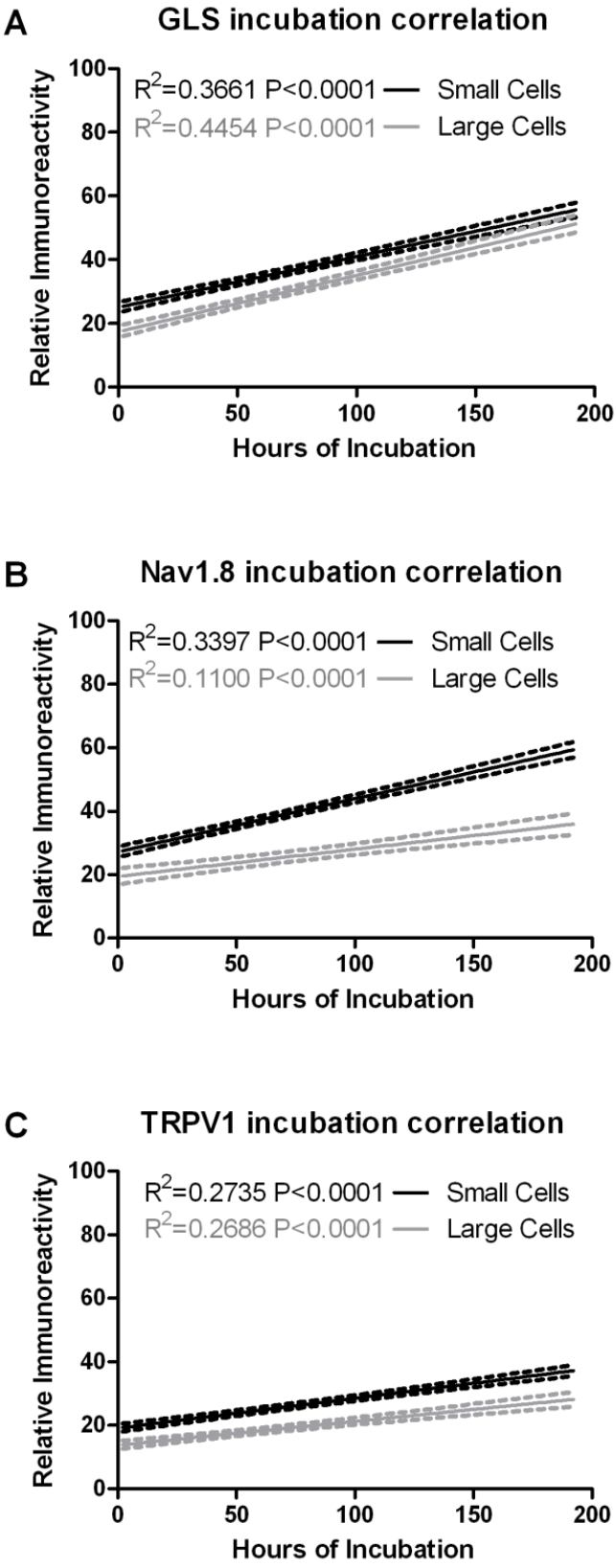
A
GLS incubation correlation
R2=0.3661 P<0.0001 Small Cells
R2=0.4454 P<0.0001 Large Cells
Relative Immunoreactivity
Hours of Incubation
B
Nav1.8 incubation correlation
R2=0.3397 P<0.0001 Small Cells
R2=0.1100 P<0.0001 Large Cells
Relative Immunoreactivity
Hours of Incubation
C
TRPV1 incubation correlation
R2=0.2735 P<0.0001 Small Cells
R2=0.2686 P<0.0001 Large Cells
Relative Immunoreactivity
Hours of Incubation

Figure 2.10. Correlations of primary antiserum incubation length with IR for GLS, $Na_v1.8$, and TRPV1. Incubation length had a significant positive correlation with IR for all three antigens in small and large DRG neurons. The correlation was strongest for GLS-IR in large DRG neurons and weakest for $Na_v1.8$-IR for large DRG neurons.

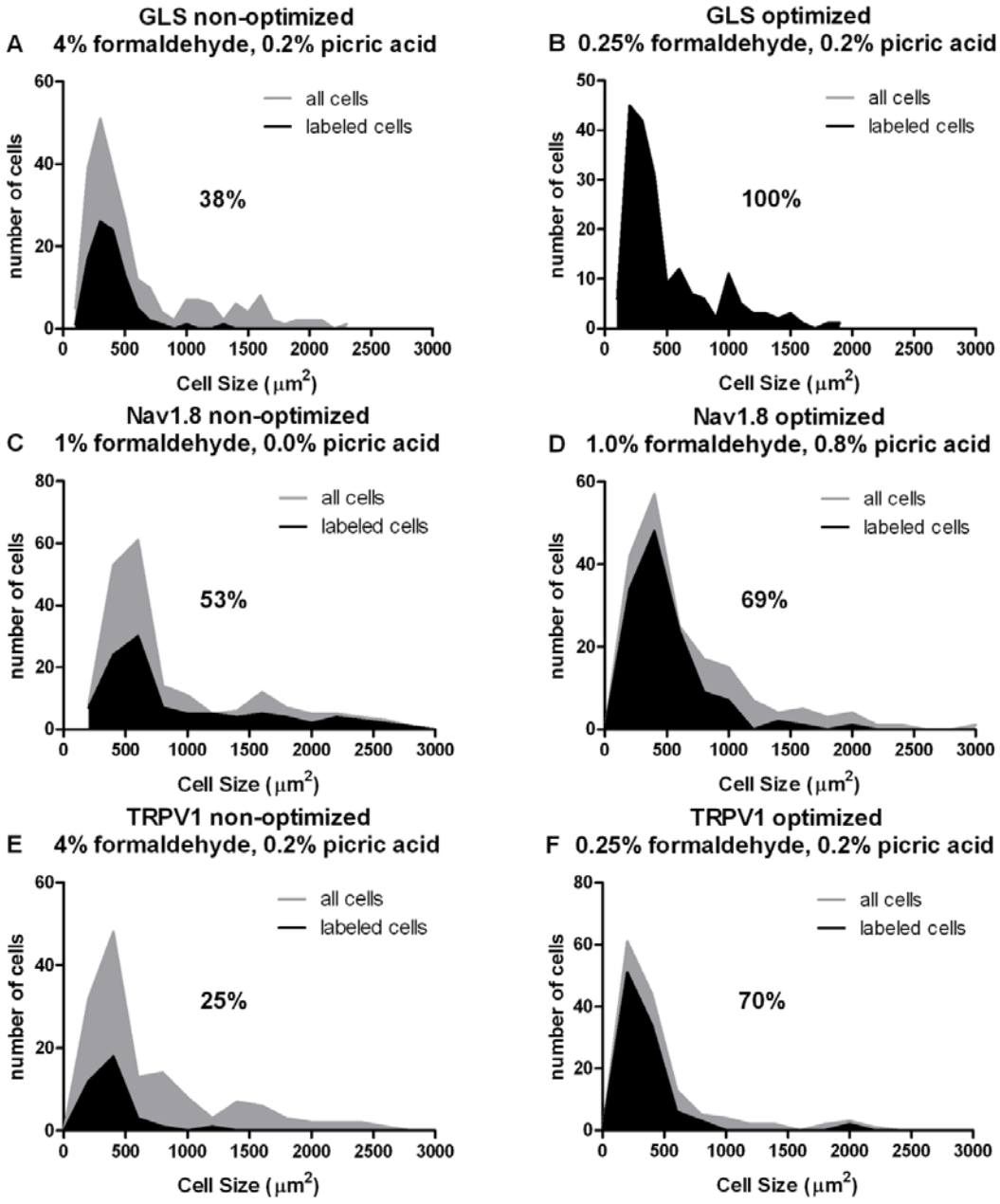

Figure 2.11. Optimization increases sensitivity of immunofluorescence detection for GLS, $Na_v1.8$, and TRPV1. Formaldehyde had a greater effect on GLS-IR in rat DRG neurons than picric acid. When 4% formaldehyde is used 38% of rat DRG neurons are labeled for GLS (A) and they are primarily small neurons. When formaldehyde is lowered to 0.25%, all rat DRG neurons are labeled (B). Adding 0.8% picric acid to the

fixative increased the total number of DRG neurons labeled for $Na_v1.8$ from 53% (C) to 69% (D), with mainly small neurons contributing to the increased labeling. TRPV1 was affected by both formaldehyde and picric acid concentrations, but only the effect of optimizing formaldehyde is shown here. Lowering the formaldehyde concentration from 4% to 0.25% increased the percentage of labeled neurons from 25% (E) to 70% (F).

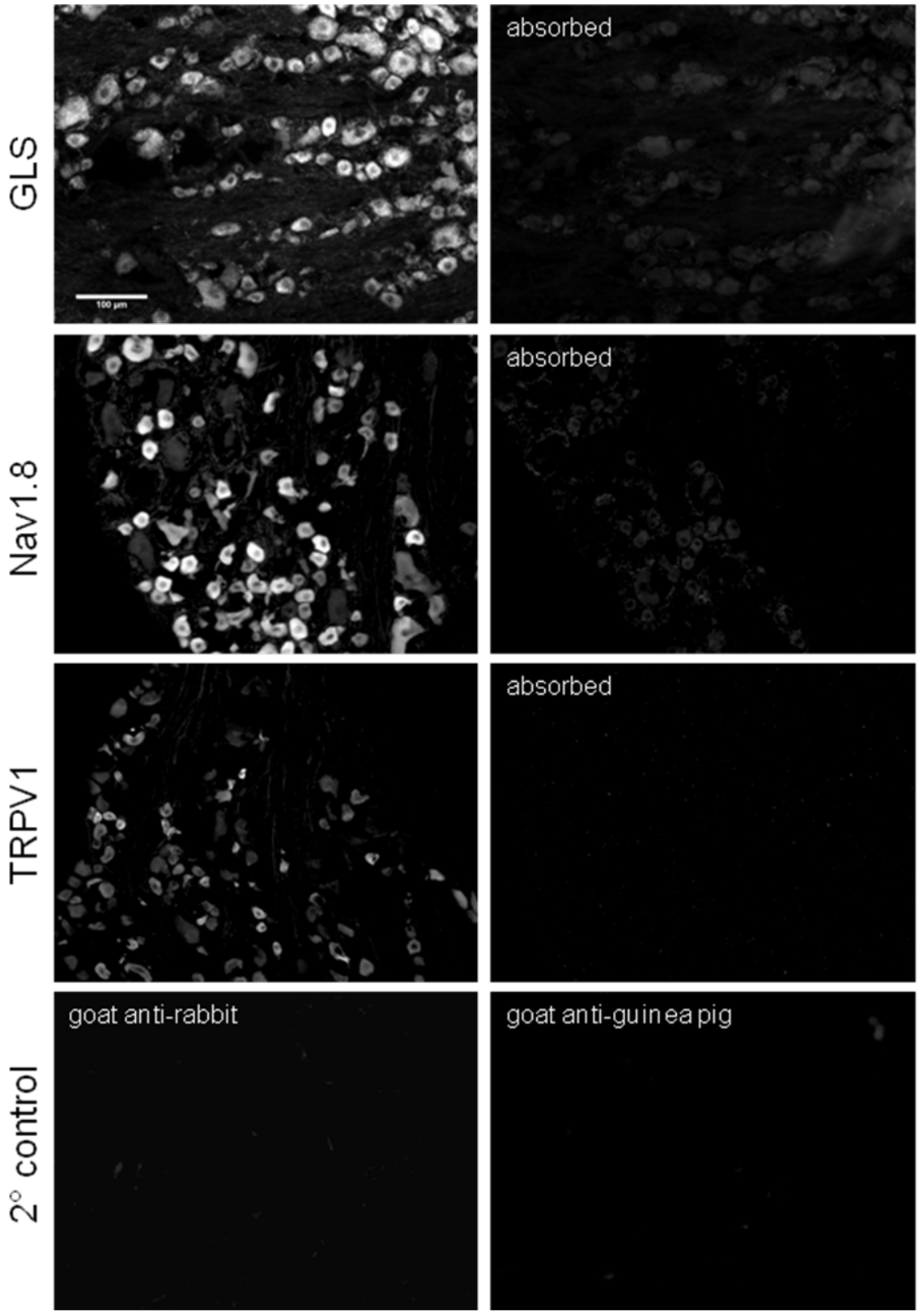
GLS
Nav1.8
TRPV1
2° control
absorbed
absorbed
absorbed
goat anti-rabbit
goat anti-guinea pig
100 µm

Figure 2.12. Control experiments for primary and secondary antisera. The optimal fixation conditions of low formaldehyde (0.25%) and high picric acid (0.8%) were used to fix the DRG. Diluted primary antisera were absorbed with antigen prior to routine processing (top three rows of panels). Sections were incubated in primary antiserum diluent only and then routinely processed with one of the two secondary antisera (bottom row of panels). IR for all three antigens was successfully absorbed out (right column, top three rows) and the two secondary antisera produced minimal labeling (bottom row).

CHAPTER 3

Glutaminase immunoreactivity is increased during inflammation

Abstract

Glutamate is implicated as a neurotransmitter for both the peripheral and central terminals of nociceptive primary sensory neurons, yet little is known concerning regulation of glutamate metabolism during situations where these neurons are sensitized, such as peripheral inflammation. Glutamate content of both the peripheral and central axons of pseudounipolar primary sensory neurons is elevated during inflammation. Glutaminase (GLS) is a constituent enzyme of the glutamate-glutamine cycle that converts glutamine into glutamate used for neurotransmission and is implicated, therefore, in producing these elevated levels of glutamate. A potential mechanism for increased glutamate is an elevation in GLS expression. To assess GLS expression during peripheral inflammation, we used the complete Freund's adjuvant model for producing peripheral inflammation in the rat hind paw and measured GLS immunoreactivity (IR) in L4 dorsal root ganglion (DRG) neurons after one, two, four, and eight days of inflammation. There was no significant elevation in GLS-IR in the DRG ipsilateral to the inflamed hind paw after one or two days of inflammation. After four days of inflammation GLS-IR was elevated significantly in all DRG neurons. After eight days of inflammation, GLS-IR only remained elevated in small ($<600\mu m^2$), presumably nociceptive neurons. The present study indicates that GLS expression is increased in the chronic stage of inflammation and may be a target for chronic pain therapy.

Introduction

Central axons of pseudounipolar primary sensory neurons of the dorsal root ganglion (DRG) terminate in spinal cord dorsal horn and medullary dorsal column nuclei for pain and touch pathways, respectively (Martin 2003). Peripheral axons of these neurons terminate in and bring sensory information from target tissues, such as viscera, muscle and skin. The central axon terminals release the neurotransmitter glutamate at both spinal (Skilling, Smullin et al. 1988; De Biasi and Rustioni 1990; Zahn, Sluka et al. 2002; Dmitrieva, Rodriguez-Malaver et al. 2004) and medullary levels (De Biasi and Rustioni 1990). Although the peripheral axon terminals are afferent receptors, some of them also have efferent capabilities (Sann and Pierau 1998), e.g., glutamate release in response to noxious stimulation (Omote, Kawamata et al. 1998; deGroot, Zhou et al. 2000; Jin, Nishioka et al. 2006). Inflammation of peripheral target tissues increases the amount of glutamate released from both the peripheral (Omote, Kawamata et al. 1998; Jin, Nishioka et al. 2006) and central axon terminals of DRG neurons (Skilling, Smullin et al. 1988; Dmitrieva, Rodriguez-Malaver et al. 2004). Similar phenomena occur with the neuropeptides substance P and calcitonin gene-related peptide (CGRP). In these instances, inflammation induces gene regulation at the transcriptional level, providing the elevated amounts of substance P and CGRP for release from peripheral and central terminals (Woolf and Salter 2000; Woolf and Ma 2007). In contrast, increasing the amount of the amino acid glutamate available for release depends on regulation at the level of the enzyme that synthesizes glutamate, glutaminase (GLS). Despite being released from the same neurons that release neuropeptides (Merighi, Polak et al. 1991)

and colocalization of GLS within peptidergic neurons (Miller, Douglas et al. 1993), very little is known about glutamate metabolism in DRG neurons during inflammation.

Glutamate metabolism in the central nervous system (CNS) has been well studied (McKenna 2007), since glutamate is the primary excitatory neurotransmitter in the CNS. Neurotransmitter glutamate is taken up and converted to glutamine by astrocytes via the enzyme glutamine synthetase, which release glutamine back to the neurons. Neurons take up glutamine and convert it to glutamate with GT. Many of the proteins necessary for the glutamate-glutamine cycle are present in DRG neurons and their glia (Berger and Hediger 2000; Miller, Richards et al. 2002; Tao, Liaw et al. 2004; Miller, Kriebel et al. 2005). Increasing the production of glutamate available for release in DRG neurons would involve an increase in flux through the glutamate-glutamine cycle near the sites of glutamate release. Long-term responses may require regulating the expression of glutamate-glutamine cycle proteins at the cell body in the DRG and then transporting them to the peripheral and central terminals. To address this issue, we hypothesized that hind paw inflammation increases GLS production in rat DRG neurons. In the present study, we examined GLS levels using immunofluorescence in rat DRG neurons after one, two, four, and eight days of hind paw inflammation. The preliminary results for this study have been presented in poster form (Hoffman, Edwards et al. 2007).

Methods

A combination of male and female Sprague-Dawley rats (n=32; 170-280g) bred on site were used for this study. They were housed on a 12 hour light: 12 hour dark cycle and given free access to food and water. Procedures in this study were conducted according to guidelines from the International Association for the Study of Pain

(Zimmermann 1983) and the National Institutes of Health (NIH 2003), and were approved by the Oklahoma State University – Center for Health Sciences Institutional Animal Care and Use Committee. All appropriate efforts were made to minimize the number of rats used in this study.

To induce a unilateral inflammation of the hind paw, rats (n=20) were immobilized while 150 µL of a 1:1 emulsion containing complete Freund's adjuvant (CFA; Sigma; St. Louis, MO, USA) and 10 mM phosphate buffered 0.9% saline (PBS) was injected into the plantar surface of the right hind paw using a 26 gauge needle. Control rats (n=12) were given an injection of 150 µL PBS in the right hind paw with the same immobilizing procedure, needle, and injection technique. Inflammation was allowed to persist for one, two, four, or eight days; at each time point, 5 CFA-injected and 3 PBS-injected animals were used for immunofluorescence experiments.

Behavioral studies were performed to verify the presence of hyperalgesia after induction of inflammation. Rats were housed in a behavioral testing room within the animal facility to familiarize them to the testing environment and to minimize the experience of transfer to and from testing chambers and housing cages. At least two handling sessions, each on a different day, occurred before starting any behavioral tests. A handling session consisted of placing rats in both types of testing chamber for one hour each and manually moving them between cages and testing chambers. This familiarized the rats to being placed into the temporary environments by the experimenters.

Three days of testing were performed prior to the injection day to obtain a baseline reading for each animal; these days were noted as days -3, -2, and -1. On injection day (day 0), the behavioral test was done prior to the injection, thus serving as a fourth and

final assessment of baseline sensitivity. Behavioral testing continued daily at the same approximate time each day throughout the remainder of each individual experiment, with the longest being until day 8 (12 total days of testing).

Thermal latencies measured in seconds were obtained using a Plantar Test apparatus (Ugo Basile, Comerio, Italy) set at an intensity of 55 mW/cm^2. Mechanical thresholds measured in grams were obtained using a Dynamic Plantar Aesthesiometer (Ugo Basile) set to apply a maximum of 50 g at a ramp rate of 5 g/s. Each testing period consisted of placing the rats into the testing chambers where acclimation was indicated by cessation of all exploratory and grooming behaviors. Two thermal latencies and two mechanical thresholds were measured from each hind paw of each rat, with measurements spaced at least ten minutes apart.

Hind paw edema was measured with a dial caliper (Mitutoyo; Aurora, IL, USA) by measuring metatarsal thickness to the nearest 0.05 mm of both hind paws on the day that the rat was perfused. All hind paw edema measurements were taken when animals were 47-48 days old so that age would not confound the results.

After one, two, four, or eight days of inflammation, 3 PBS-injected and 5 CFA-injected rats were anesthetized with intraperitoneal (i.p.) injections of 1.5 mL 2.5% (w/v) Avertin followed by 0.5 mL xylazine. Rats were perfused with 75 mL of calcium-free Tyrode's solution, pH 7.3 followed by 325 mL of 0.96% (w/v) picric acid and 0.2% (w/v) formaldehyde in 0.1M sodium phosphate buffer, pH 7.3. We chose this fixative because low aldehyde concentration results in optimal immunolabeling of GLS (Kaneko, Itoh et al. 1989; Hoffman, Edwards et al. 2008). The left and right L4 DRG were carefully dissected and placed in the same fixative for 24 hours at 4°C before being transferred to

20% (w/v) sucrose in 0.1M sodium phosphate buffer, pH 7.3 for 48 hours at 4°C. The sixteen DRG from a given set of animals were embedded in a single frozen block and cut in 10 µm sections on a Microm HM 550 OMVP cryostat (Richard Allan Scientific; Kalamazoo, MI, USA). Every fourth section was thaw mounted on gelatin-coated SuperFrost slides (Fischer Scientific; Pittsburg, PA, USA) with two sections per slide. Five slides of DRG sections from each time point were dried at 37°C for two hours. After three 10 minute rinses in PBS, DRG sections were blocked for one hour at room temperature in 10% (v/v) normal goat serum, 10% (v/v) fetal bovine serum, 10% (v/v) normal horse serum, 2% (w/v) polyvinylpyrollidone, 2% (w/v) bovine serum albumin, and 0.3% (v/v) Triton X-100 in PBS. A polyclonal rabbit antiserum against glutaminase was a generous gift from Norman Curthoys (Colorado State University, Ft. Collins, CO, USA). The primary antiserum was diluted 1:10,000 in PBS containing 0.3% (w/v) Triton X-100 (PBS-T) and DRG sections were incubated for four days at 4°C. After primary antiserum incubation, DRG sections were rinsed three times for 10 minutes in PBS and incubated for one hour at room temperature in biotinylated goat anti-rabbit (Vector Laboratories; Burlingame, CA, USA) diluted in PBS-T to 1.5 µg/mL. DRG sections were rinsed two times in PBS for 10 minutes and one time in 0.1M sodium carbonate buffered 0.9% (w/v) saline (SCBS) for 10 minutes before one hour of incubation at room temperature in fluorescein isothiocyanate conjugated avidin (Vector Laboratories) diluted to 1 µg/mL in SCBS. After three 10 minute rinses in PBS, cover slips were affixed with ProLong Gold (Invitrogen; Carlsbad, CA, USA) to retard fading of immunofluorescence.

Images were acquired on a BX51 epifluorescence microscope (Olympus; Center Valley, PA, USA) using a SPOT RT740 camera (Diagnostic Instruments; Sterling

Heights, MI, USA). An exposure and gain combination was determined empirically for each of the four slide sets in which the dimmest regions of tissue could be discerned visually for tracing, but the brightest regions were not oversaturated. Three fields of view were captured randomly from each section of each DRG. All nucleated cells were analyzed in ImageJ (National Institutes of Health; Bethesda, MD, USA) by using the freehand selection tool to identify the cells as regions of interest (ROIs). Once all ROIs for a given image were selected and added to the ROI manager, the area (in μm^2) and mean gray values were measured for each cell and exported for subsequent statistical analysis. Each pixel of an 8-bit grayscale image can have a value from 0-255. We converted each mean gray value (C) into a relative mean gray value that ranged from 1-100 (Fang, Djouhri et al. 2006), because images from each of the four slide sets were taken at slightly different gain and exposure settings. To do this, we found the mean gray value of the most weakly labeled neuron in each data set (A) and the mean gray value of the most intensely labeled neuron in each data set (B); each neuron was given a relative mean gray value = $(100 \times (C-A)/(B-A))$. Mean gray values quantitate the immunoreactivity (IR) and therefore estimate protein expression. The relative mean gray value and size (in μm^2) for each cell were shown in x-y scatterplots. Frequency distributions of relative mean gray values were also generated for each time point. At each of the four time points assessed, the mean relative mean gray value were calculated for small ($<600\ \mu m^2$) and large ($>600\ \mu m^2$) neurons of each L4 DRG.

Graphs and statistical calculations were performed in GraphPad Prism version 5.01 for Windows (GraphPad Software; San Diego, CA, USA). Two-way ANOVAs were done to determine if effects of inflammation or time were significant on thermal latency,

mechanical threshold, and hind paw edema data. Bonferroni post-tests were performed to determine which groups differed and when. A two way ANOVA was done on each of the four sets of GLS-IR data to determine if effects of inflammation were significant on the mean GLS-IR of small and large L4 DRG neurons. Bonferroni post-tests were performed to determine which DRG and which neuron populations differed significantly in GLS-IR. All graphical results represent mean plus or minus the standard deviation. Results were considered significant when p values were less than 0.05.

Results

Thermal latencies and mechanical thresholds of the hind paws contralateral to the PBS injection, ipsilateral to the PBS injection or contralateral to the CFA injection were never significantly different from each other. Baseline thermal latencies of the hind paws ipsilateral to the CFA injection were not significantly different than the other baseline measurements, but they were always significantly different from the three other groups after the injection at day 0 through day 4. Thermal latencies of hind paws ipsilateral to the CFA injection were not different than those from hind paws ipsilateral to the PBS injection on days 5, 7 or 8 (Figure 3.1A). Baseline mechanical thresholds of the hind paws ipsilateral to the CFA injection were not significantly different than the other baseline measurements, but they were always significantly different from the three other groups after the injection at day 0 through day 8 (Figure 3.1B).

Metatarsal thickness of the hind paws contralateral to PBS and CFA injections were not significantly different from the PBS injected paws at any of the four time points. Metatarsal thickness was increased significantly ($p < 0.001$) in the hind paws ipsilateral to CFA injection compared to the other three groups of hind paw at all four time points

with a peak increase at 2 days (Figure 3.1C). The relative increases of the CFA-injected paw versus the PBS-injected paw were 67%, 84%, 52%, and 28%, for days 1, 2, 4, and 8, respectively.

Representative images from the DRG ipsilateral to the CFA injection after one, two, four, and eight days of inflammation showed a qualitative difference in the GLS-IR, especially after four days of inflammation (Figure 3.2, left bottom panel). The area (in μm^2) and GLS-IR (relative mean gray value) for each neuron profile were plotted on the x and y axes, respectively for each time point in the study (Figure 3.3). There did not appear to be any obvious differences in GLS-IR after one or two days of inflammation (Figure 3.3A and 3.3B). However, a robust elevation in GLS was evident after four days of inflammation (Figure 3.3C) that appeared to persist in some small neurons even after eight days of inflammation (Figure 3.3D). For a better appreciation of the GLS-IR changes, frequency distributions were made for GLS-IR (Figure 3.4). The frequency distributions of GLS-IR intensity appear similar between different groups of DRG after one and two days of inflammation (Figures 3.4A and 3.4B); whereas there is an observable "right shift" in the distribution of GLS-IR intensity in DRG ipsilateral to the CFA injection after four days of inflammation (Figure 3.4C). The GLS-IR frequency distribution in the DRG ipsilateral to CFA injection after eight days of inflammation is slightly right shifted from the frequency distributions of other DRG at this time point (Figure 3.4D). The means of the relative mean gray values for DRG contralateral to the CFA injection showed a significant increase after one day of inflammation (Figure 3.5A), but there were no significant differences after two days of inflammation (Figure 3.5B). After four days of inflammation, the GLS-IR in the DRG ipsilateral to the CFA injections

was significantly increased over all three other groups of DRG in both small and large DRG neurons (Figure 3.5C). The approximate magnitude of GLS-IR elevation in small and large neurons after four days of inflammation was similar. There was a smaller albeit significant elevation of GLS-IR in small and large neurons of the DRGs ipsilateral to the PBS injection and contralateral to the CFA injection. By eight days post injection, there was still a significant elevation of GLS-IR in the small neuron ipsilateral to the CFA injection, but there were no differences in the other groups of DRG (Figure 3.5D). GLS-IR in large neurons ipsilateral to the CFA injection was not significantly different from the three other groups of DRG after eight days of inflammation.

Discussion

Peripheral sensitization of DRG neurons during inflammation initiates a sensitizing cascade along the pain pathway resulting in the chronic pain state. Both post-translational and expression dependent mechanisms are involved in peripheral sensitization; the former for initiation of sensitization during the acute stage of inflammatory pain and the latter for maintaining the sensitization during the chronic stage (Woolf and Ma 2007). Many proteins involved in peripheral sensitization undergo both types of changes. For instance, transient receptor potential vanilloid subfamily member 1 (TRPV1) is released from phosphatidylinositol-4,5-bisphosphate inhibition (Chuang, Prescott et al. 2001) and is phosphorylated by protein kinase C (Sugiura, Tominaga et al. 2002) in the acute stage of inflammatory pain, and its synthesis increases in the chronic stage (Ji, Samad et al. 2002; Xue, Jong et al. 2007). Both mechanisms contribute to sensitization of the DRG neuron (Chuang, Prescott et al. 2001; Sugiura, Tominaga et al. 2002) and behavioral hyperalgesia (Ji, Samad et al. 2002; Ferreira, da Silva et al. 2004).

While GLS does not have a phosphorylation site, its activity can be modulated by allosteric factors such as calcium and inorganic phosphate (Kvamme, Torgner et al. 2001), whose concentrations would increase in an activated peripheral or central axon terminal. For example, increased synaptic activity increases hydrolysis of ATP into ADP and inorganic phosphate and it increases calcium influx through voltage-gated calcium channels (Altier and Zamponi 2004) and members of the TRP family (Bautista, Jordt et al. 2006). Therefore, increased synaptic activity during the acute stage of inflammation could increase GLS activity and account for the elevated amounts of glutamate seen in the skin (Omote, Kawamata et al. 1998; Jin, Nishioka et al. 2006), peripheral axons (Westlund, Sun et al. 1992), and spinal cord dorsal horn within hours after the induction of inflammation (Skilling, Smullin et al. 1988; Dmitrieva, Rodriguez-Malaver et al. 2004). In the current study, however, DRG neurons also appear to increase expression of GLS and possibly transport it out of the cell body in the chronic stage of inflammation. Based on the timescale of increased GLS production, it is possible that a retrogradely transported neurotrophic factor such as nerve growth factor (NGF) is responsible for this regulation. The timescale of GLS up-regulation is similar to the up-regulation of substance P and CGRP after five days of inflammation, which was preventable with anti-NGF treatment (Donnerer, Schuligoi et al. 1992). Retrograde NGF signaling also could account for subsequent anterograde transport out of newly synthesized GLS out of the cell body via mitochondrial axonal transport (Chada and Hollenbeck 2003; Chada and Hollenbeck 2004). This type of regulation parallels the post-translational modification followed by expressional regulation dogma mentioned earlier (Woolf and Ma 2007). Moreover, NGF regulates expression of several other proteins important for nociception

(Pezet and McMahon 2006), and has the ability to affect GLS expression in DRG neurons (McDougal, Yu et al. 1981; Miller, Akesson et al. 1999; Miller, Caire et al. 2001) and retina (Tomita, Ishiguro et al. 1999).

Glutamate is implicated not only as a neurotransmitter released by nociceptive peripheral axon terminals but also as a sensitizer of these terminals. Injecting glutamate or glutamate receptor agonists sensitize nociceptors in *ex vivo* (Du, Koltzenburg et al. 2001) studies and causes hyperalgesia *in vivo* in rodents (Carlton, Hargett et al. 1995; Jackson, Graff et al. 1995; Carlton, Zhou et al. 1996; Zhou, Bonasera et al. 1996; Davidson, Coggeshall et al. 1997; Lawand, Willis et al. 1997; Carlton, Zhou et al. 1998; Carlton and Coggeshall 1999; Giovengo, Kitto et al. 1999; Bhave, Karim et al. 2001) and humans (Gazerani, Wang et al. 2006). The role of glutamate in mediating hyperalgesia during inflammation is evidenced by high glutamate levels in inflamed tissues (Nordlind, Johansson et al. 1993; Lawand, McNearney et al. 2000) and the attenuation of hyperalgesia with glutamate receptor antagonists in inflammatory animal models (Jackson, Graff et al. 1995; Lawand, Willis et al. 1997; Bhave, Karim et al. 2001; Du, Zhou et al. 2003) and burn injury in humans (Warncke, Jorum et al. 1997). Glutamate may exacerbate the neurogenic component of inflammation by further activation of SP and SP and CGRP release (Yu, Sessle et al. 1996). The numbers of glutamate receptors on peripheral axons also increases during inflammation (Carlton and Coggeshall 1999; Du, Zhou et al. 2003), which could lead to an escalating cycle wherein the peripheral terminals are able to maintain their own sensitization and exacerbate chronic pain (Carlton 2001). Similarly, glutamate is involved in sensitization of dorsal horn neurons to afferent stimulation (Dougherty and Willis 1991; Dougherty, Palecek et al. 1993; Hu,

Alter et al. 2007; Pezet, Marchand et al. 2008). The presence of glutamate receptors on central axon terminals (Liu, Wang et al. 1994) could enhance central glutamate release via a positive feedback mechanism. Therefore, increased glutamate production may be involved in both peripheral and central sensitization mechanisms that culminate in chronic pain.

Since GLS is only one of many proteins involved in the glutamate-glutamine cycle, other proteins within the cycle may need to increase their activities and/or expressions in order to effectively increase the flux of glutamate through the cycle. Although many of these proteins have at least been localized to the DRG and peripheral nerve, very little is known about the glutamate-glutamine cycle during inflammation. The neuronal glutamate transporter responsible for reuptake of glutamate, excitatory amino acid transporter 3 (EAAT3), localizes to primarily small diameter DRG neurons (Tao, Liaw et al. 2004) and the glial glutamate transporter, EAAT1, localizes to satellite glial cells of the DRG (Berger and Hediger 2000). Glutamine synthetase, the glial enzyme that converts glutamate to glutamine, not only serves as a specific marker for satellite glial cells in the rat DRG (Miller, Richards et al. 2002) and mouse trigeminal ganglia (TG) (Weick, Cherkas et al. 2003; Hanani 2005), but increases along with glutamine in satellite glial cells after inflammation (Miller and Kriebel 2003). Increases in GS and glutamine concur with the notion that multiple glutamate-glutamine cycle proteins and substrates increase in response to inflammation. Little is known concerning glutamine transporters in the DRG, but we have detected sodium-coupled neutral amino acid transporters (SNAT) 1 (Miller, Kriebel et al. 2005) and 2 (unpublished results) in DRG neurons. Vesicular glutamate transporters (VGLUTs) are necessary at sites of glutamate

neurotransmission and VGLUT1 and 2 localize to different size classes of DRG (Morris, Konig et al. 2005; Brumovsky, Watanabe et al. 2007) and TG (Li, Xiong et al. 2003) neuron cell bodies in addition to the peripheral (Nunzi, Pisarek et al. 2004; Brumovsky, Watanabe et al. 2007) and central (Li, Fujiyama et al. 2003; Morris, Konig et al. 2005) terminals. Regulation of VGLUT1 and 2 levels at the cell body occurs after peripheral axotomy (Brumovsky, Watanabe et al. 2007) and VGLUT2 expression appears to regulate glutamate release during neuropathic pain (Moechars, Weston et al. 2006). However, information about alterations of VGLUT during inflammation is lacking. We hypothesize that post-translational and/or expression dependent mechanisms may act on some or all of the aforementioned proteins to increase glutamate production during inflammation and contribute to peripheral and central sensitization. Support for this hypothesis comes from the observations that pharmacological intervention of GLS with an irreversible inhibitor at the peripheral terminal (Miller, Herzog et al. 2006) or glutamine transporter (Chiang, Li et al. 2008) and GS (Chiang, Wang et al. 2007) inhibition at the central terminals and second order neurons in dorsal horn provide analgesia during inflammation.

The present results indicate that an increase in GLS production occurs during the chronic stage of inflammatory pain. Further study of glutamate-glutamine cycle proteins both peripherally and centrally during inflammation is necessary to fully understand the role glutamate metabolism plays in peripheral and central sensitization. It is expected that such knowledge of glutamate metabolism will provide useful targets for chronic pain.

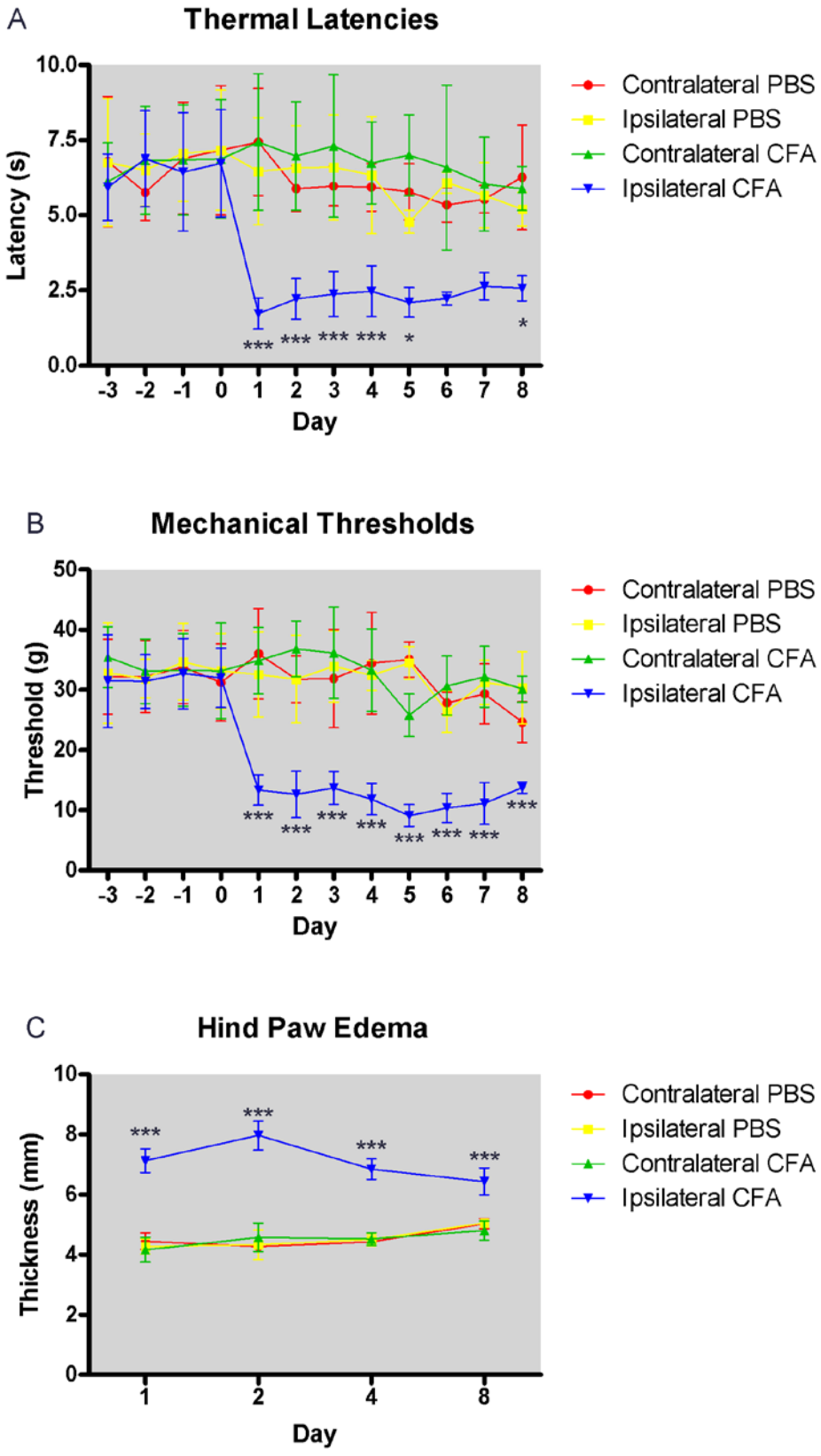
A
Thermal Latencies
Latency (s)
10.0
7.5
5.0
2.5
0.0
-3 -2 -1 0 1 2 3 4 5 6 7 8
Day
*** *** *** *** * *
Contralateral PBS
Ipsilateral PBS
Contralateral CFA
Ipsilateral CFA
B
Mechanical Thresholds
Threshold (g)
50
40
30
20
10
0
-3 -2 -1 0 1 2 3 4 5 6 7 8
Day
*** *** *** *** *** *** *** ***
Contralateral PBS
Ipsilateral PBS
Contralateral CFA
Ipsilateral CFA
C
Hind Paw Edema
Thickness (mm)
10
8
6
4
2
0
1 2 4 8
Day
*** *** *** ***
Contralateral PBS
Ipsilateral PBS
Contralateral CFA
Ipsilateral CFA

Figure 3.1. Thermal latencies , mechanical thresholds , and metatarsal thicknesses from rat hind paws after injection with PBS or CFA on day 0. Injection of CFA caused significant decreases in thermal latencies (A) for days 1 through 4 and mechanical thresholds (B) for days 1 through 8. Thermal latencies appeared to be decreased for days 5 through 8, but significance could not be shown with sample sizes of n = 3 for PBS and n = 5 for CFA. Behavioral data from all four sets were combined; therefore, the number of rats contributing data declines as the study progressed. Edema measurements (C) for each time point consist of 3 PBS-injected rats and 5 CFA-injected rats. There was always a significant increase in edema in the CFA-injected hind paw, with peak swelling occurring after two days of inflammation. Data are graphed as means (±SD). *$p < 0.05$, **$p < 0.01$, ***$p < 0.001$.

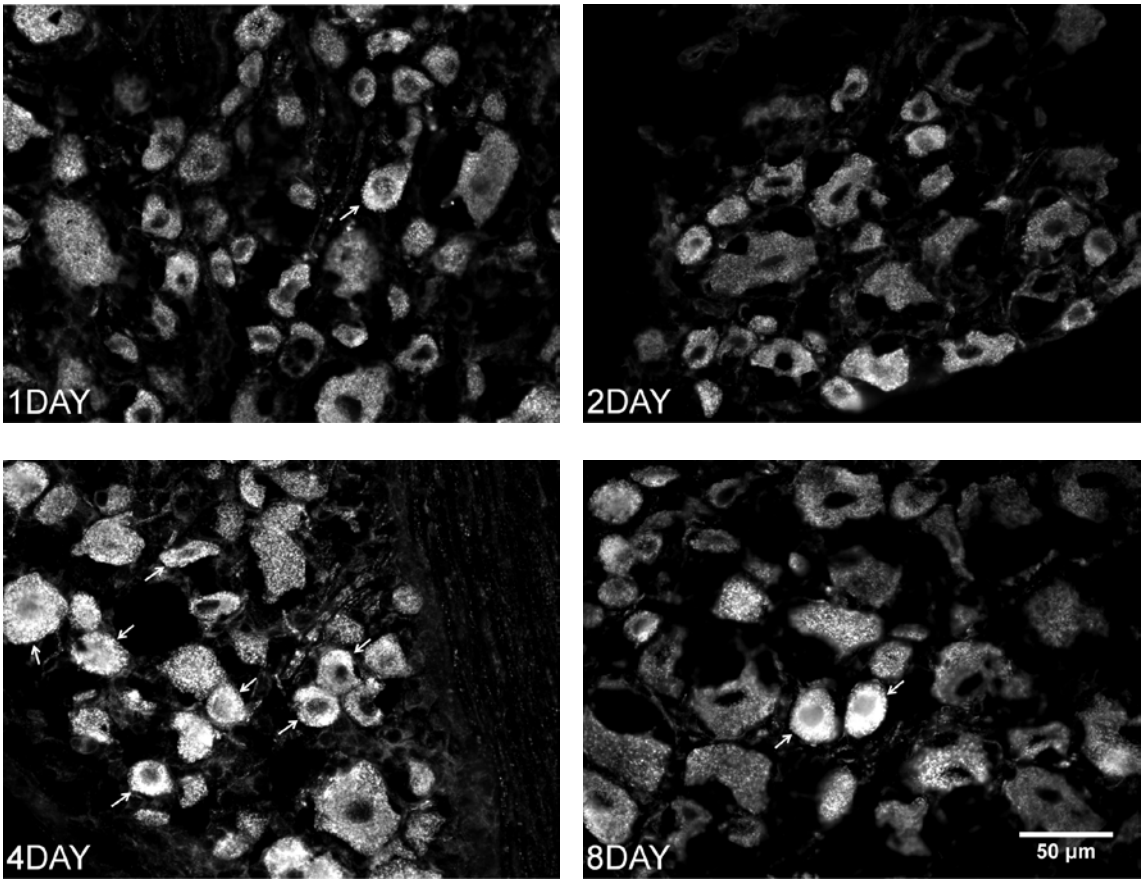

Figure 3.2. Representative images of GLS immunofluorescence of L4 DRG neurons ipsilateral to the CFA-injected hind paw after one, two, four, and eight days of inflammation. Very few neurons had high GLS-IR after one and two days of inflammation (arrows). However, after four days of hind paw inflammation GLS-IR in many neurons increased (arrows). After eight days of inflammation GLS-IR was still elevated in some small neurons (arrows).

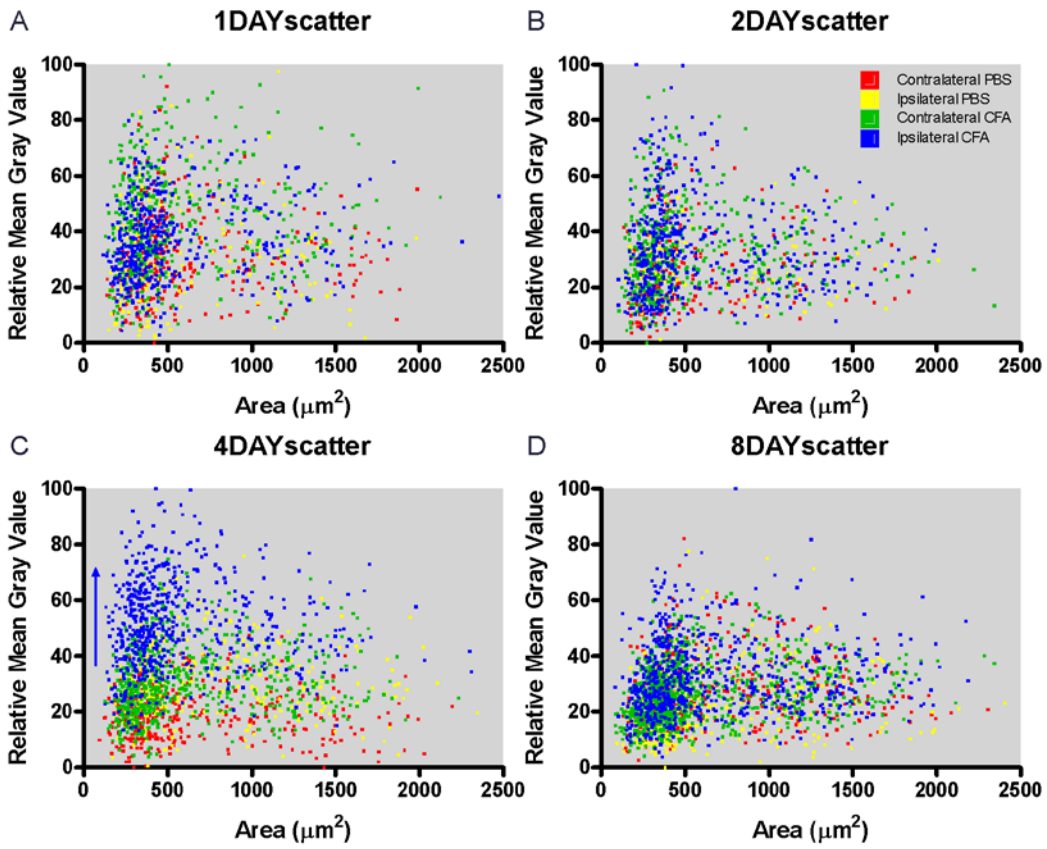

Figure 3.3. Scatter plots of the GLS-IR as relative mean gray values (y-axis) and the cell size in square microns (x-axis). Each point represents a single neuron profile after one (A), two (B), four (C), or eight (D) days of inflammation. The different types of DRG are indicated by color. Plots for different types of DRG look similar after one and two days of inflammation. Elevation of GLS-IR intensities is apparent after four days of inflammation in cells of all sizes from the DRG ipsilateral to CFA injection. After eight days of inflammation, some small DRG neurons still have elevated GLS-IR.

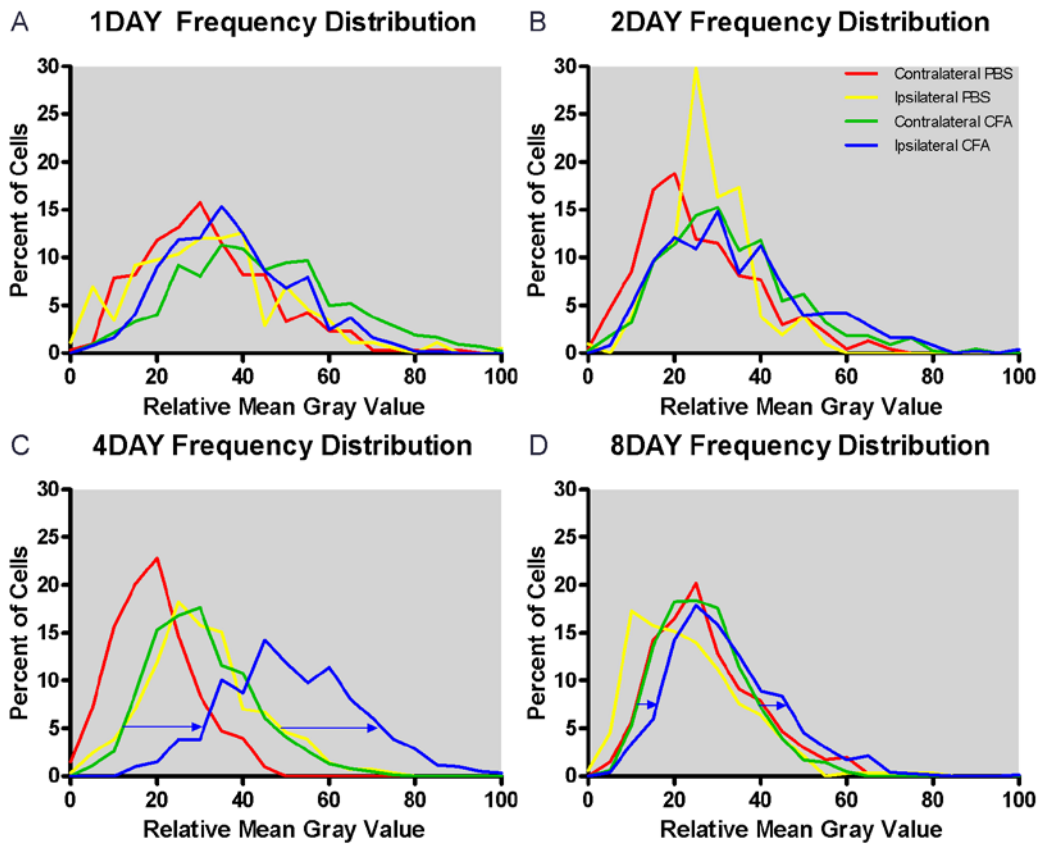

Figure 3.4. Frequency distributions for GLS-IR in L4 DRG neurons after hind paw inflammation. There was a subtle shift to the right in the frequency distribution for DRG neurons contralateral to the CFA injection after one day of inflammation. After four days of inflammation, there was a right shift of the GLS-IR frequency distributions for the DRG neurons ipsilateral to the PBS injection and contralateral to the CFA injection as compared to the DRG neurons contralateral to the PBS injection. In addition, there was a larger shift to the right in the frequency distribution for the neurons ipsilateral to the CFA injection at the four day time point. After eight days of inflammation, there was only a slight right shift of the frequency distribution for the DRG neurons ipsilateral to the CFA injection.

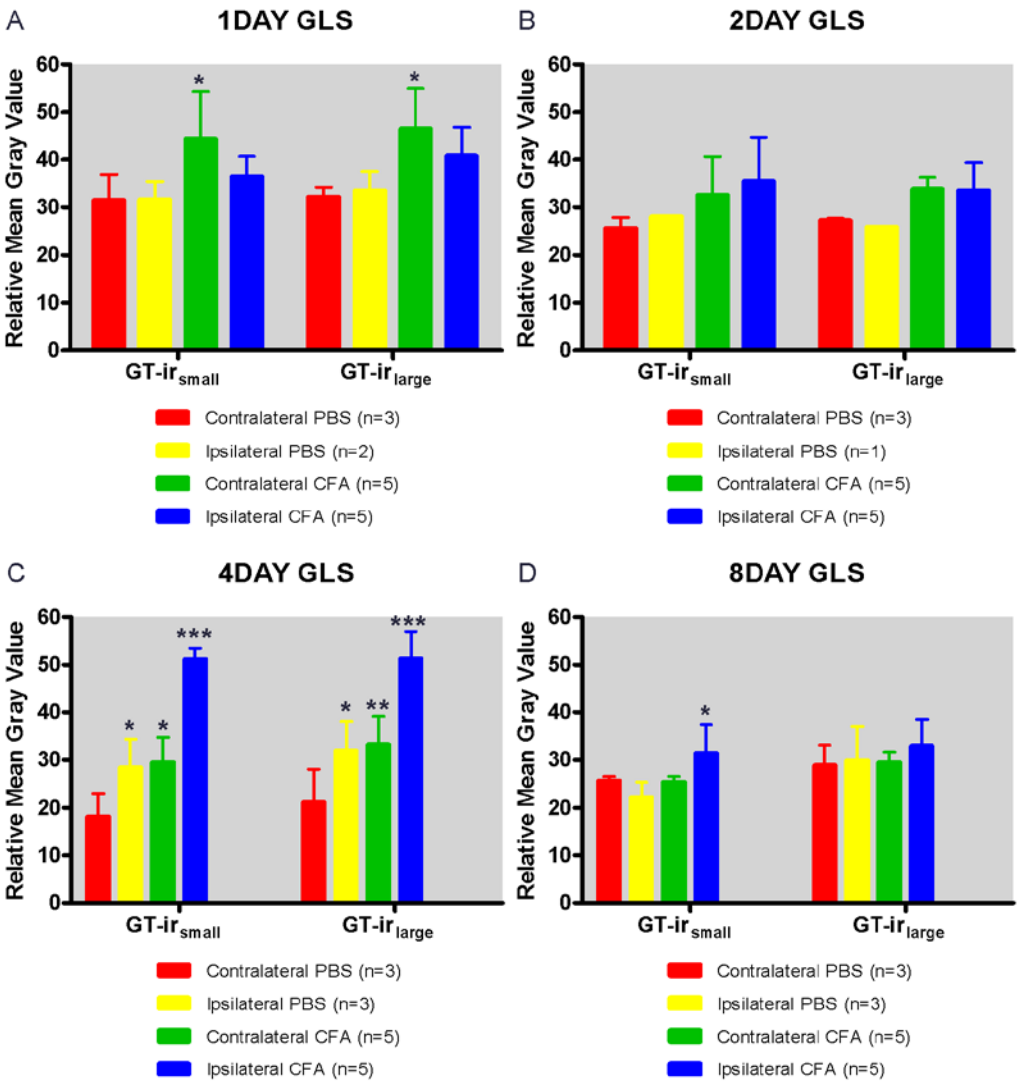

Figure 3.5. Mean GLS-IR in small and large L4 DRG neurons after hind paw inflammation. The means of the relative mean gray values for DRG contralateral to the CFA injection showed a significant increase after one day of inflammation (A), but there were no significant differences after two days of inflammation (B). After four days of inflammation, the GLS-IR in the DRG ipsilateral to the CFA injections was significantly increased over all three other groups of DRG in both small and large DRG neurons (Figure 5C). By eight days post injection, there was still a significant elevation of GLS-IR in the small neurons ipsilateral to the CFA injection (D).

CHAPTER 4

Effect of nerve growth factor deprivation on dorsal root ganglion glutaminase and $Na_v1.8$ expression

Abstract

Nerve growth factor (NGF) levels are elevated during inflammation, which increases sensitivity of nociceptive nerve fibers innervating inflamed tissue. Antagonism of NGF is gaining support as a novel therapy for inflammatory and neuropathic pain. The most effective NGF antagonists to date are anti-NGF antibodies, which are presumed to sequester endogenous NGF and prevent its interaction with NGF receptors. Autoimmunization with NGF is a useful experimental model for studying the effects of chronic, steady levels of anti-NGF antibodies. High serum anti-NGF levels were previously correlated with hypoalgesia after NGF autoimmunization, but the mechanism was not determined. In the present study, we studied this mechanism by immunizing rats against NGF and evaluating their sensory sensitivity, serum anti-NGF levels, degree of NGF deprivation as indicated by sympathetic ganglion atrophy, and two markers of dorsal root ganglion (DRG) neuron function: glutaminase (GLS) and voltage-gated sodium channel 1.8 ($Na_v1.8$). All DRG neurons express the enzyme GLS for making the neurotransmitter glutamate, while only nociceptive DRG neurons express $Na_v1.8$. Impairment of GLS expression could, therefore, reduce fidelity of DRG neuron communication with the central nervous system for all sensory modalities, while

decreased $Na_v1.8$ expression would only affect nociception. We found that NGF deprivation decreased sensitivity to pain and decreased basal $Na_v1.8$ expression in a subpopulation of nociceptive DRG neurons, but it did not affect basal GLS expression in these neurons or other sensory modalities. We conclude that the mechanism of hypoalgesia during NGF deprivation does not involve decreased GLS expression, but may involve decreased $Na_v1.8$ expression.

Introduction

Nerve growth factor (NGF) is produced by peripheral tissues and influences the function of afferent and autonomic nerve fibers innervating these tissues. Inflammation increases production of NGF (Woolf, Safieh-Garabedian et al. 1994; Sivilia, Paradisi et al. 2008), which in turn sensitizes nociceptive afferents through post-translational and expression dependent mechanisms (Pezet and McMahon 2006). Therefore, antagonizing NGF has become a research focus for treatment of inflammatory pain (Hefti, Rosenthal et al. 2006; Watson, Allen et al. 2008). Although small molecule NGF receptor antagonists have been developed (Owolabi, Rizkalla et al. 1999; Colquhoun, Lawrance et al. 2004), antibodies against NGF remain the most effective means of blocking NGF-induced changes in nociceptors (Koltzenburg, Bennett et al. 1999; Covaceuszach, Cattaneo et al. 2005; Sevcik, Ghilardi et al. 2005; Hefti, Rosenthal et al. 2006; Abdiche, Malashock et al. 2008). Administering anti-NGF antibodies systemically (Ma and Woolf 1997) or locally (Bennett, Koltzenburg et al. 1998; Gould, Gould et al. 2000; Djouhri, Dawbarn et al. 2001) at the site of inflammation attenuates nociceptor sensitization and provides analgesia in animal inflammatory pain models (McMahon 1996).

Autoimmunization against NGF is an effective experimental model for studying the effects of NGF deprivation on peripheral neurons. Sympathetic neurons, which rely on continual NGF release from their peripheral targets, undergo severe atrophy after NGF autoimmunization (Otten, Goedert et al. 1979; Gorin and Johnson 1980; Johnson, Gorin et al. 1982). Sensory neurons in the adult dorsal root ganglion (DRG) undergo slight atrophy and have decreased expression of specific proteins like SP and the voltage-gated sodium channel $Na_v1.8$ (Schwartz, Pearson et al. 1982; Fjell, Cummins et al. 1999). NGF autoimmunization leads to sympathectomy (Gorin and Johnson 1979; Otten, Goedert et al. 1979) and hypoalgesia (Chudler, Anderson et al. 1997), which are symptoms similar to those of humans affected by congenital insensitivity to pain with anhydrosis (CIPA) where the high affinity NGF receptor TrkA is mutated (Indo 2001). Sympathectomy is due to severe atrophy of autonomic neurons, whereas the mechanism underlying hypoalgesia is less clear. Aside from being required for survival of sensory neurons during development, NGF plays a role in regulating normal sensitivity of nociceptors (McMahon, Bennett et al. 1995; McMahon 1996; Bennett, Koltzenburg et al. 1998), which still express TrkA in adulthood (McMahon, Armanini et al. 1994; Phillips and Armanini 1996). This is thought to occur by regulating basal expression of proteins important for nociception, such as SP and calcitonin gene-related peptide (CGRP), which contribute to edema and vasodilation (Pezet and McMahon 2006).

All DRG neurons use the neurotransmitter glutamate for release from central terminals onto second order sensory neurons in the spinal cord dorsal horn (Merighi, Polak et al. 1991; Zahn, Sluka et al. 2002) and medullary dorsal column nuclei (De Biasi and Rustioni 1990; Giuffrida and Rustioni 1992). Glutaminase (GLS) is the neuronal

enzyme that converts glutamine into glutamate and all DRG neurons express this enzyme (Miller, Douglas et al. 1993; Li, Ohishi et al. 1996). In addition to SP and CGRP, nociceptors also have the ability to release glutamate at their peripheral terminals (Omote, Kawamata et al. 1998; deGroot, Zhou et al. 2000; Carlton 2001; Jin, Nishioka et al. 2006; Brumovsky, Watanabe et al. 2007). If GLS expression is decreased in nociceptors, then both peripheral and central glutamatergic transmission may be affected, which could lead to decreased fidelity of nociceptive transmission.

$Na_v1.8$ is exclusively expressed in nociceptive DRG neurons (Djouhri, Fang et al. 2003), and $Na_v1.8$ mRNA expression as well as current density are decreased after NGF deprivation via autoimmunization (Fjell, Cummins et al. 1999). The aim of the current study was to determine if there is a change in GLS or $Na_v1.8$ expression in nociceptive DRG neurons after NGF deprivation via autoimmunization. Immunization effectiveness was evaluated by obtaining serum anti-NGF titers. Deprivation of NGF was confirmed by observing superior cervical ganglion (SCG) morphology. Previous anti-NGF studies (Chudler, Anderson et al. 1997) had only examined hot plate responses, so we used additional sensory tests to better determine the behavioral effects of NGF deprivation.

Methods

Sprague-Dawley rats (n = 31) were housed on a 12 hour light: 12 hour dark cycle and given free access to food and water. Procedures were conducted according to guidelines from the International Association for the Study of Pain (Zimmermann 1983) and were approved by the Oklahoma State University Center for Health Sciences Institutional Animal Care and Use Committee. All appropriate efforts were made to minimize the number of animals used in this study.

To determine the effect of immunization on behavioral responses, the proportion of rats expected to have high anti-NGF titer, and the duration of antibody production, 12 rats were immunized against cytochrome C, and their behavioral responses and antibody titers were compared to naïve rats (n = 3). To determine the effects of NGF deprivation, rats in a second experiment were randomly assigned to either the control/cytochrome C group (cytC; n=6) or experimental/NGF group (n=10). At six weeks of age, rats in both experiments were immunized with the appropriate antigen: cytochrome C from horse heart (Sigma) or 2.5S NGF from mouse submandibular gland (Affinity BioReagents). Each rat was anesthetized with isoflurane prior to giving four dorsal paraspinal subcutaneous injections (~25 µL each) of antigen in complete Freund's adjuvant (CFA; Sigma); the total initial immunization dose for each rat was 20 µg in 100 µL CFA. At ten weeks of age, rats were given a booster immunization with the appropriate antigen using the same injection method used for the initial immunization; the total booster immunization dose for each rat was 50 µg in 100 µL CFA.

Antibody titer measurements were obtained from serum and cerebrospinal fluid (CSF) samples using an enzyme-linked immunosorbant assay (ELISA). For serum collection, rats were anesthetized with isoflurane and laid on a heating pad to aid in vasodilatation. A 26G needle attached to a syringe with the plunger removed was used to collect ~150 µL of blood from one of the lateral tail veins (Brown 2006). Whole blood was incubated at 37°C for one hour to aid clotting and then stored overnight at 4°C. The sample was centrifuged at 10,000 × *g* for 15 minutes at 4°C to dislodge the clot. Serum (~50 µL) was collected from the top of the supernatant. The following dilutions of serum were made in PBS-Tween (100 mM sodium phosphate, 150 mM sodium chloride, 0.05%

(v/v) Tween-20, pH 7.2): 1:2000, 1:4000, 1:8000, 1:16000, 1:32000, 1:48000, 1:64000, 1:96000. Multi-well plates were coated with 2 µg/mL of appropriate antigen (cytC or NGF) diluted in 50 mM sodium carbonate buffer, pH 9.6 overnight at 4°C. Wells were rinsed three times for five minutes with PBS-Tween. Wells were blocked with 5% (v/v) normal goat serum in PBS-Tween for one hour at room temperature. Dilutions of sera were applied and incubated for one hour at 37°C. Wells were rinsed three times for five minutes with PBS-Tween and incubated for one hour at 37° in horseradish peroxidase-conjugated goat anti-rat (Sigma) diluted 1:1000 in PBS-Tween. Wells were rinsed three more times with PBS-Tween before adding 100 µL 0.04% (w/v) *o*-phenylenediamine (OPD) in 50 mM phosphate-citrate buffer, pH 5.0 containing 0.012% (v/v) hydrogen peroxide. The OPD reaction was stopped with 50 µL 2.5 N sulfuric acid. The reaction product was measured by determining the absorption at 492 nm. Titer was determined as the most dilute sera that gave an absorbance reading at least twice that of pre-immune serum samples from each rat taken at 5 weeks of age. Sera of rats in the first experiment (n=15) were measured at 8, 11, 12, 13, and 14 weeks of age. Sera of rats in the second experiment (n=16) were measured at 11, 12, and 14 weeks of age, and CSF was measured only at 14 weeks of age from high titer NGF and cytC rats. Cerebrospinal fluid was sampled immediately prior to tissue collection by surgically revealing the dura mater over cisterna magna in anesthetized rats and piercing it with the collection needle to avoid contamination with blood. Additional controls performed with each ELISA include: minus antigen control, minus primary control, and minus secondary control.

Behavioral studies were performed to determine if sensory thresholds were affected by immunization with cytC or NGF as previously reported (Otten, Ruegg et al. 1982;

Chudler, Anderson et al. 1997). Four different tests were used: thermal latency, mechanical threshold, hot plate, and tail flick. Thermal latencies and mechanical thresholds were assessed at 5, 9, 11, 12, and 14 weeks of age by measuring each hind paw three times with at least 10 minutes between measurements. Thermal latencies were measured with the Plantar Test apparatus (Ugo Basile) set at 55 mW/cm^2. Mechanical thresholds were measured with the Dynamic Plantar Aesthesiometer apparatus (Ugo Basile) set to apply a maximum force of 50 g at a ramp rate of 5 g/sec. The hot plate test was performed at 11, 12, 13, and 14 weeks of age by measuring the response time to lick a hind paw with at least 10 minutes between the three measurements from each rat. The Model 39D Analgesia Meter hot plate (IITC) was set at 52°C. The tail flick test was performed only at 14 weeks. Tails were blackened with ink and tested three times with a Tail Flick Analgesia Meter apparatus (IITC).

At 14 weeks of age, rats in the second experiment (n=16) were anesthetized with Avertin and xylazine and transcardially perfused with 75 mL calcium-free Tyrode's solution followed by 300 mL 1.0% (w/v) formaldehyde, 0.8% (w/v) picric acid in 0.1 M sodium phosphate buffer. SCG and the fifth lumbar (L_5) DRG were removed and post-fixed in the same fixative overnight at 4°C. Ganglia were cryopreserved in antifreeze solution (Hoffman and Le 2004) and stored at -20°C. Prior to sectioning, they were rinsed for three days in 25% (w/v) sucrose in 0.01 M phosphate buffered 0.9% (w/v) saline (PBS). One DRG and one SCG from each rat were used for immunofluorescence. All DRG were embedded in a frozen block and all SCG were embedded in a second frozen block. Both blocks were sectioned at 14 µm on a Microm HM 550 OMVP cryostat (Richard Allan Scientific). Sections were dried at 37° for one hour and rinsed

three times with PBS. After blocking in 10% (v/v) normal goat serum, 2% bovine serum albumin, 2% polyvinylpyrolidone in PBS with 0.2% (v/v) Triton X-100 (PBS-T), sections were incubated for four days at 4°C in primary antisera diluted in PBS-T. Sections of DRG were incubated in either rabbit anti-GLS (gift of N. Curthoys at Colorado State University) diluted to 1:10000 or rabbit anti-$Na_v1.8$ (Sigma) diluted to 1:4000 while SCG sections were incubated with rabbit anti-tyrosine hydroxylase (TH) diluted to 1:1000 (Chemicon). Sections were rinsed three times in PBS before incubating in 1.0 µg/mL biotinylated goat anti-rabbit IgG (Vector Laboratories) diluted in PBS-T for one hour at room temperature. Sections were rinsed twice in PBS and once in sodium carbonate buffered saline, pH 9.6 (SCBS) before incubating for one hour in 1.0 µg/mL avidin-FITC diluted in SCBS. Sections were rinsed three times in PBS and then incubated for 30 minutes at room temperature in 0.5 µg/mL AlexaFluor 568-conjugated isolectin B4 and 300 mM DAPI diluted in PBS with 1 mM $CaCl_2$. After three more PBS rinses, coverslips were apposed with ProLong Gold (Invitrogen).

Images were acquired on a BX51 epifluorescence microscope (Olympus) using a SPOT RT740 camera (Diagnostic Instruments). An exposure and gain combination was determined empirically for each antigen in which the dimmest regions of tissue could be discerned visually for tracing, but the brightest regions were not oversaturated. Three fields of view were captured randomly from each section of each DRG using filters for FITC, AlexaFluor 568, and DAPI. All nucleated cells were analyzed in ImageJ (National Institutes of Health) by using the freehand selection tool to identify the cytoplasm of each neuron as regions of interest. Once all ROIs for a given image were selected and added to the ROI manager, measurements for each cytoplasmic profile from the FITC and

AlexaFluor 568 images were exported to a spreadsheet for statistical analysis (Hoffman and Miller 2008).

GraphPad Prism version 5.01 was used to make graphs and perform statistical tests. Significant effects of NGF deprivation (5 high anti-NGF rats vs. 5 low anti-NGF rats vs. 6 cytC rats) on thermal latencies, mechanical thresholds, hot plate responses, and immunofluorescence were determined with two-way ANOVA's with post-hoc Bonferroni tests for multiple comparisons. Differences in tail-flick responses were determined with one-way ANOVA with post-hoc Bonferroni test for multiple comparisons. Graphs display means with error bars representing standard error of the mean (SEM). P values less than 0.05 were considered significant.

Results

The first experiment provided needed information about the duration and magnitude of immunologic response to the immunization protocol used (Figure 4.1A). Of the 12 rats immunized against cytC, four were put in a low titer group because their titers were 0 one week after the booster immunization. Their titers eventually started to rise at 12 weeks, but never got higher than 16000. Three rats were put in a medium titer group because they had positive serum titers at week 11, but had not reached 96000 by week 12. The remaining five rats were considered high titer, because they all reached a titer of 96000 by week twelve and maintained it through week 14. Naïve rats never showed a positive titer. No significant differences in behavioral responses were noted between rats of different groups (data not shown). Since cytC and 2.5S NGF are similar in molecular weight, we predicted a comparable immune response to NGF. Power analysis of behavioral data from the first experiment indicated that at least four high anti-NGF titer

rats would be needed for 80% power (beta = 0.2). In order to have enough rats with high anti-NGF titer, we immunized ten rats against NGF. We determined to measure expression of GLS and $Na_v1.8$ after three weeks of exposure to high amounts of anti-NGF by letting the rats of the second experiment survive until they were 14 weeks old since anti-cytC titers remained elevated at 14 weeks in the first experiment.

Rats immunized against cytC for the second experiment did not show the same magnitude of response as the rats in the first experiment did; however, all but one rat did have a positive titer for anti-cytC antibodies (Figure 4.1B). The responses to NGF immunization were split into high and low titer groups (Figure 4.1B). Five rats were considered high titer, because they had titers of 96000 by 12 weeks and maintained the high titer to 14 weeks. The remaining five rats were put into the low titer group. All of the low titer rats had titers of 32000 or less at 14 weeks. Cerebrospinal fluid of four of the NGF immunized rats with high titer and three of the cytC immunized rats was tested for presence of anti-NGF and anti-cytC respectively. Antibody titers of cerebrospinal fluid were zero in all cases as previously reported (Chudler, Anderson et al. 1997).

The responses, in seconds and grams, respectively, increased significantly between the pre- and post-immunization periods (Figures 4.2A and 4.2B). The presence of high NGF titer had no effect on thermal latency or mechanical threshold at any of the time points tested. Rats in the high NGF titer group had significantly longer response times for the hot plate test at 11, 12, and 14 weeks, which were approximately twice as long as cytC and low NGF titer rats (Figure 4.2C). Responses of low NGF titer rats were never significantly different from cytC rats for the hot plate test. There were no differences

among the three groups for the tail flick test at 14 weeks (data not shown); the average response time was between 6 and 10 seconds for all three groups.

The size of SCG neurons was measured by examining TH-positive neuron profiles. Qualitatively, SCG neurons from all rats immunized against NGF except one showed some degree of atrophy. SCG from rats with high and low anti-NGF titers had decreased neuronal cytoplasmic area, increased number of heterochromatic nuclei (non neuronal), and neuronal cell loss (Figure 4.3). The SCG's of rats immunized against cytC had a similar morphology to the SCG's of naive rats.

DRG neuron profiles were separated into small (<600 μm^2) and large (>600 μm^2) cell size populations (Figure 4.4A). Small neurons were separated further into IB4 positive and negative populations based on a threshold set at the minimum between two peaks of a frequency distribution for IB4 intensity (Figure 4.4B). Mean gray values of the FITC image for each cell were used as a measure of IR. Mean IR's were calculated for three neuron populations (small IB4 positive, small IB4 negative, and large) for each rat. GLS-IR did not change significantly among the three groups (cytC, low NGF, high NGF) for any of the three cell populations even though there was a trend for GLS-IR to be lower in small DRG neurons of NGF-immunized rats as compared to cytC-immunized rats (Figure 4.5 and 4.7A). $Na_v1.8$-IR was significantly lower in large cells as compared to small cells of cytC and low NGF titer rats. Small IB4 negative DRG neurons from high NGF titer rats had decreased $Na_v1.8$-IR as compared to small IB4 negative DRG neurons of low NGF titer and cytC rats and small IB4 positive neurons of all three groups of rats (Figure 4.6 and 4.7B). There was no significant effect of NGF immunization on DRG neuron size for any of the three populations tested.

Discussion

The immunization protocol used in this study was very similar to that used in other studies (Doubleday and Robinson 1994; Doubleday and Robinson 1995; Chudler, Anderson et al. 1997); however, there has been little published information regarding the weekly antibody titer progression after the booster immunization. We determined immunization efficacy and temporal progression by immunizing rats against cytC and monitoring serum anti-cytC weekly after the booster immunization. A previous study indicated that approximately 25% of the rats immunized were high titer (Chudler, Anderson et al. 1997). In our experiment, 5/12 (42%) rats were high titer. As expected (Bean 2001), a peak in anti-cytC of high titer rats was observed two weeks following the booster immunization (Figure 1A) when the rats were 12 weeks old, and it remained elevated when the rats were 14 weeks old. These results prompted us to immunize ten rats against NGF in the second experiment and end the study when rats were 14 weeks old in anticipation of having at least four rats with high anti-NGF titers. Behavioral responses of naïve rats compared to rats immunized against cytC for the first experiment were not significantly different. We, therefore, decided to use cytC immunized rats as controls for the second experiment.

Five of the ten NGF immunized rats were placed into a high titer group since they had a 96000 titer at 12 weeks that remained at 14 weeks. The other five NGF immunized rats were placed in a low titer group. Antibodies for cytC and NGF were not present in the cerebrospinal fluid, which indicated that any effects of immunization were due to peripheral actions of the antibodies and were not consequences of antibody interactions with the central nervous system.

Although NGF deprivation did not significantly change thermal latencies or mechanical thresholds, both measures of sensory function were increased at 9 weeks of age and later time points as compared to responses at 5 weeks of age. This effect is likely due to the age of the rats rather than immunizations since all three groups were similarly affected. The hot plate test detected differences between the high NGF titer group but not the low NGF titer group versus the cytC group at 11, 12, and 14 weeks. This is similar to the previous study that reported hypoalgesia when using the hot plate test in adult rats immunized against NGF (Chudler, Anderson et al. 1997). Our results further support that there is a critical level of anti-NGF that needs to be present for hypoalgesia to occur, and this should be taken into consideration when evaluating cellular responses to NGF immunization. The lack of change in mechanical threshold in NGF immunized rats indicated that NGF immunization was impairing only nociception, not all sensory modalities. NGF immunization did not change responses to the tail flick test, which was only performed at 14 weeks because the tails had to be blackened with ink. This would have hindered blood collection from the lateral tail vein during the other weeks. The difference in the responses to the three thermal nociception tests (thermal latency, hot plate, tail flick) may reveal clues as to the mechanism of hypoalgesia induced by NGF deprivation. One reason for the discrepancy may be that the thermal latency test is more suited for detecting changes in hyperalgesia during inflammation than hypoalgesia (Hargreaves, Dubner et al. 1988; Le Bars, Gozariu et al. 2001). Other reasons may be that the rapid and focal radiant heating of the skin in the thermal latency and tail flick tests selectively activates Aδ fibers, whereas the hot plate test activates C fibers (Le Bars, Gozariu et al. 2001).

Morphology of SCG was used to verify NGF deprivation in rats immunized against NGF. High and low titer rats exhibited SCG neuron atrophy, whereas cytC immunized rats had SCG similar to naïve rats. The degree of atrophy was more severe in high titer NGF rats than in low titer rats. Peripheral sympathetic neurons are very dependent on NGF for maintenance and survival, which is why even the low titer NGF rats had SCG atrophy. However, levels of anti-NGF capable of depriving SCG neurons of sufficient NGF, does not affect peripheral sensory neurons (Gorin and Johnson 1980). Our results support these findings since low titer NGF animals showed no impairment of nociception but did have SCG atrophy.

Sensory neurons are only dependent on NGF for survival during development and early postnatal life (Gorin and Johnson 1979; Gorin and Johnson 1980; Johnson, Gorin et al. 1980; Miller, Akesson et al. 1999). In the adult rat, NGF levels in peripheral tissues are thought to establish the basal nociceptive threshold through regulation of proteins important for nociception, such as SP and CGRP (Pezet and McMahon 2006). Glutamate is released from both the peripheral (Omote, Kawamata et al. 1998; deGroot, Zhou et al. 2000; Jin, Nishioka et al. 2006) and central terminals (Skilling, Smullin et al. 1988; Dmitrieva, Rodriguez-Malaver et al. 2004) of DRG neurons during nociceptive stimulation. DRG neurons use GLS to convert glutamine into neurotransmitter glutamate, so a decrease in GLS expression may limit the amount of glutamate available for release by DRG neurons and decrease responses to noxious stimuli. In the present study, we studied GLS-IR in several populations of DRG neurons after NGF deprivation to determine if basal levels of NGF are necessary for normal GLS expression. We found no significant difference in the GLS-IR due to NGF deprivation, indicating that basal

GLS expression is not regulated by NGF. This finding, however, does not preclude the possibility that increased NGF, such as that produced during inflammation, may up regulate GLS expression. For instance, we found that GLS-IR is increased four days after intraplantar CFA injection (Hoffman, Edwards et al. 2007). Since inhibition of GLS has been reported to provide analgesia (Miller, Herzog et al. 2006), it would be important to know if it is among the targets regulated by elevated NGF levels during inflammation even though basal expression does not seem to be affected by decreased NGF.

The voltage-gated sodium channel $Na_v1.8$ is expressed in nociceptive neurons and influences the electrophysiological response properties of these cells (Djouhri, Fang et al. 2003). There is disagreement as to whether expression of $Na_v1.8$ is altered after inflammation, which may be dependent on the inflammatory model used. No increase in $Na_v1.8$ expression occurs 72 hours after intraplantar CFA injection or at 4 or 24 hours after NGF injection (Okuse, Chaplan et al. 1997), whereas $Na_v1.8$ is up regulated at four days after intraplantar carrageenan injection (Tanaka, Cummins et al. 1998; Black, Liu et al. 2004). Basal expression of mRNA for $Na_v1.8$ has been shown to be decreased in small diameter IB4 negative DRG neurons after NGF deprivation (Fjell, Cummins et al. 1999) and the results of the present study support these findings. The neuroanatomical marker IB4 is frequently used to distinguish two populations of nociceptive DRG neurons: peptidergic, trkA-expressing neurons (IB4-negative) from nonpeptidergic, c-Ret-expressing neurons (IB4-positive). IB4 preferentially labels nonpeptidergic neurons that respond to glial-derived neurotrophic factor (GDNF) with the c-Ret receptor. These neurons do not typically contain the peptides SP or CGRP. Nociceptive DRG neurons that do not label with IB4 respond to NGF with the trkA receptor and do contain SP and

CGRP. Similar to Fjell et al (1999), we found that the IB4-negative population of DRG neurons from rats with high anti-NGF titers had decreased expression of $Na_v1.8$, indicating that NGF may regulate basal expression of NGF through the trkA receptor. Combined with the behavioral results of this study and that of Chudler et al (1997), we conclude that normal levels of NGF in peripheral tissues determine nociceptive sensitivity, at least in part, by regulating $Na_v1.8$ expression.

One previous study showed a decrease in DRG neuron size after NGF deprivation in the adult rat (Rich, Yip et al. 1984). We found that NGF did not have a significant effect on the mean cross sectional area for any of the three populations of DRG neurons examined. Our findings support the conclusion that NGF deprivation does not cause appreciable atrophy in adult DRG neurons (Gorin and Johnson 1980; Johnson, Gorin et al. 1982; Schwartz, Pearson et al. 1982).

This study determined that basal GLS expression is not affected by NGF, but previous results indicate it may be important for inflammatory pain (Miller, Herzog et al. 2006; Hoffman, Edwards et al. 2007). $Na_v1.8$ expression was decreased in NGF deprived rats, indicating that the mechanism of hypoalgesia after NGF deprivation involves decreased expression of $Na_v1.8$. It is probable, however, that $Na_v1.8$ is not the only down-regulated protein important for nociception in these rats. Glutamate sensitizes peripheral terminals of DRG neurons (Du, Koltzenburg et al. 2001) and dorsal horn neurons in the spinal cord (Dougherty and Willis 1991; Dougherty, Palecek et al. 1993), and antagonizing glutamate receptors provides analgesia during inflammation (Jackson, Graff et al. 1995; Davidson, Coggeshall et al. 1997; Lawand, Willis et al. 1997). All DRG neurons have the enzyme GLS for making glutamate (Miller, Douglas et al. 1993;

Li, Ohishi et al. 1996), yet little attention has been given to the role of this enzyme in pain during inflammation. The mainstay of current pain medications are non-steroidal anti-inflammatory drugs (NSAIDs), which inhibit the enzymes that make prostaglandins. Glutamate levels increase during inflammation like other sensitizing molecules such as the prostaglandins. Therefore, peripheral GLS inhibition should be investigated as a potential therapeutic target for pain.

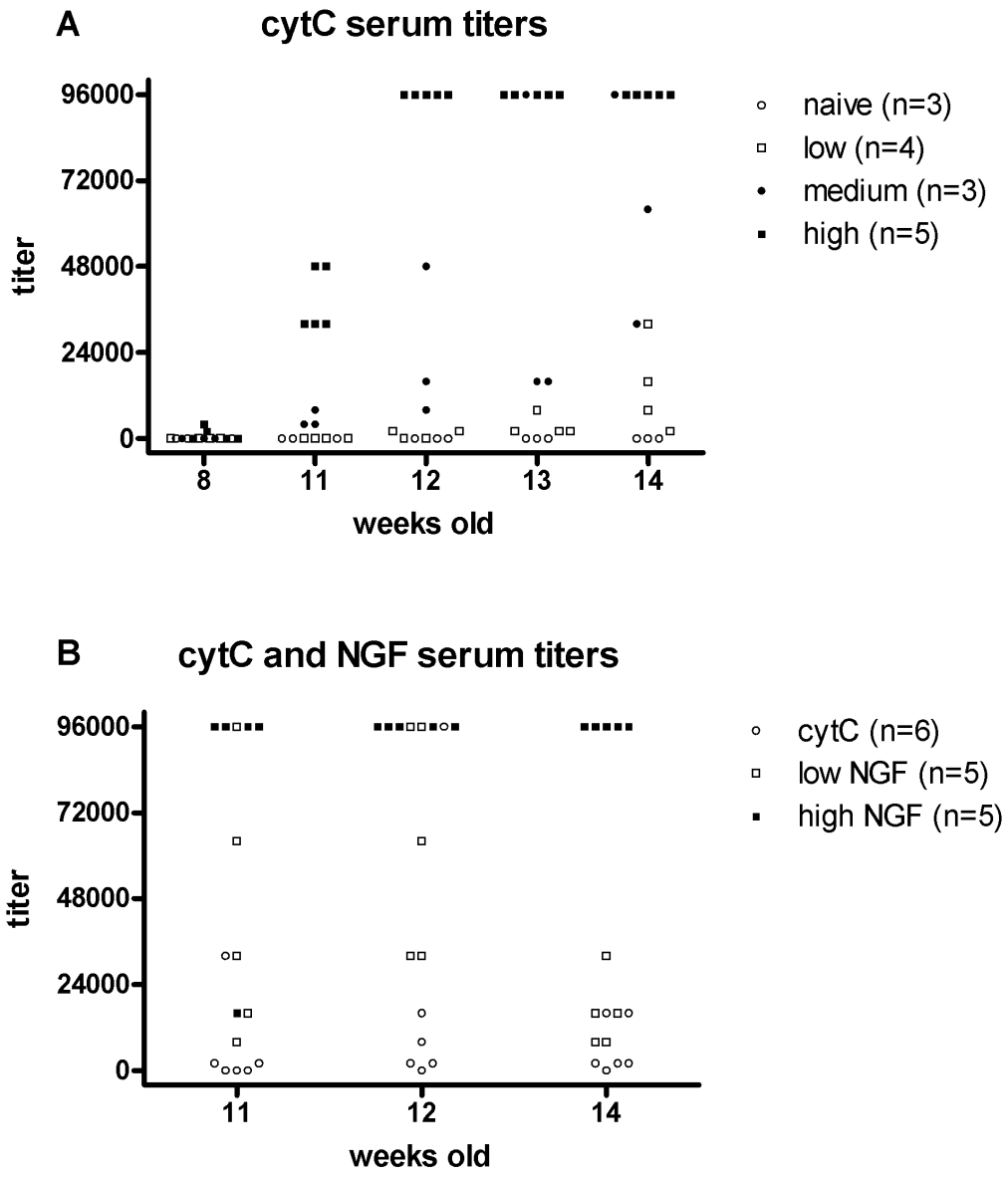

Figure 4.1. Detection of antibody titers in immunized rats. A) Serum anti-cytC titers as assessed by ELISA. Twelve rats were given an initial immunization against cytC when they were six weeks old and a booster immunization when they were ten weeks old. Immunized rats were placed into low, medium, and high titer groups. A steady increase in anti-cytC serum levels was apparent after the booster immunization. The high titer

group reached the peak titer at 12 weeks of age and maintained it through 14 weeks of age. B) Serum anti-cytC and ant-NGF titers as assessed by ELISA. Ten rats were immunized against NGF and six were immunized against cytC to serve as controls. The NGF-immunized rats were place in high and low titer groups. Anti-NGF titers increased to peak levels by 12 weeks of age and remained elevated at 14 weeks.

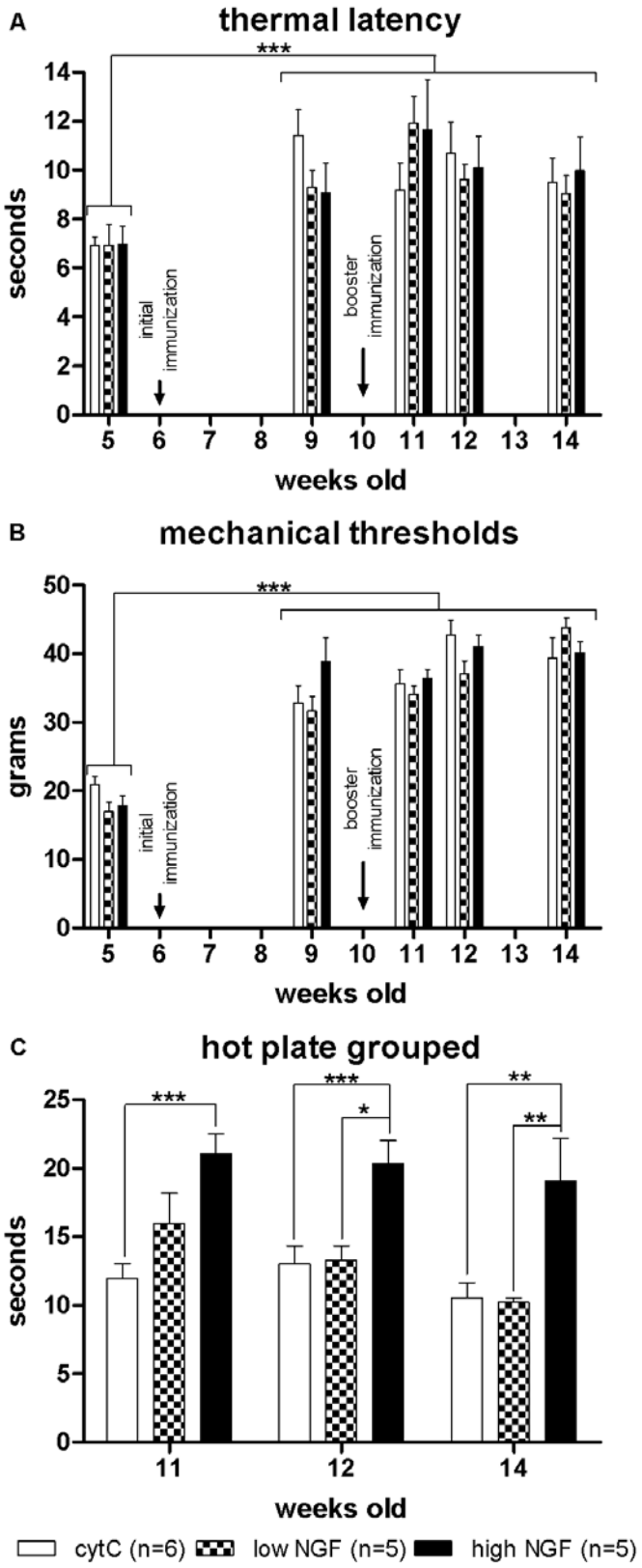
A
thermal latency
***
seconds
initial immunization
booster immunization
weeks old
B
mechanical thresholds
***
grams
initial immunization
booster immunization
weeks old
C
hot plate grouped
***
***
*
**
**
seconds
weeks old
cytC (n=6)
low NGF (n=5)
high NGF (n=5)

Figure 4.2. Sensory testing in immunized rats. A) Thermal latencies of rats immunized against cytC or NGF. Thermal latencies were longer at 9, 11, 12, and 14 weeks as compared to 5 weeks for all three groups of rats (an age effect rather than an immunization effect). Immunization with NGF had no significant effect on thermal latencies, even after the booster immunization when anti-NGF titers were highest. B) Mechanical thresholds of rats immunized against cytC or NGF. Mechanical thresholds were higher at 9, 11, 12, and 14 weeks as compared to 5 weeks for all three groups of rats. Immunization with NGF had no significant effect on mechanical thresholds, even after the booster immunization when anti-NGF titers were highest. C) Hot plate response times of rats immunized against cytC or NGF. Response times were significantly higher in rats with high anti-NGF titers as compared to cytC immunized rats at 11, 12, and 14 weeks of age. Rats with low anti-NGF titers never responded significantly different than cytC immunized rats. High titer NGF rats had significantly longer response times than low titer NGF rats at 12 and 14 weeks. *$P<0.05$; **$P<0.01$; ***$P<0.001$

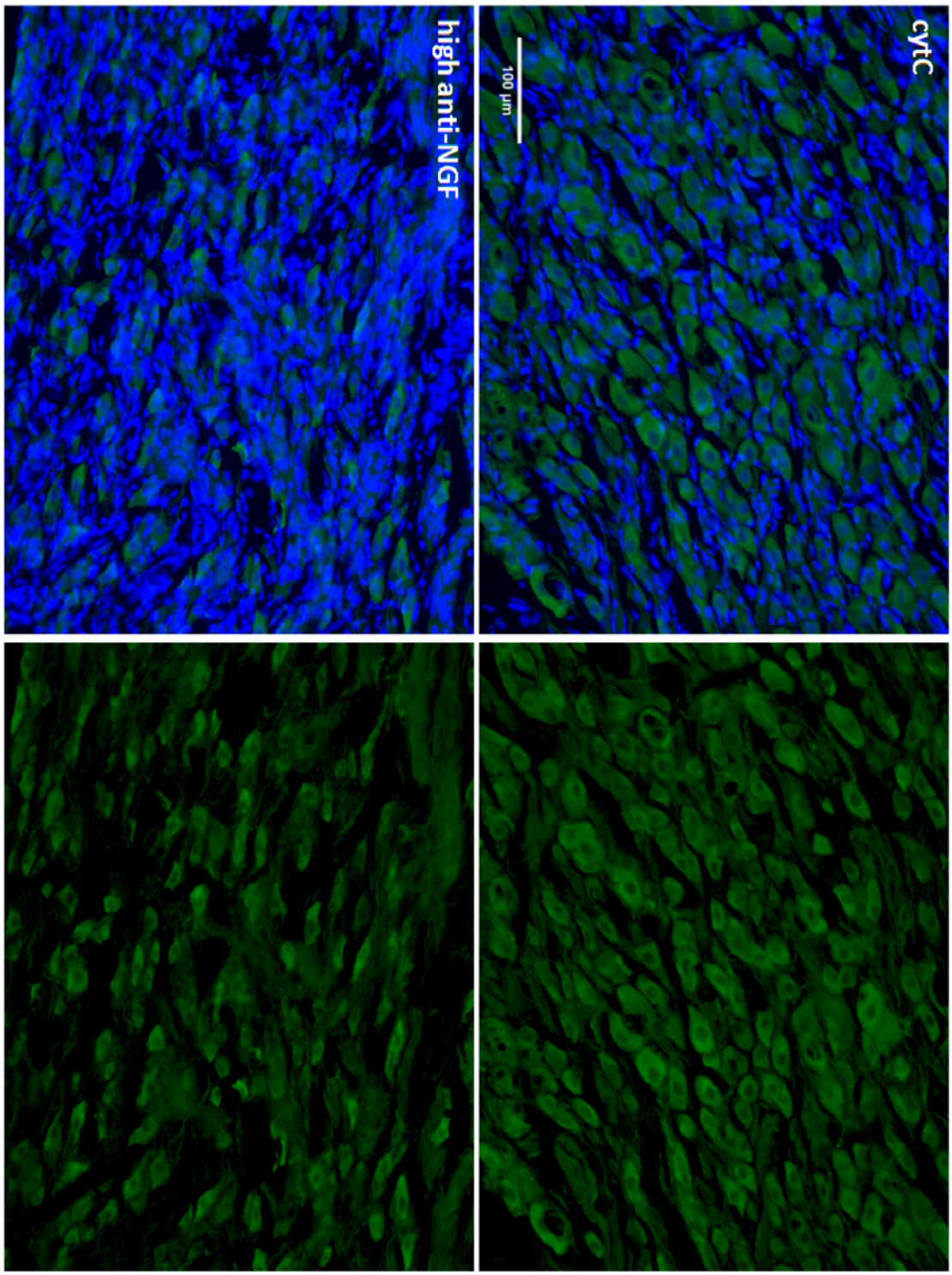

Figure 4.3. Superior cervical ganglion morphology in immunized rats. Representative images of SCG from rats immunized against cytC (upper panels) or with high anti-NGF

titers (lower panels). Immunofluorescence for TH is shown in green (right panels) and is merged with the blue DAPI image (left panels). SCG neurons from rats with high anti-NGF titers appeared atrophied as compared to SCG neurons from cytC immunized rats. There was also an increase in the number of DAPI stained nuclei in SCG from high anti-NGF titer rats.

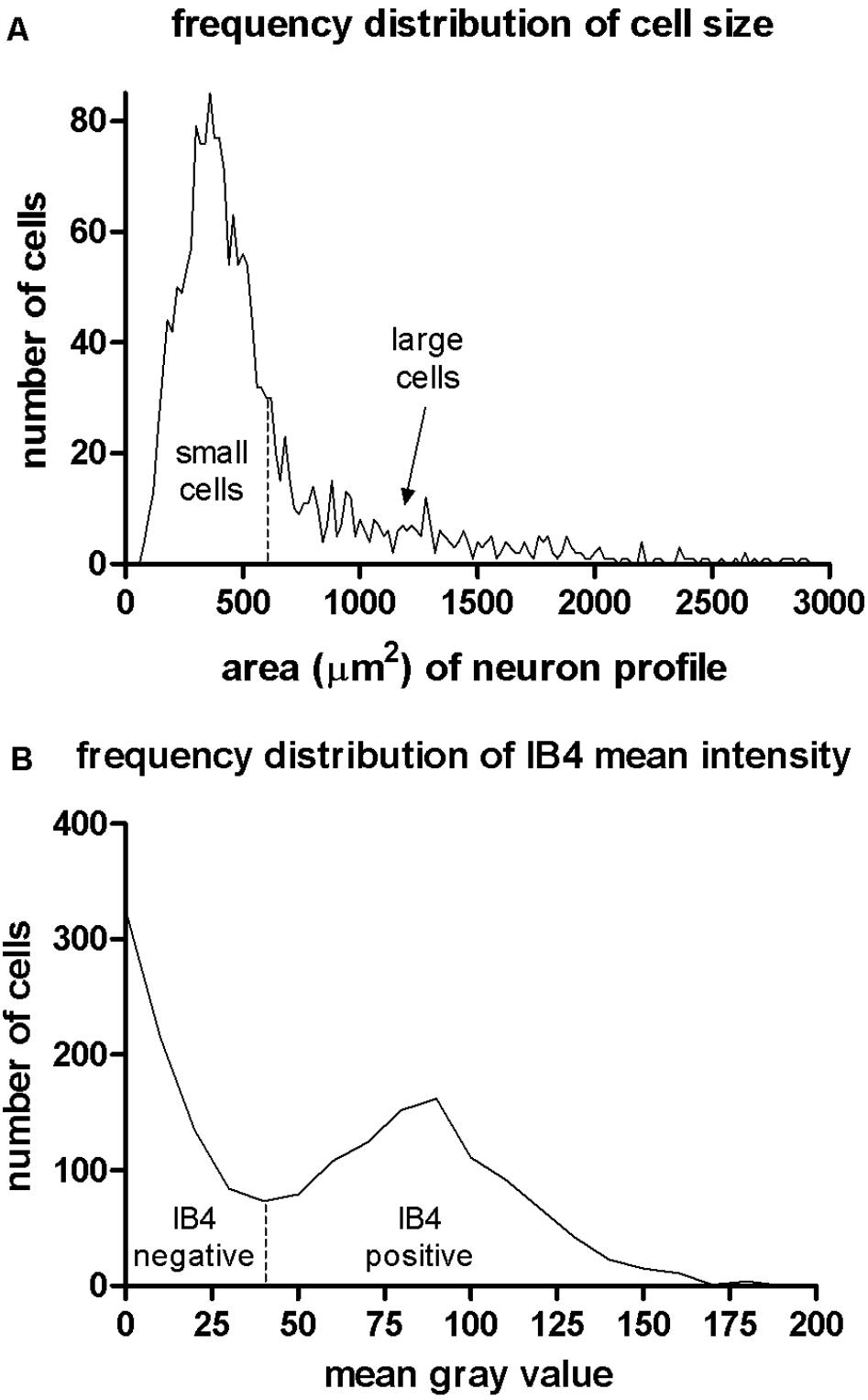
A
frequency distribution of cell size
number of cells
80
60
40
20
0
small cells
large cells
0
500
1000
1500
2000
2500
3000
area (μm2) of neuron profile
B
frequency distribution of IB4 mean intensity
number of cells
400
300
200
100
0
IB4 negative
IB4 positive
0
25
50
75
100
125
150
175
200
mean gray value

Figure 4.4. Dividing DRG neurons into subpopulations based on size and IB4 labeling. A) The frequency distribution for the cross sectional area (in μm^2) for all 1,824 cells analyzed was plotted and divided into small and large cell populations using 600 μm^2 as the dividing point. B) The frequency distribution for the IB4 labeling intensity (mean gray value from ImageJ) was plotted and a threshold was placed at the minimum between the two peaks indicating IB4 positive and IB4 negative DRG neurons.

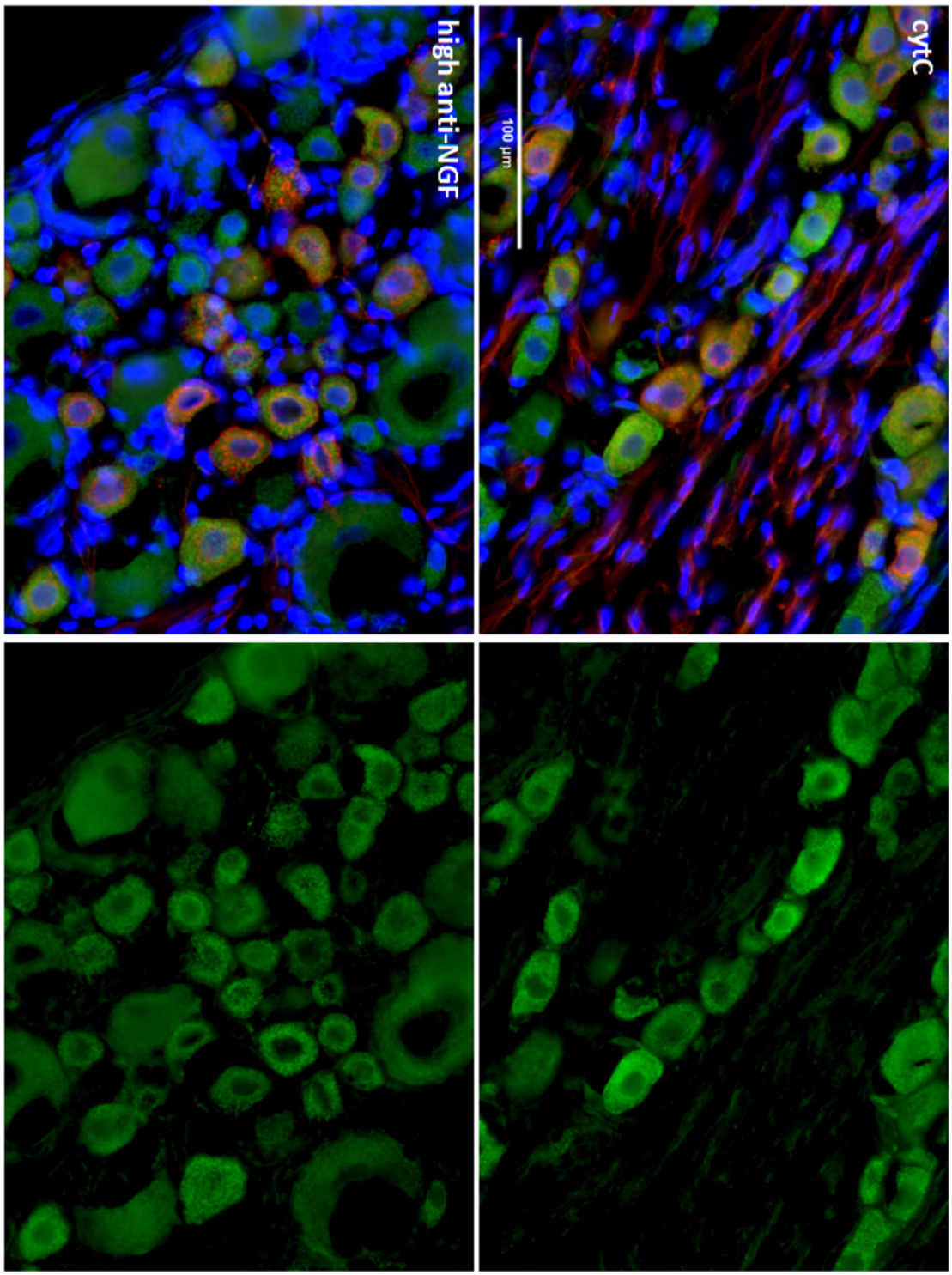

Figure 4.5. Glutaminase immunoreactivity in dorsal root ganglia of immunized rats. Representative images of DRG from rats immunized against cytC (upper panels) or with

high anti-NGF titers (lower panels). Immunofluorescence for GLS is shown in green (right panels) and is merged with the blue DAPI and red IB4 images (left panels). GLS-IR was not significantly affected by high anti-NGF titers.

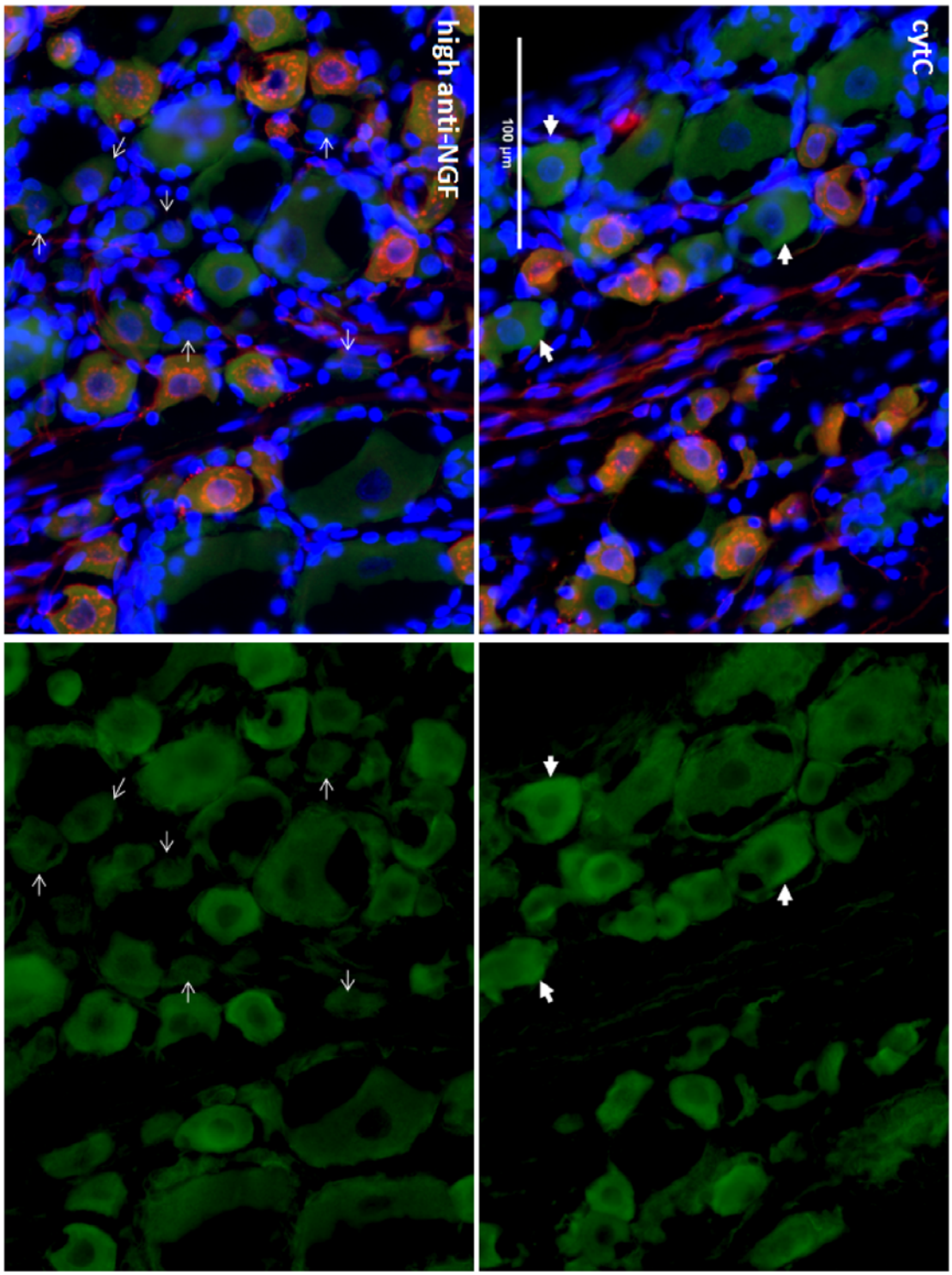

Figure 4.6. $Na_v1.8$ immunoreactivity in dorsal root ganglia of immunized rats. Representative images of DRG from rats immunized against cytC (upper panels) or with

high anti-NGF titers (lower panels). Immunofluorescence for $Na_v1.8$ is shown in green (right panels) and is merged with the blue DAPI and red IB4 images (left panels). $Na_v1.8$-IR appeared less intense in large DRG neurons as compared to small diameter neurons. In addition, high anti-NGF titers decreased $Na_v1.8$-IR in small IB4 negative DRG neurons (thin arrows) as compared to this population in cytC immunized rats (bold arrows).

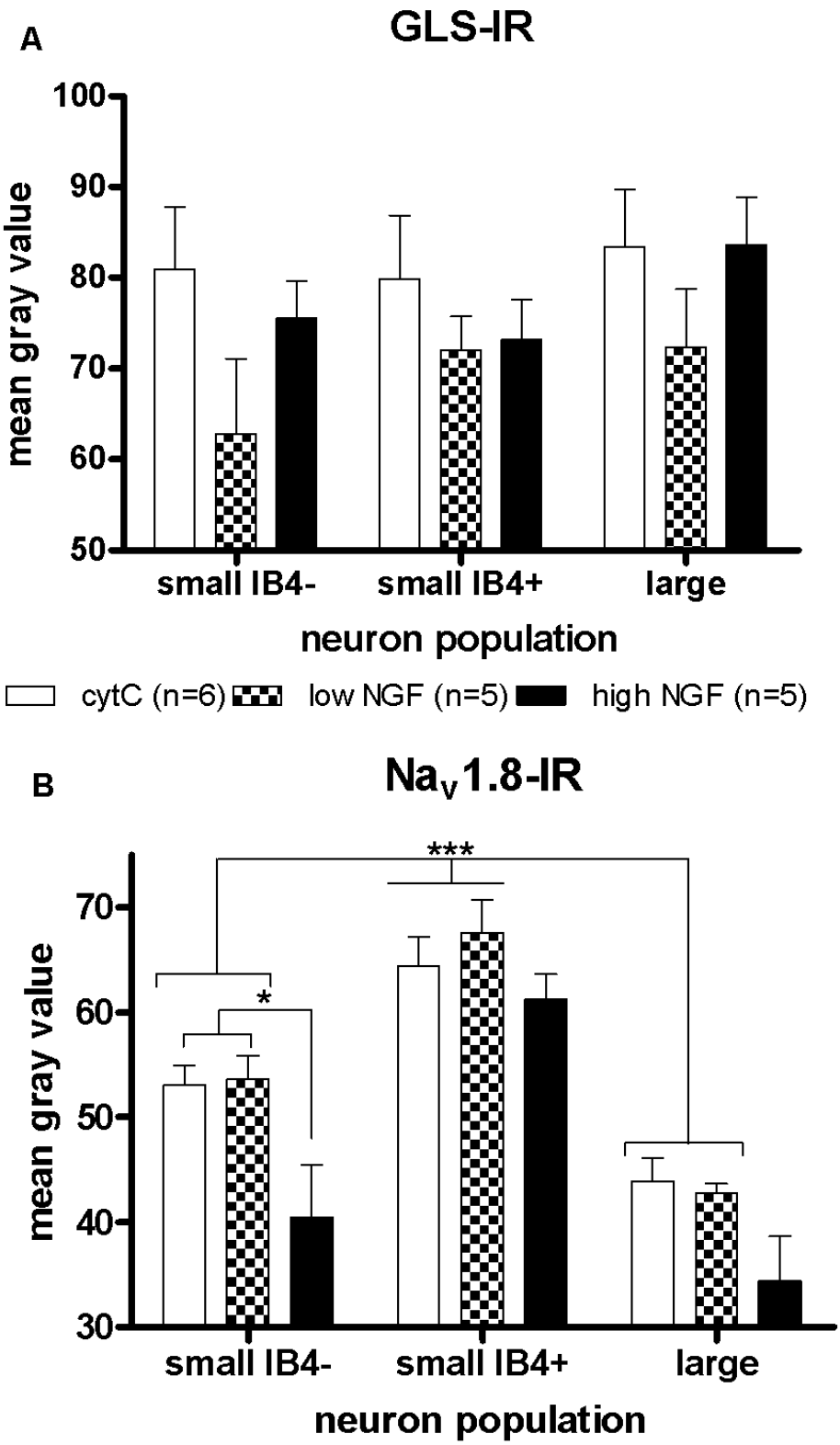
A
GLS-IR
mean gray value
100
90
80
70
60
50
small IB4-
small IB4+
large
neuron population
cytC (n=6)
low NGF (n=5)
high NGF (n=5)
B
Na$_V$1.8-IR
***
*
mean gray value
70
60
50
40
30
small IB4-
small IB4+
large
neuron population

Figure 4.7. Quantitative image analysis of GLS- and $Na_v1.8$-IR of DRG neurons from rats immunized against cytC and NGF. A) Levels of anti-NGF had no significant effect on GLS in any of the three DRG neuron populations examined. B) Large DRG neurons had significantly lower $Na_v1.8$-IR than the small DRG neurons and the IB4 negative neurons had significantly lower $Na_v1.8$-IR than IB4 positive neurons. Rats with high anti-NGF titers had decreased $Na_v1.8$-IR in small IB4 negative neurons. *$P<0.05$; ***$P<0.001$

CHAPTER 5

Peripheral inhibition of glutaminase reduces spinal Fos expression during inflammation

Abstract

Levels of the excitatory amino acid glutamate are increased in inflamed tissues. Glutamate sensitizes peripheral axons of primary afferent neurons during inflammation leading to decreased firing threshold and hyperexcitability. One proposed source of glutamate is the primary afferent itself. Antagonizing glutamate receptors on peripheral axons of primary afferents during inflammation provides analgesia in animals and humans. The enzyme glutaminase is used by primary sensory neurons to convert glutamine to glutamate. Peripheral inhibition of glutaminase with 6-diazo-5-oxo-L-norleucine (DON) provides long lasting analgesia during inflammation. In this study, we measured the effects of glutaminase inhibition on carrageenan induced spinal Fos expression. Rats were given intraplantar injections of carrageenan and treated locally with either vehicle or DON. After three hours of inflammation, hind paw swelling and spinal expression of Fos were examined. CellProfiler was used to automate Fos nuclei counting in five laminar groupings in the spinal cord (I-II, III-IV, V-VI, VII-IX, X). Carrageenan increased hind paw thickness by ~70% and spinal Fos expression in superficial (I-II) and deep (V-VI) laminae by 10-fold and 5-fold, respectively. Treatment with DON reduced hind paw swelling by ~13% and suppressed Fos expression in the

laminae I-II by ~54%, but not the deep laminae. Our results further support the notion of glutamate as a peripheral inflammatory mediator and indicate that glutaminase should be considered as a novel therapeutic target for treatment of inflammatory pain.

Introduction

Exogenous glutamate excites and sensitizes peripheral axons of primary afferent neurons (Du, Koltzenburg et al. 2001), and it is generally accepted that glutamate is involved in the sensitization of primary afferents during inflammation (Carlton 2001) through both ionotropic (Carlton, Hargett et al. 1995; Zhou, Bonasera et al. 1996; Davidson, Coggeshall et al. 1997)and metabotropic (Bhave, Karim et al. 2001) glutamate receptors. The source of endogenous glutamate that interacts with primary afferents is not clear, although a probable candidate is the peripheral terminal itself. Antidromic stimulation of the sciatic nerve increases glutamate concentrations in peripheral tissues, indicating a neural source of glutamate (deGroot, Zhou et al. 2000; Jin, Nishioka et al. 2006). Furthermore, increases in peripheral glutamate concentration after capsaicin stimulation are attenuated by local morphine (Jin, Nishioka et al. 2006), which suggests that glutamate is released by heat sensing nociceptors. Increased glutamate concentrations resulting from inflammation (Omote, Kawamata et al. 1998; Lawand, McNearney et al. 2000) can be diminished by nerve block (Lawand, McNearney et al. 2000), which again suggests the primary afferent as the source of glutamate. Lastly, peripheral terminals of primary afferent neurons are immunoreactive for vesicular glutamate transporters (Brumovsky, Watanabe et al. 2007) and have varicosities that contain small clear vesicles akin to those that contain glutamate in the central nervous

system (Kruger, Kavookjian et al. 2003). These studies, therefore, support the idea of glutamate autostimulation of nociceptive afferent fibers.

Injection of carrageenan into the plantar surface of the rat hind paw increases the expression of *c-fos* mRNA (Draisci and Iadarola 1989) and Fos protein (Honore, Buritova et al. 1995) in the lumbar spinal cord. Many analgesics attenuate the Fos increase induced by carrageenan, which indicates that Fos expression is a measure of activation in pain pathways and can serve to quantitate analgesia (Coggeshall 2005). Non-steroidal anti-inflammatory drugs (NSAIDs) decrease the formation of inflammatory mediators that can sensitize primary afferents (Popp, Haussler et al. 2008) by inhibiting the enzyme cyclooxygenase (COX). Peripheral inhibition of COX suppresses carrageenan induced Fos expression (Buritova and Besson 1998). If glutamate is to be considered among the molecules that sensitize primary afferent fibers during inflammation, then a similar approach would be to target the enzyme that synthesizes neurotransmitter glutamate from the precursor glutamine, glutaminase (GLS). We have previously shown that the irreversible GLS inhibitor, 6-diazo-5-oxo-L-norleucine (DON), provides long term analgesia in a dose dependent manner (Miller, Herzog et al. 2006) and that GLS expression is increased (Hoffman, Edwards et al. 2007) in the complete Freund's adjuvant (CFA) monoarthritis model. In the present study, we use spinal Fos expression to quantify the analgesic effect of DON on carrageenan induced hind paw inflammation. Our goal is to determine if glutamate that sensitizes peripheral terminals is produced by GLS during inflammation.

Methods

Sprague-Dawley rats (n = 15; 200-300 g) were housed on a 12 hour light: 12 hour dark cycle and given free access to food and water. Procedures were conducted according to guidelines from the National Institutes of Health (NIH 2003) and were approved by the Oklahoma State University Center for Health Sciences Institutional Animal Care and Use Committee. All appropriate efforts were made to minimize discomfort and the number of animals used in this study.

To test the effects of DON on carrageenan-evoked spinal Fos expression, rats (n=6) were injected with 10 µmol/25 µL DON (Sigma) in 0.01 M sodium phosphate buffered 0.9% (w/v) saline (PBS) in the right hind paw one day before being injected with 10 µmol DON in 100 µL of 1% (w/v) λ-carrageenan (Sigma) diluted in PBS. This dose of DON was chosen based on previous behavioral experiments (Miller, Herzog et al. 2006). Controls consisted of rats injected with vehicle (PBS) and carrageenan (n=5) in the same manner and naïve rats (n=4). Three hours after carrageenan injection, hind paw metatarsal thickness was measured with calipers (Mitutoyo) to the nearest 0.05 mm. All rats were anesthetized with 2.5% (w/v) Avertin and xylazine and then transcardially perfused with 75 mL PBS followed by 325 mL 4% formaldehyde in 0.1M sodium phosphate buffer. L4 spinal cord segments were dissected and post fixed for four hours at 4°C and then cryoprotected in 30% sucrose (w/v) for two days. Serial 20 µm frozen sections were cut and thaw mounted to slides. Sections were dried at 37°C for one hour and rinsed three times with PBS. After being blocked in 5% (v/v) NGS diluted in PBS with 0.25% Triton X-100 (PBS-T), sections were incubated overnight at 4°C in rabbit anti-Fos (Ab-5 Calbiochem) diluted 1:8000 in the blocking solution. Sections were

rinsed five times in PBS and incubated for two hours at room temperature in biotinylated goat anti-rabbit (Vector Laboratories) diluted to 1.0 µg/mL in PBS-T. After three PBS rinses, the sections were incubated for one hour at room temperature in Vectastain ABC reagent (Vector Laboratories) prepared as per the manufacturer's instructions. Sections were rinsed two times in PBS and once in tris-buffered saline, pH 7.6 (TBS) before incubating for five minutes at room temperature in 3,3'-diaminobenzidene tetrahydrochloride (Sigma) diluted to 10 mg/24 mL in TBS with 0.5% hydrogen peroxide. Sections were rinsed three times with PBS to stop the reaction and dehydrated in an alcohol series (50%, 70%, 90% × 2, 100% × 2). Sections were cleared in xylene twice and coverslipped with Permount (Fisher).

Ten sections from each rat were photographed using the 4X objective on a BX51 microscope (Olympus) with a SPOT RT740 camera (Diagnostic Instruments). Laminar groupings I-II, III-IV, V-VI, VII-IX, and X (Molander, Xu et al. 1984) on the side ipsilateral to hind paw injection were traced manually with a Cintiq 21UX interactive pen display (Wacom) in ImageJ (NIH). Traced laminar groupings were made into binary mask images with white laminar groupings on a black background. Fos positive nuclei were identified automatically and counted in each image by CellProfiler (Broad Institute Imaging Platform) (Carpenter, Jones et al. 2006) using the binary mask images to obtain Fos positive nuclei counts per laminar grouping. The CellProfiler pipeline used is summarized in Table 5.1.

Hind paw thickness measurements were compared with a two-way ANOVA with the fixed factors being hind paw (contralateral or ipsilateral to injection) and treatment groups (naïve, PBS, DON). Numbers of Fos-positive nuclei also were compared with

two-way ANOVA but with fixed factors being laminar groups (I-II, III-IV, V-VI, VII-IX, and X) and treatment groups. Multiple comparisons were made with Bonferroni post-tests. P values less than 0.05 were considered significant. Values are reported as mean ± standard error of the mean.

Results

Intraplantar carrageenan injection elicited an inflammatory response that caused significant swelling (~70% increase) of the metatarsal thickness in the ipsilateral hind paw (8.4±0.4 mm) versus the naïve rats (4.9±0.1 mm; Figure 5.1). Pretreatment and co-injection with DON, the GLS inhibitor, had a small but significant effect (~13% decrease) on carrageenan mediated hind paw swelling (7.3±0.3 mm), but it did not reduce hind paw thickness to that of naïve rats. Automated counting of Fos nuclei per laminar grouping provided a strictly objective criteria for identifying nuclei labeled for Fos that was consistent for all images analyzed. After laminar groupings were traced on all images, CellProfiler took an average of 14.1 seconds to process each image through the pipeline (Table 5.1). Naïve rats had less than five Fos nuclei per laminar grouping. Carrageenan significantly increased the number of Fos nuclei in ipsilateral laminae I-II (23±5) and laminae V-VI (28±4), without significantly affecting the number of Fos nuclei in other laminae (Figures 5.2 & 5.3). Pretreatment and co-injection with DON significantly decreased (~54%) the number of Fos nuclei in ipsilateral laminae I-II (11±1), but not laminae V-VI (22±3), as compared to PBS treated rats. There were still significantly more Fos nuclei in laminae I-II and laminae V-VI in DON treated rats than in naïve rats.

Discussion

Peripheral processes of primary afferent neurons have been implicated as the source of elevated glutamate released during inflammation (Carlton 2001). We hypothesized that inhibiting the enzyme GLS at the site of inflammation would suppress carrageenan induced Fos expression in spinal cord. Our finding that peripheral DON injection was able to suppress Fos expression in spinal cord supports the long-lasting analgesic effects of DON observed in the CFA inflammation model (Miller, Herzog et al. 2006). Antagonism of NMDA glutamate receptors systemically suppresses spinal Fos expression during peripheral inflammation throughout all laminar groupings in spinal cord, even ventral horn, but does not affect hind paw edema (Chapman, Honore et al. 1995). Such findings indicate that effects of systemic NMDA antagonism are mediated primarily acting in central nervous system. Peripheral NMDA antagonism also suppresses spinal Fos expression by ~35% during inflammation (Wang, Liu et al. 1997), which indicates glutamate sensitization of primary afferents at least partially accounts for increased spinal Fos expression. In addition to glutamate, intraplantar antagonism of two other sensitizing factors, the enzyme COX (Buritova and Besson 1998) and the bradykinin B2 receptor (Buritova, Chapman et al. 1997), also reduces carrageenan-induced spinal Fos expression. Peripheral COX inhibition with the highest dose of flurbiprofen resulted in a 52±5% suppression of the increase in Fos expression in laminae I-II and a 62±2% suppression in laminae V-VI (Buritova and Besson 1998). Antagonism of the B2 receptor with the highest dose of HOE140 resulted in a 51±6% suppression of the increase in Fos expression in laminae I-II and a 48±7% suppression in laminae V-VI (Buritova, Chapman et al. 1997). The highest doses of flurbiprofen and HOE140 also

decreased hind paw edema by 67±7% and 41±3%, respectively. COX is already the target of many analgesics, and bradykinin antagonism is being considered as a new analgesic strategy (Chen and Johnson 2007; Kuduk and Bock 2008). The finding that GLS inhibition has similar effects on Fos expression in laminae I-II to COX and bradykinin inhibition supports glutamate as a sensitizer of primary afferents and suggests GLS as a potential therapeutic target for inflammatory pain. The smaller anti-inflammatory effect of DON as compared to flurbiprofen and HOE140 may account for the lack of a significant effect on Fos suppression in laminae V-VI. Although much evidence points toward the primary afferent as the source of increased glutamate during inflammation, other peripheral cell types cannot be ruled out. Keratinocytes (Nguyen and Keast 1991), fibroblasts (Sarantos, Abouhamze et al. 1994), and white blood cells (Newsholme, Crabtree et al. 1985) all have GLS and may have a role in producing glutamate that acts on primary afferent fibers.

Primary afferent nociceptors have an efferent role during inflammation (Sann and Pierau 1998). Following transection of the sciatic nerve or neonatal destruction of capsaicin sensing DRG neurons, plasma extravasation during inflammation is markedly attenuated (Jancso, Kiraly et al. 1977). The component of inflammation contributed by the primary afferent has been called neurogenic inflammation, and it is presumed to be mediated by release of the neuropeptides substance P and calcitonin gene related peptide which results in vasodilatation and edema (Alvarez, Cervantes et al. 1988; Donnerer, Schuligoi et al. 1992). Exogenous glutamate causes overt nociception and swelling that can be blocked by antagonizing substance P (Beirith, Santos et al. 2003). Glutamate, therefore, may cause release of SP and CGRP from primary afferents. In this study, a

13% decrease in hind paw edema was observed after DON inhibition of carrageenan inflammation. We hypothesize that decreasing the concentration of glutamate with DON may suppress the amount of substance P released, decreasing the neurogenic component of inflammation.

Antagonism of glutamate receptors at the periphery provides analgesia during inflammatory pain models (Jackson, Graff et al. 1995; Davidson, Coggeshall et al. 1997; Bhave, Karim et al. 2001; Du, Zhou et al. 2003). Such analgesic effects have been attributed to glutamate receptors on the primary afferents themselves (Sato, Kiyama et al. 1993; Carlton, Hargett et al. 1995; Carlton and Coggeshall 1999; Kinkelin, Brocker et al. 2000). Exogenous glutamate injection causes pain and vasomotor responses in humans as well, and glutamate receptor antagonists can provide analgesia (Warncke, Jorum et al. 1997). In light of this information, our study further indicates that antagonism of glutamate at the periphery is a viable pain therapy, and we propose the enzyme GLS as novel therapeutic target.

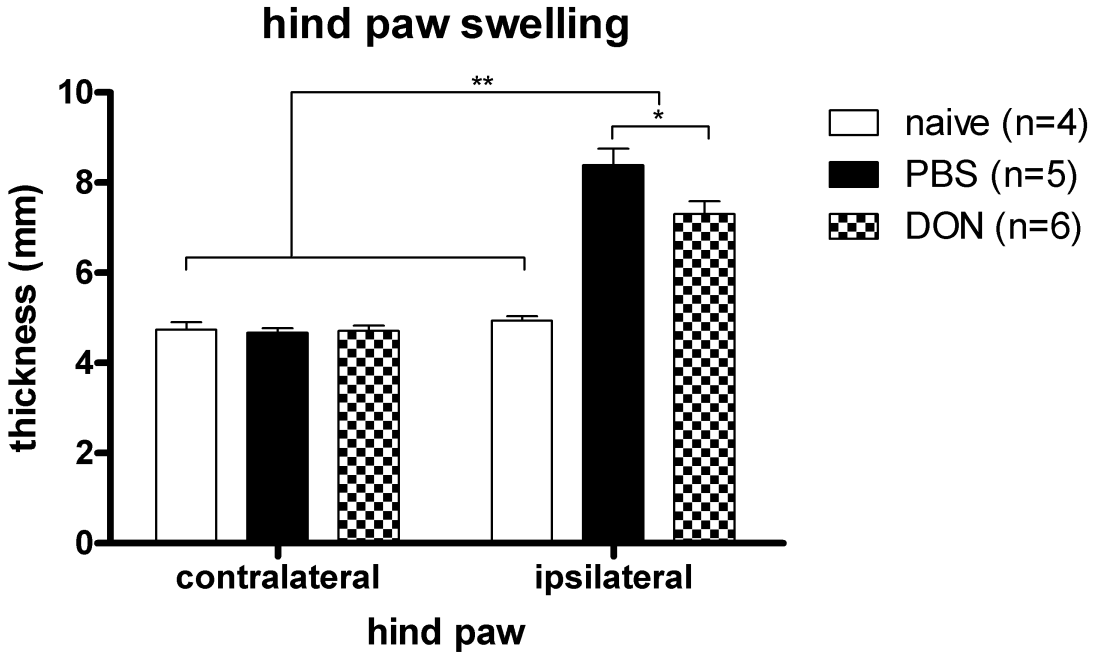

Figure 5.1. Effects of peripheral GLS inhibition on carrageen induced hind paw swelling. Intraplantar carrageenan injection caused a unilateral inflammation of the hind paw. Swelling was slightly reduced (13%) by DON treatment, but not brought to normal.

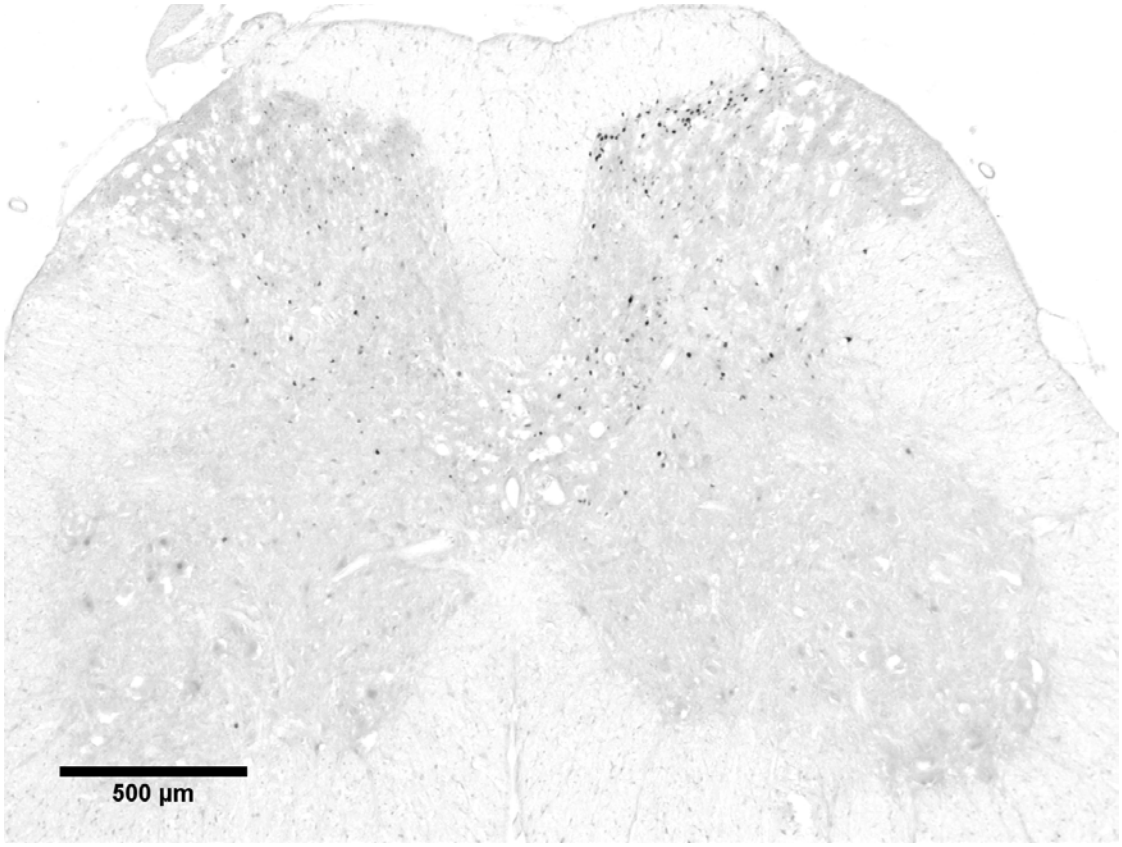
500 µm

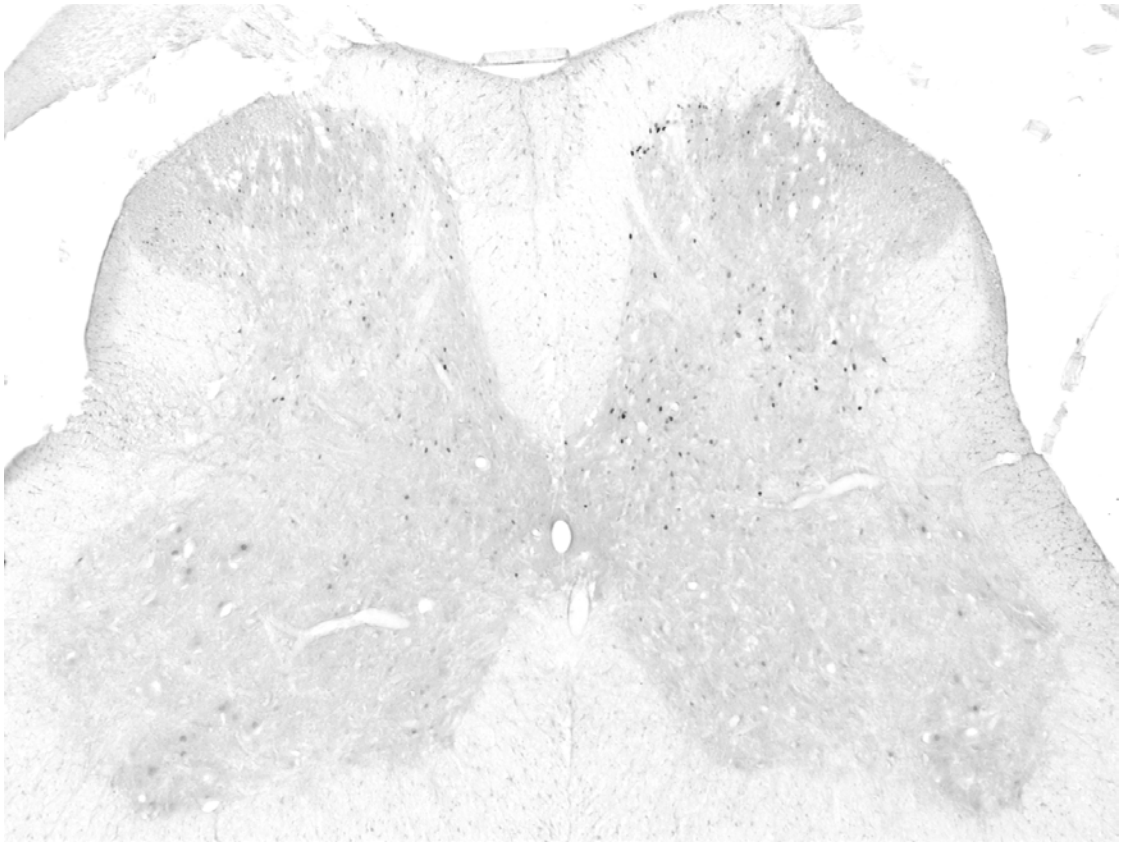

Figure 5.2. Representative images of spinal Fos immunohistochemistry after carrageenan induced inflammation. Carrageenan injection with PBS treatment induced Fos expression in superficial (I-II) and deep laminae (V-VI) of the ipsilateral spinal cord dorsal horn (top). Inhibition of GLS with DON decreased the number of carrageenan induced Fos nuclei in superficial laminae (54%) without affecting the number of Fos nuclei in the deep layers (bottom).

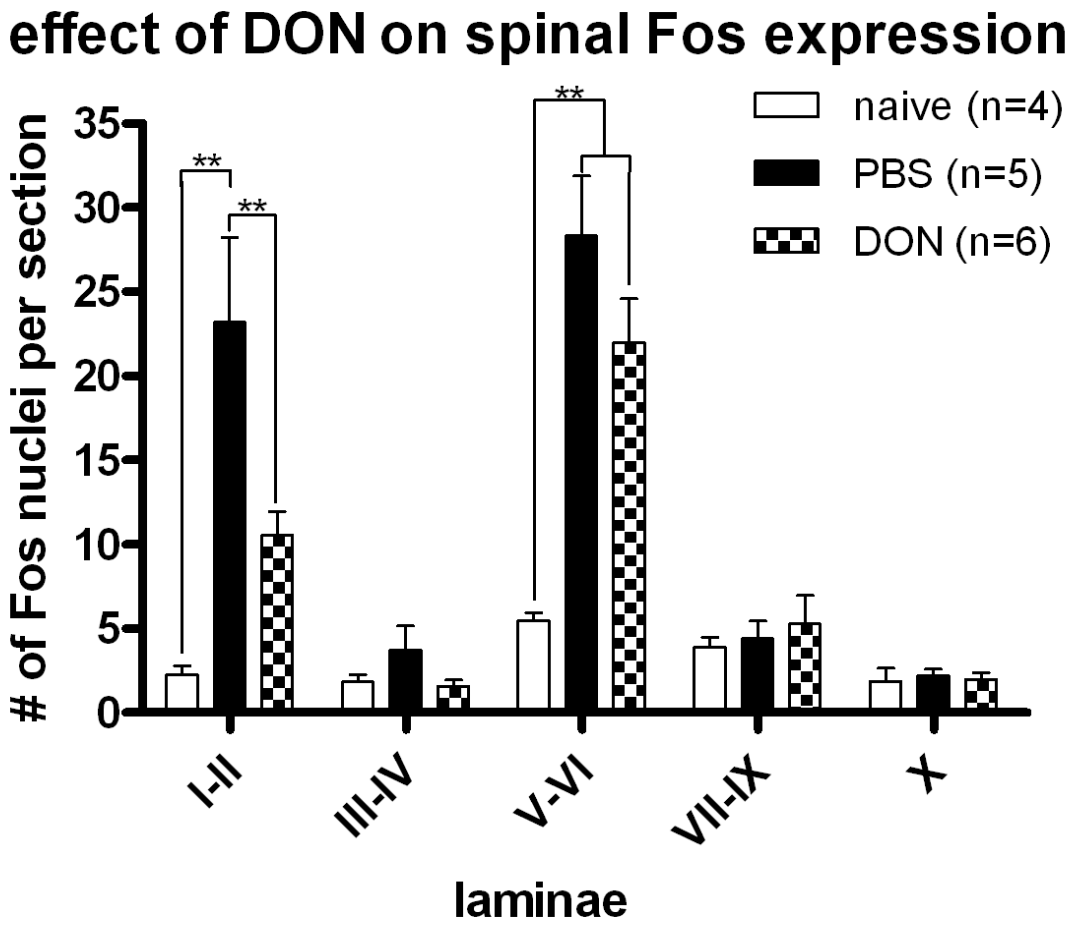

Figure 5.3. Effects of peripheral GLS inhibition on carrageen induced Fos expression. Automated counting of Fos nuclei for five laminar grouping revealed significant increases in Fos expression in the superficial (I-II) and deep (V-VI) dorsal horn after carrageenan injection with PBS treatment. Treatment with DON significantly reduced Fos expression in the superficial (54%) but not the deep laminae. *P<0.01, **P<0.001

Module	Description
LoadImages	loads image pairs (binary mask of laminae and original)
IdentifyPrimAutomatic	identifies laminae as objects from binary mask image
InvertIntensity	inverts intensity of original so Fos nuclei are white
ApplyThreshold	sets all gray values below a certain intensity to black
IdentifyPrimAutomatic	identifies Fos nuclei by shape and intensity
MeasureObjectAreaShape	obtains area measurements for laminae and nuclei
MeasureObjectIntensity	obtains intensity measurements for laminae and nuclei
Relate	counts number of Fos nuclei within each laminar grouping
ExportToExcel	exports all measurement data to Excel spreadsheet

Table 5.1. Summary of pipeline used in CellProfiler for automated detection and counting of Fos nuclei in images of spinal cord sections. Manual identification of laminar groupings was required prior to using the CellProfiler software. Each module listed has additional parameters that are set to specify in detail how to handle the data.

CHAPTER 6

Conclusion

Novel strategies to manage inflammatory pain could improve the quality of life for those suffering intractable pain and the health of those experiencing negative side effects of current analgesics. The advantages of targeting nociceptive neurons in the peripheral ganglia are that: (1) they are the beginning of the "pain pathway", (2) they are outside of the CNS, and (3) they uniquely express specific proteins used for nociception. This allows for fewer side effects and the potential for topical drug application at the site of inflammation. Identification of such molecular targets requires precise characterization of protein expression in nociceptive neuron populations. Due to differences in laboratory technique, reported distributions for many proteins vary. These issues were addressed in Chapter 2. By comparing concentrations of formaldehyde and picric acid in the fixative used for immunofluorescence studies, we determined that each antigen-antibody pair has an optimal concentration of these two fixatives that gives maximal sensitivity. We concluded that such optimization should be performed when determining antigen distribution.

Since its accidental discovery as a fixative in the late nineteenth century (Blum 1893), formaldehyde has remained the most popular fixative used for both histopathology and basic science (Fox, Johnson et al. 1985). It has long been recognized, however, that formaldehyde fixation is not optimal for preserving tissue antigenicity (Hopwood 2002).

Our current understanding of the mechanism of formaldehyde fixation dates back to the 1940s, when it was shown that formaldehyde cross-links amino acid residues in proteins (Fraenkel-Conrat and Olcott 1948; Fraenkel-Conrat and Olcott 1948; Fraenkel-Conrat and Mecham 1949). Unlike glutaraldehyde ($C_5H_8O_2$), which is a dialdehyde, formaldehyde (CH_2O) has only one reactive group (Figure 6.1). In aqueous solution, formaldehyde exists mainly as its monohydrate (CH_4O_2), methylene glycol (Le Botlan, Mechin et al. 1983), that can oligomerize and/or form methylene cross bridges between amino acids in proteins (Puchtler and Meloan 1985). It is postulated that when amino acids are cross-linked with one another, antigens are "masked" and are unavailable for interaction with antibodies (Sompuram, Vani et al. 2004). Certain techniques called antigen retrieval have been developed to "unmask" antigens after formaldehyde fixation and reestablish immunolabeling (Shi, Key et al. 1991). The success of such techniques is variable and there is not a single technique that works for all antigen-antibody combinations (Shi, Liu et al. 2007). Our results indicate a way to circumvent the need for antigen retrieval techniques by optimizing the formaldehyde concentration in the fixative in order to obtain maximal antigen detection sensitivity, while maintaining adequate fixation by addition of other fixative component (picric acid). Our results are more likely to influence basic science research where greater control over fixation methods is possible. This could lead to more accurate determinations of antigen distribution in not just the rat dorsal root ganglion, but any tissue used for basic science research. Once the susceptibility of antigens processed routinely in pathology laboratories is known, specific concentrations of formaldehyde may become standard for certain antigen labeling protocols in the clinical setting as well.

Even less is known about the mechanism of picric acid fixation, but it is thought to be a precipitant/coagulant fixative that denatures proteins (Polak and Van Noorden 2003). Picric acid has three nitro groups (Figure 6.1) that react with histones and basic proteins and forms crystalline picrates with free amino acids. Tissues, therefore, retain little affinity for basic dyes and exhibit prominent shrinkage (Hopwood 2002). Usually, picric acid is used in combination with other fixatives in both the clinical and basic science research settings. A popular picric acid-containing fixative was introduced in 1897 by Pol Andre Bouin for optimal viewing of gametes in the rat testis and has since been referred to as Bouin's fluid. Subsequent picric acid fixatives also were named after those that introduced them (i.e., Rossman's, Gendre's, and Zamboni's), and were found to be advantageous for viewing of carbohydrates (Hopwood 2002). Qualitative comparisons such as that done for GLS in brain (Kaneko, Itoh et al. 1989) have been performed to determine if picric acid has an effect on immunoreactivity. Our study in Chapter 2 showed that picric acid either had no effect on immunoreactivity or increased it, but it never had a negative effect like formaldehyde. Adding picric acid increased detection sensitivity for $Na_v1.8$ and TRPV1, and it may have a similar effect for other antigen-antibody combinations. As with formaldehyde, it would be beneficial to optimize picric acid concentration in the fixative used for preservation of tissue used for research or clinical diagnosis.

The neurotransmitter glutamate is released from peripheral and central terminals of DRG neurons, but the distribution of the synthetic enzyme for glutamate, GLS, was not clear. Very few studies had investigated the distribution of GLS in the DRG, and there was not a consensus among those that had. A few reports had determined that 30-40% of

DRG neurons expressed GLS, and these were mainly small diameter neurons. Other studies had determined that 80% or more of DRG neurons expressed GLS, regardless of size. The main difference between the methodologies in these two sets of studies was the fixative used. As part of the optimization study in Chapter 2, we found that sensitivity for GLS detection was optimal when low formaldehyde was used, and that picric acid concentration did not have any effect. These findings indicated that the latter group of studies was closer to describing the true distribution of GLS in the DRG, which we determined was ubiquitous among DRG neurons. Our results are supported by the need of all DRG neurons to synthesize glutamate for release from central terminals (Figure 6.2).

Glutamate concentrations increase in inflamed tissue and sensitize peripheral terminals of DRG neurons. In addition, glutamate concentrations in spinal cord dorsal horn increase following noxious inflammatory stimulation. Sensitization can regulate the expression of proteins in DRG neurons, which accounts for long-term changes in threshold and excitability. Prior to our studies, there was no information regarding glutamate metabolism in DRG neurons during inflammation. In Chapter 3, we investigated expression of the enzyme GLS, which is responsible for neurotransmitter glutamate synthesis, in a long-term inflammatory pain model. We determined that GLS expression is elevated after four days of inflammation in all DRG neurons and remains elevated in the small DRG neuron population after eight days of inflammation. We presume that increased GLS expression could supply the elevated amounts of glutamate released at the peripheral and/or central terminals of DRG neurons (Figure 6.3).

Many of the expression changes that occur in DRG neurons during inflammation are the result of retrograde NGF signaling. NGF binds to membrane receptors on peripheral terminals, is endocytosed, and transported on microtubules toward the cell body in the DRG in signaling endosomes (Delcroix, Valletta et al. 2003). The signaling cascade proteins associated with the endosomes lead to regulatory changes of gene expression at the cell body (Figure 6.4). For instance, TRPV1's dual promoter system has been found to be positively regulated by NGF (Xue, Jong et al. 2007). It is postulated that basal expression of proteins upregulated during inflammation is under the control of peripherally produced NGF. Sequestering NGF with anti-NGF antibodies deprives DRG neurons of their peripheral source of NGF and causes hypoalgesia (Chudler, Anderson et al. 1997). The exact mechanism for this hypoalgesia is not certain, but one study has implicated that decreased $Na_v1.8$ expression is involved (Fjell, Cummins et al. 1999). Since GLS was found to be upregulated during inflammation in Chapter 3, we decided to determine if NGF deprivation via autoimmunization decreased GLS expression in Chapter 4. We found that basal GLS expression is not affected by NGF deprivation (Figure 6.5). NGF production is increased in inflamed tissues, making more NGF available for retrograde transport to the cell body in the DRG. These elevated amounts of NGF may still account for the upregulation of GLS that we observed in Chapter 3. Further experiments, where NGF is blocked during inflammation will need to be performed to determine if this is the case (see future directions section below).

Since glutamate is a sensitizer of nociceptor peripheral terminals and it is produced in elevated amounts in inflamed tissues, it would be advantageous to know how it is being produced. The results of Chapter 3 indicated that it may be made by neuronal GLS,

which is upregulated during inflammation. Cyclooxygenase (COX) is another enzyme that makes sensitizing molecules (prostaglandins), and it is also upregulated in inflamed tissues (Schuligoi, Ulcar et al. 2003). Inhibition of COX with NSAIDs is a first choice treatment for many types of inflammatory pain and reduces Fos expression in spinal cord during inflammatory stimulation in animals. If GLS can also reduce Fos expression in spinal cord, the argument for GLS as a novel analgesic target will be strengthened. In Chapter 5, we showed that peripheral inhibition of GLS during carrageenan induced hind paw inflammation attenuates the usual increase in spinal cord Fos expression. We used a glutamine analog called DON (Figure 6.6) to inhibit GLS in the periphery and used Fos expression in spinal cord as a measure of analgesic efficacy. It should be noted that Fos expression has limitations, and inferences that elevated spinal Fos expression indicates increased electrical activity in spinal neurons should not be made without electrophysiological confirmation. Despite the limitations of quantifying spinal Fos expression, a review on spinal Fos expression as a marker for nociception referenced 485 articles (Coggeshall 2005), and the majority of cited references were original reports that used Fos immunohistochemistry on spinal cord sections during some form of noxious stimulation. Although studies of Fos expression may not be reliable at indicating precise electrical activity, the vast number of Fos studies allows for relative comparisons to be made. Experimental analgesics that have been proven by other methodologies and analgesics used to treat clinical pain provide benchmarks for comparison of novel analgesics. For instance, peripheral inhibition COX with the highest tested dose of flurbiprofen suppresses the increase in Fos expression by 52±5% in laminae I-II and by 62±2% in laminae V-VI three hours after carrageenan induced inflammation. Peripheral

inhibition of the NMDA glutamate receptor with the highest dose of MK-801 suppresses the increase in total Fos expression by ~35% (counting was not performed for individual laminar groupings) one hour after formalin induced inflammation. GLS inhibition with DON suppressed the increase of Fos expression in laminae I-II by 54% after three hours of carrageenan induced inflammation (Figure 6.7). However, GLS inhibition had no effect on Fos expression in laminae V-VI. The magnitude of the effect of DON on Fos in the superficial dorsal horn, therefore, was similar to that of COX inhibition. Coupled with previous evidence that peripheral GLS inhibition reduces hyperalgesia during a CFA inflammatory pain model, this new finding further supports the idea that GLS inhibition may be a successful analgesic strategy for inflammatory pain. However, if GLS inhibition becomes an analgesic strategy, measures must be taken to minimize effects on the central nervous system since all glutamatergic and GABAergic CNS neurons use glutaminase. We support the use of GLS inhibitors topically to decrease the concentration of drug in the CNS.

Future directions

In this study, GLS expression was shown to be increased during inflammation (Chapter 3; Figure 6.3), but its basal expression was not affected by NGF depletion (Chapter 4; Figure 6.5). NGF is implicated in the upregulation of proteins in DRG neurons during inflammation, and the results of this study do not rule out the possibility that NGF is responsible for the upregulation of GLS during inflammation. A future direction, therefore, should be to examine GLS expression in DRG neuron subpopulations during a long-term inflammation in chronically NGF deprived rats. The autoimmunization protocol used in Chapter 4 should be performed, and rats that develop

high anti-NGF titers and control rats immunized against cytC should be given an injection of CFA in the hind paw as in Chapter 3. If the elevated NGF present during inflammation is responsible for GLS up-regulation, then the NGF deprived rats should have lower GLS expression as compared to rats immunized against cytC. In addition, it would be expected that the NGF autoimmunization might be an effective "pain vaccine" in the sense that it may be able to prevent the development of hyperalgesia.

Although GLS is widely expressed throughout the body (i.e., kidney, intestine, skin, immune system, CNS), topical application of GLS inhibitors to inflamed areas will limit the negative side effects. The COX inhibitor trolamine and the TRPV1 agonist capsaicin have already been marketed as analgesic topical creams (Aspercreme® and Arthricare®, respectively), indicating the effectiveness of topical analgesics for treatment of inflammatory pain in deeper tissues such as muscles and joints. The GLS inhibitor DON has been administered locally by injection into the rat hind paw (Chapter 5). While this is convenient for experimentation with rats, it does not represent how the inhibitor will be used clinically. Another future direction should, therefore, be to formulate DON in a topical cream that can be applied to the hind paw skin prior to or during inflammation and measure behavioral responses and spinal Fos expression. A novel GLS inhibitor, bis-2-(5-phenylacetamido-1,2,4-thiadiazol-2-yl)ethyl sulfide (Robinson, McBryant et al. 2007), should be tested alongside DON to compare efficacy and potency. This information could lead to the design of more GLS inhibitors with optimal pharmacokinetics for topical administration.

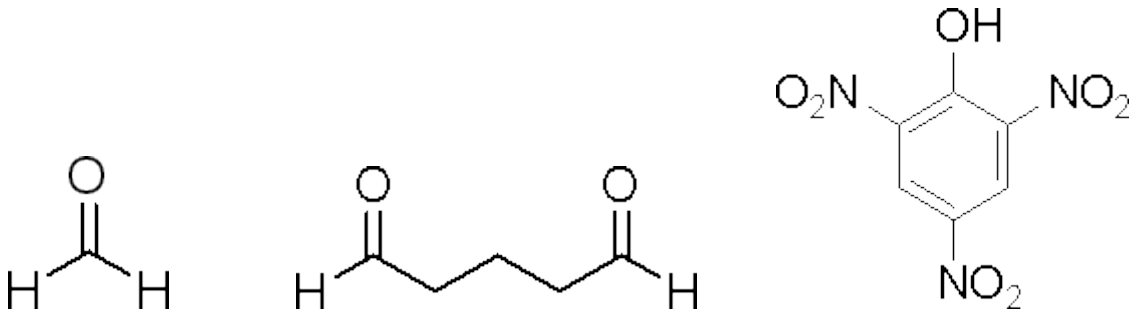

formaldehyde glutaraldehyde picric acid

Figure 6.1. Chemical structures of fixative components. Formaldehyde monomer (left) has only one functional group as compared to the dialdehyde, glutaraldehyde (middle). Picric acid has three nitro (NO_2) groups that can react with tissue constituents.

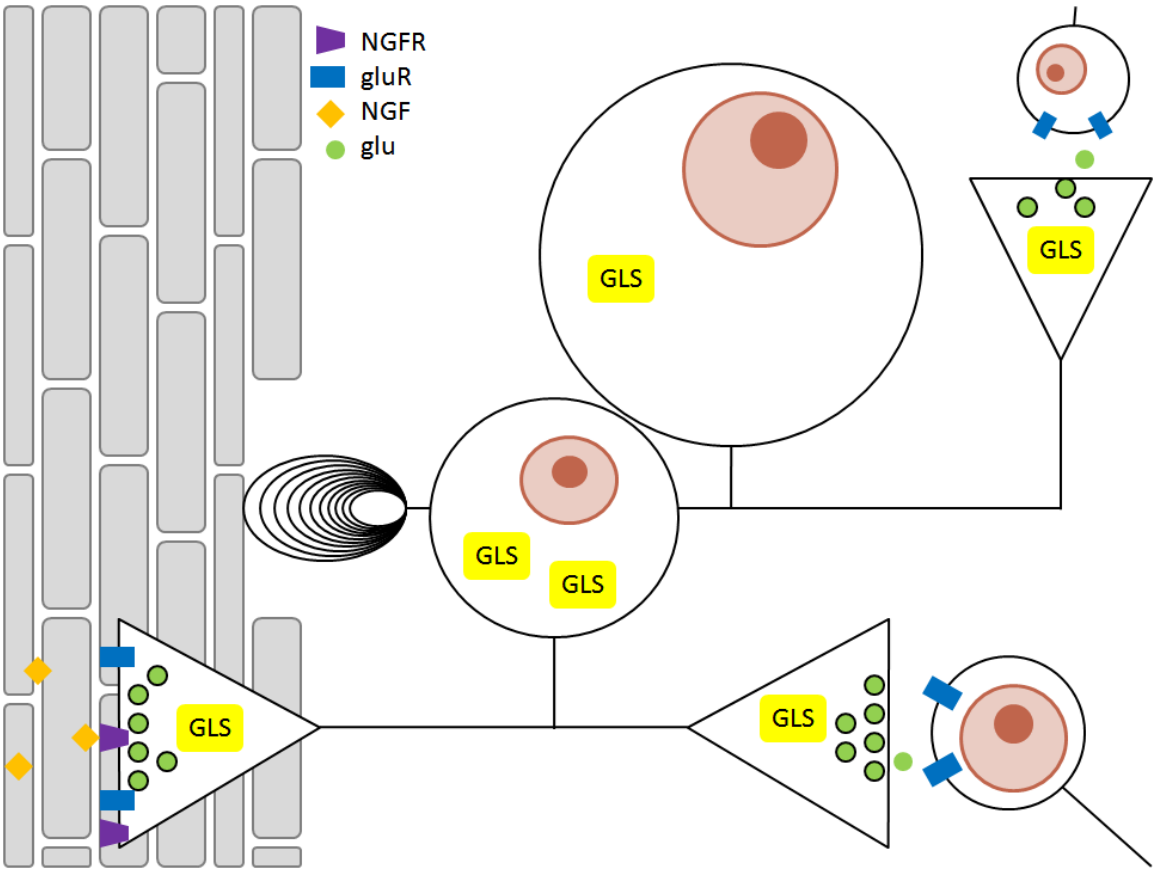

Figure 6.2. Summary of Chapter 2 findings. Two DRG neurons are depicted. The lower one is a small diameter nociceptive neuron with a bare nerve ending peripheral process and a central process that terminates in the spinal cord dorsal horn. The upper one is a large diameter touch responsive neuron with an encapsulated (Pacinian corpuscle) ending peripheral process and a central process that terminates in the medulla. Both neurons use glutamate for neurotransmission. The nociceptive neuron uses glutamate at both the peripheral and central terminals, while the large diameter neuron uses glutamate on the its central terminal only. GLS, the enzyme that synthesizes glutamate, was localized in all DRG neurons in Chapter 2. However, small neurons had relatively higher expression levels than large neurons.

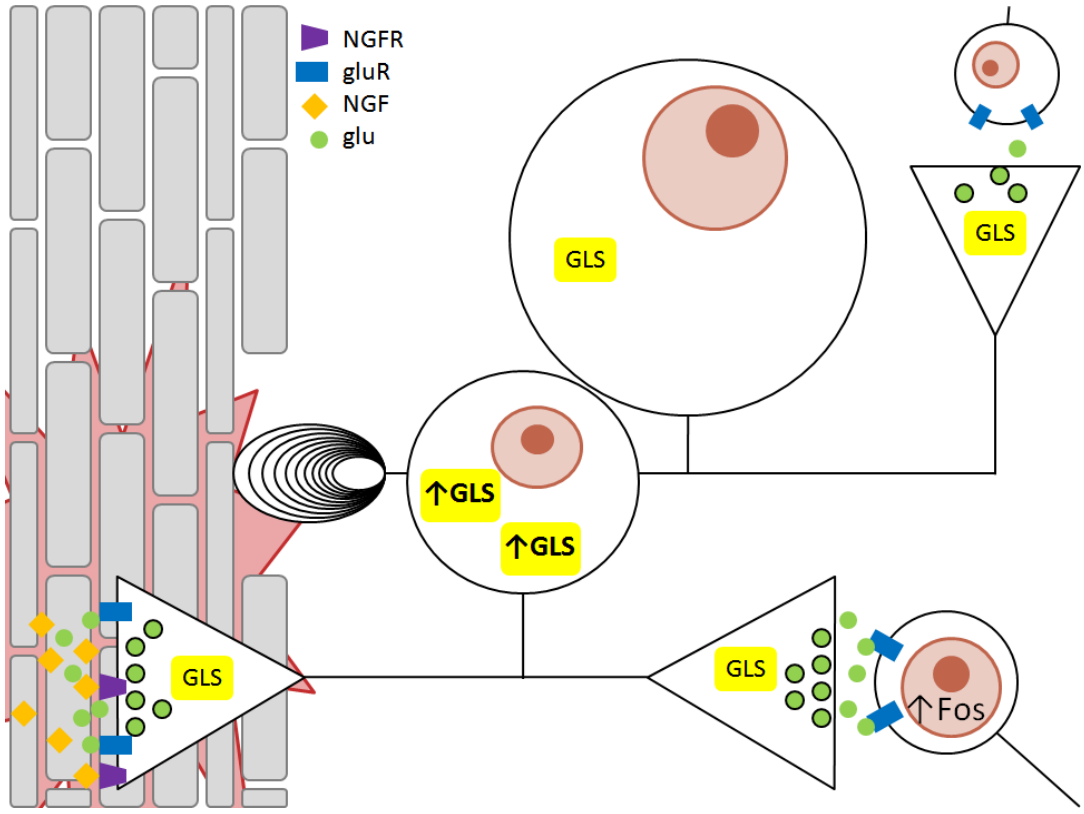

Figure 6.3. Summary of Chapter 3 findings. Inflammation was induced in the rat hind paw. NGF and glutamate levels are increased in inflamed tissue. Glutamate concentrations increase in dorsal horn of spinal cord during peripheral inflammation and Fos expression is increased in the nuclei of dorsal horn neurons. We found that GLS expression was elevated in small diameter DRG neurons after four and eight days of inflammation. Up-regulation of GLS may account for increased glutamate concentrations in the periphery and spinal cord. NGF is retrogradely transported to the cell body and is known to affect the expression of genes important for nociception (see Figure 6.4). GLS up-regulation may be among the genes under positive regulatory control of the high NGF levels during inflammation. Further experiments are necessary to determine this.

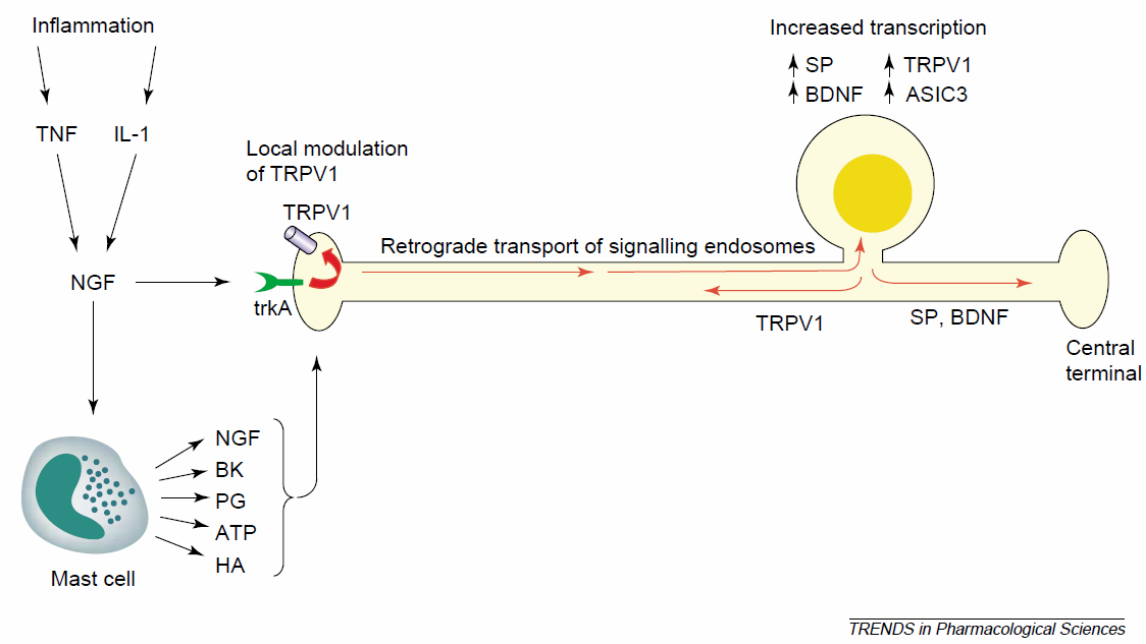

Figure 6.4. The role of NGF in peripheral sensitization. NGF is involved in post-translational changes to proteins already present in the peripheral terminal as well as increasing expression of proteins by retrograde transport to the cell body in signaling endosomes. Basal levels of NGF may regulate the sensitivity of nociceptive DRG neurons by regulating the expression of proteins important for pain sensation (Hefti, Rosenthal et al. 2006).

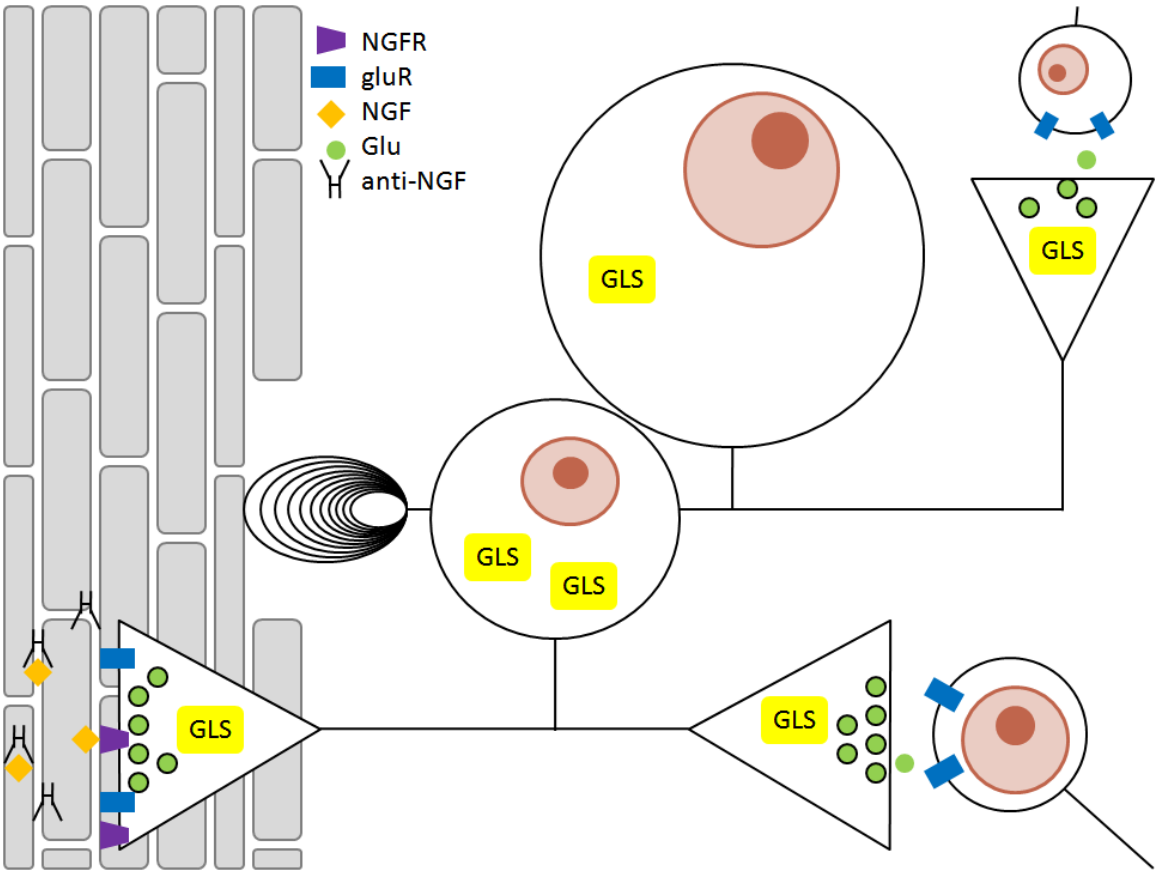

Figure 6.5. Summary of Chapter 4 findings. Immunization with NGF produced a constant level of anti-NGF antibodies that could bind to NGF and prevent its endocytosis by primary afferent terminals and subsequent retrograde transport. High anti-NGF levels resulted in hypoalgesia, but did not affect GLS expression.

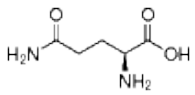

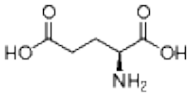

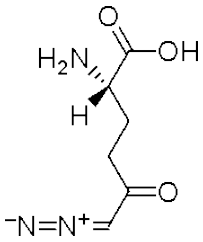

glutamine glutamate DON

Figure 6.6. Chemical structures of glutamine, glutamate, and DON. DON is a glutamine analog, and it is identical in structure to glutamine except for the 6-diazo group that replaces the terminal amino group.

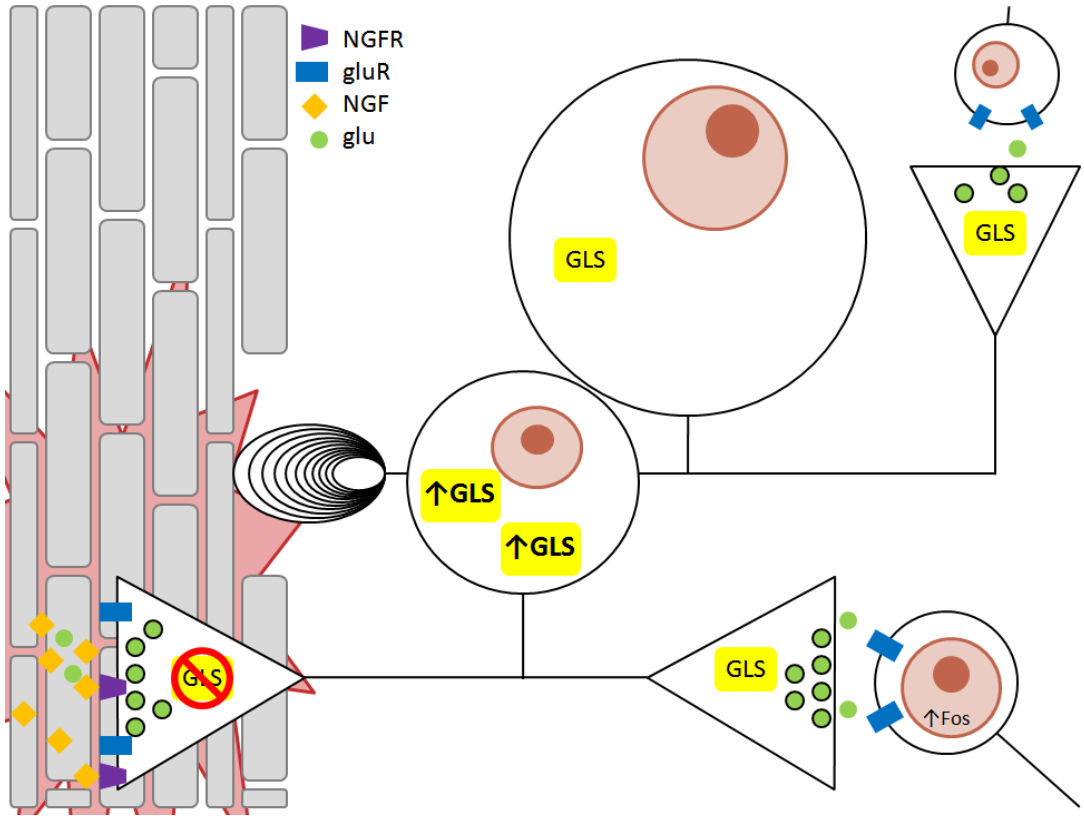

Figure 6.7. Summary of Chapter 5 findings. Hind paw inflammation was induced while simultaneously blocking GLS with DON. We observed a suppression of Fos up-regulation in dorsal horn of spinal cord as compared to inflammation alone (represented by decreased font size). Previously, DON inhibition has been shown to be an effective analgesic. We hypothesize that GLS inhibition with DON decreased peripheral glutamate levels, which resulted in less peripheral sensitization and fewer action potentials reaching the spinal cord (less glutamate release onto dorsal horn neuron). We postulate that the suppression of Fos expression in the spinal cord was due to reduced electrical activity in dorsal horn neurons, but electrophysiological data are required to confirm this.

REFERENCES

Abdiche, Y. N., D. S. Malashock, et al. (2008). "Probing the binding mechanism and affinity of tanezumab, a recombinant humanized anti-NGF monoclonal antibody, using a repertoire of biosensors." Protein Sci **17**(8): 1326-35.

Altier, C. and G. W. Zamponi (2004). "Targeting Ca2+ channels to treat pain: T-type versus N-type." Trends Pharmacol Sci **25**(9): 465-70.

Alvarez, F. J., C. Cervantes, et al. (1988). "Presence of calcitonin gene-related peptide (CGRP) and substance P (SP) immunoreactivity in intraepidermal free nerve endings of cat skin." Brain research **442**(2): 391-5.

Amann, R., R. Schuligoi, et al. (1995). "Intraplantar injection of nerve growth factor into the rat hind paw: local edema and effects on thermal nociceptive threshold." Pain **64**(2): 323-9.

Averill, S., S. B. McMahon, et al. (1995). "Immunocytochemical localization of trkA receptors in chemically identified subgroups of adult rat sensory neurons." Eur J Neurosci **7**(7): 1484-94.

Battaglia, G. and A. Rustioni (1988). "Coexistence of glutamate and substance P in dorsal root ganglion neurons of the rat and monkey." J Comp Neurol **277**(2): 302-12.

Bautista, D. M., S. E. Jordt, et al. (2006). "TRPA1 mediates the inflammatory actions of environmental irritants and proalgesic agents." Cell **124**(6): 1269-82.

Bean, E. S. (2001). Polyclonal Antibodies. Basic methods in antibody production and characterization. G. C. Howard. Boca Raton, CRC Press**:** 31-43.

Beirith, A., A. R. Santos, et al. (2003). "The role of neuropeptides and capsaicin-sensitive fibres in glutamate-induced nociception and paw oedema in mice." Brain Res **969**(1-2): 110-6.

Benn, S. C., M. Costigan, et al. (2001). "Developmental expression of the TTX-resistant voltage-gated sodium channels Nav1.8 (SNS) and Nav1.9 (SNS2) in primary sensory neurons." J Neurosci **21**(16): 6077-85.

Bennett, D. L., M. Koltzenburg, et al. (1998). "Endogenous nerve growth factor regulates the sensitivity of nociceptors in the adult rat." Eur J Neurosci **10**(4): 1282-91.

Berger, U. V. and M. A. Hediger (2000). "Distribution of the glutamate transporters GLAST and GLT-1 in rat circumventricular organs, meninges, and dorsal root ganglia." J Comp Neurol **421**(3): 385-99.

Bhave, G., F. Karim, et al. (2001). "Peripheral group I metabotropic glutamate receptors modulate nociception in mice." Nat Neurosci **4**(4): 417-23.

Black, J. A., S. Liu, et al. (2004). "Changes in the expression of tetrodotoxin-sensitive sodium channels within dorsal root ganglia neurons in inflammatory pain." Pain **108**(3): 237-47.

Blum, F. (1893). "Der formaldehyd als hartungsmittel." Z Wiss. Mikrosc **10**: 314.

Bocchini, V. and P. U. Angeletti (1969). "The nerve growth factor: purification as a 30,000-molecular-weight protein." Proc Natl Acad Sci U S A **64**(2): 787-94.
Bolay, H. and M. A. Moskowitz (2002). "Mechanisms of pain modulation in chronic syndromes." Neurology **59**(5 Suppl 2): S2-7.
Brown, C. (2006). "Blood collection from the tail of a rat." Lab Anim (NY) **35**(8): 24-5.
Brumovsky, P., M. Watanabe, et al. (2007). "Expression of the vesicular glutamate transporters-1 and -2 in adult mouse dorsal root ganglia and spinal cord and their regulation by nerve injury." Neuroscience **147**(2): 469-90.
Buritova, J. and J. M. Besson (1998). "Peripheral and/or central effects of racemic-, S(+)- and R(-)-flurbiprofen on inflammatory nociceptive processes: a c-Fos protein study in the rat spinal cord." Br J Pharmacol **125**(1): 87-101.
Buritova, J., V. Chapman, et al. (1997). "The contribution of peripheral bradykinin B2 receptors to carrageenan-evoked oedema and spinal c-Fos expression in rats." Eur J Pharmacol **320**(1): 73-80.
Cangro, C. B., P. M. Sweetnam, et al. (1984). "Selective localization of glutaminase in spinal and sensory nerve cells. A potential marker for glutamate neurotransmission." JAMA **251**(6): 797.
Cangro, C. B., P. M. Sweetnam, et al. (1985). "Localization of elevated glutaminase immunoreactivity in small DRG neurons." Brain Res **336**(1): 158-61.
Carlton, S. M. (2001). "Peripheral excitatory amino acids." Curr Opin Pharmacol **1**(1): 52-6.
Carlton, S. M. and R. E. Coggeshall (1999). "Inflammation-induced changes in peripheral glutamate receptor populations." Brain Res **820**(1-2): 63-70.
Carlton, S. M., G. L. Hargett, et al. (1995). "Localization and activation of glutamate receptors in unmyelinated axons of rat glabrous skin." Neurosci Lett **197**(1): 25-8.
Carlton, S. M., S. Zhou, et al. (1996). "Localization and activation of substance P receptors in unmyelinated axons of rat glabrous skin." Brain Res **734**(1-2): 103-8.
Carlton, S. M., S. Zhou, et al. (1998). "Evidence for the interaction of glutamate and NK1 receptors in the periphery." Brain Res **790**(1-2): 160-9.
Carpenter, A. E., T. R. Jones, et al. (2006). "CellProfiler: image analysis software for identifying and quantifying cell phenotypes." Genome Biol **7**(10): R100.
Caterina, M. J., M. A. Schumacher, et al. (1997). "The capsaicin receptor: a heat-activated ion channel in the pain pathway." Nature **389**(6653): 816-24.
Chada, S. R. and P. J. Hollenbeck (2003). "Mitochondrial movement and positioning in axons: the role of growth factor signaling." J Exp Biol **206**(Pt 12): 1985-92.
Chada, S. R. and P. J. Hollenbeck (2004). "Nerve growth factor signaling regulates motility and docking of axonal mitochondria." Curr Biol **14**(14): 1272-6.
Chapman, V., P. Honore, et al. (1995). "The contribution of NMDA receptor activation to spinal c-Fos expression in a model of inflammatory pain." Br J Pharmacol **116**(1): 1628-34.
Chen, J. J. and E. J. Johnson (2007). "Targeting the bradykinin B1 receptor to reduce pain." Expert Opin Ther Targets **11**(1): 21-35.
Chiang, C. Y., Z. Li, et al. (2008). "Glutamine uptake contributes to central sensitization in the medullary dorsal horn." Neuroreport **19**(11): 1151-4.

Chiang, C. Y., J. Wang, et al. (2007). "Astroglial glutamate-glutamine shuttle is involved in central sensitization of nociceptive neurons in rat medullary dorsal horn." J Neurosci **27**(34): 9068-76.

Chuang, H. H., E. D. Prescott, et al. (2001). "Bradykinin and nerve growth factor release the capsaicin receptor from PtdIns(4,5)P2-mediated inhibition." Nature **411**(6840): 957-62.

Chudler, E. H., L. C. Anderson, et al. (1997). "Nerve growth factor depletion by autoimmunization produces thermal hypoalgesia in adult rats." Brain Res **765**(2): 327-30.

Coggeshall, R. E. (2005). "Fos, nociception and the dorsal horn." Prog Neurobiol **77**(5): 299-352.

Coggeshall, R. E. and S. M. Carlton (1998). "Ultrastructural analysis of NMDA, AMPA, and kainate receptors on unmyelinated and myelinated axons in the periphery." J Comp Neurol **391**(1): 78-86.

Colquhoun, A., G. M. Lawrance, et al. (2004). "Differential activity of the nerve growth factor (NGF) antagonist PD90780 [7-(benzolylamino)-4,9-dihydro-4-methyl-9-oxo-pyrazolo[5,1-b]quinazoline-2 -carboxylic acid] suggests altered NGF-p75NTR interactions in the presence of TrkA." J Pharmacol Exp Ther **310**(2): 505-11.

Costigan, M. and C. J. Woolf (2000). "Pain: molecular mechanisms." J Pain **1**(3 Suppl): 35-44.

Covaceuszach, S., A. Cattaneo, et al. (2005). "Neutralization of NGF-TrkA receptor interaction by the novel antagonistic anti-TrkA monoclonal antibody MNAC13: a structural insight." Proteins **58**(3): 717-27.

Davidson, E. M., R. E. Coggeshall, et al. (1997). "Peripheral NMDA and non-NMDA glutamate receptors contribute to nociceptive behaviors in the rat formalin test." Neuroreport **8**(4): 941-6.

De Biasi, S. and A. Rustioni (1990). "Ultrastructural immunocytochemical localization of excitatory amino acids in the somatosensory system." J Histochem Cytochem **38**(12): 1745-54.

deGroot, J., S. Zhou, et al. (2000). "Peripheral glutamate release in the hindpaw following low and high intensity sciatic stimulation." Neuroreport **11**(3): 497-502.

Delcroix, J. D., J. S. Valletta, et al. (2003). "NGF signaling in sensory neurons: evidence that early endosomes carry NGF retrograde signals." Neuron **39**(1): 69-84.

Della Seta, D., L. de Acetis, et al. (1994). "NGF effects on hot plate behaviors in mice." Pharmacol Biochem Behav **49**(3): 701-5.

Djouhri, L., D. Dawbarn, et al. (2001). "Time course and nerve growth factor dependence of inflammation-induced alterations in electrophysiological membrane properties in nociceptive primary afferent neurons." J Neurosci **21**(22): 8722-33.

Djouhri, L., X. Fang, et al. (2003). "The TTX-resistant sodium channel Nav1.8 (SNS/PN3): expression and correlation with membrane properties in rat nociceptive primary afferent neurons." J Physiol **550**(Pt 3): 739-52.

Dmitrieva, N., A. J. Rodriguez-Malaver, et al. (2004). "Differential release of neurotransmitters from superficial and deep layers of the dorsal horn in response to acute noxious stimulation and inflammation of the rat paw." Eur J Pain **8**(3): 245-52.

Donnerer, J., R. Schuligoi, et al. (1992). "Increased content and transport of substance P and calcitonin gene-related peptide in sensory nerves innervating inflamed tissue: evidence for a regulatory function of nerve growth factor in vivo." Neuroscience **49**(3): 693-8.

Doubleday, B. and P. P. Robinson (1994). "Nerve growth factor depletion reduces collateral sprouting of cutaneous mechanoreceptive and tooth-pulp axons in ferrets." J Physiol **481 (Pt 3)**(Pt 3): 709-18.

Doubleday, B. and P. P. Robinson (1995). "The effect of NGF depletion on the neurotropic influence exerted by the distal stump following nerve transection." J Anat **186 (Pt 3)**(Pt 3): 593-605.

Dougherty, P. M., J. Palecek, et al. (1993). "Combined application of excitatory amino acids and substance P produces long-lasting changes in responses of primate spinothalamic tract neurons." Brain Res Brain Res Rev **18**(2): 227-46.

Dougherty, P. M. and W. D. Willis (1991). "Enhancement of spinothalamic neuron responses to chemical and mechanical stimuli following combined micro-iontophoretic application of N-methyl-D-aspartic acid and substance P." Pain **47**(1): 85-93.

Douglas, W. W. and J. M. Ritchie (1957). "Nonmedullated fibres in the saphenous nerve which signal touch." J Physiol **139**(3): 385-99.

Draisci, G. and M. J. Iadarola (1989). "Temporal analysis of increases in c-fos, preprodynorphin and preproenkephalin mRNAs in rat spinal cord." Brain Res Mol Brain Res **6**(1): 31-7.

Du, J., M. Koltzenburg, et al. (2001). "Glutamate-induced excitation and sensitization of nociceptors in rat glabrous skin." Pain **89**(2-3): 187-98.

Du, J., S. Zhou, et al. (2003). "N-methyl-D-aspartate-induced excitation and sensitization of normal and inflamed nociceptors." Neuroscience **118**(2): 547-62.

Duce, I. R. and P. Keen (1983). "Selective uptake of [3H]glutamine and [3H]glutamate into neurons and satellite cells of dorsal root ganglia in vitro." Neuroscience **8**(4): 861-6.

Dyck, P. J., S. Peroutka, et al. (1997). "Intradermal recombinant human nerve growth factor induces pressure allodynia and lowered heat-pain threshold in humans." Neurology **48**(2): 501-5.

Fang, X., L. Djouhri, et al. (2006). "Intense isolectin-B4 binding in rat dorsal root ganglion neurons distinguishes C-fiber nociceptors with broad action potentials and high Nav1.9 expression." J Neurosci **26**(27): 7281-92.

Fang, X., S. McMullan, et al. (2005). "Electrophysiological differences between nociceptive and non-nociceptive dorsal root ganglion neurones in the rat in vivo." J Physiol **565**(Pt 3): 927-43.

Ferreira, J., G. L. da Silva, et al. (2004). "Contribution of vanilloid receptors to the overt nociception induced by B2 kinin receptor activation in mice." Br J Pharmacol **141**(5): 787-94.

Fjell, J., T. R. Cummins, et al. (1999). "In vivo NGF deprivation reduces SNS expression and TTX-R sodium currents in IB4-negative DRG neurons." J Neurophysiol **81**(2): 803-10.

Follenfant, R. L. and M. Nakamura-Craig (1992). Glutamate induces hyperalgesia in the rat paw. Br J Pharmacol.

Fox, C. H., F. B. Johnson, et al. (1985). "Formaldehyde fixation." J Histochem Cytochem **33**(8): 845-53.
Fraenkel-Conrat, H. and D. K. Mecham (1949). "The reaction of formaldehyde with proteins; demonstration of intermolecular cross-linking by means of osmotic pressure measurements." J Biol Chem **177**(1): 477-86.
Fraenkel-Conrat, H. and H. S. Olcott (1948). "The reaction of formaldehyde with proteins; cross-linking between amino and primary amide or guanidyl groups." J Am Chem Soc **70**(8): 2673-84.
Fraenkel-Conrat, H. and H. S. Olcott (1948). "Reaction of formaldehyde with proteins; cross-linking of amino groups with phenol, imidazole, or indole groups." J Biol Chem **174**(3): 827-43.
Fukuoka, T., K. Kobayashi, et al. (2008). "Comparative study of the distribution of the alpha-subunits of voltage-gated sodium channels in normal and axotomized rat dorsal root ganglion neurons." J Comp Neurol **510**(2): 188-206.
Gazerani, P., K. Wang, et al. (2006). "Effects of subcutaneous administration of glutamate on pain, sensitization and vasomotor responses in healthy men and women." Pain **124**(3): 338-48.
Giovengo, S. L., K. F. Kitto, et al. (1999). "Parenterally administered kainic acid induces a persistent hyperalgesia in the mouse and rat." Pain **83**(2): 347-58.
Giuffrida, R. and A. Rustioni (1992). "Dorsal root ganglion neurons projecting to the dorsal column nuclei of rats." J Comp Neurol **316**(2): 206-20.
Goldstein, M. E., S. B. House, et al. (1991). "NF-L and peripherin immunoreactivities define distinct classes of rat sensory ganglion cells." J Neurosci Res **30**(1): 92-104.
Gorin, P. D. and E. M. Johnson (1979). "Experimental autoimmune model of nerve growth factor deprivation: effects on developing peripheral sympathetic and sensory neurons." Proc Natl Acad Sci U S A **76**(10): 5382-6.
Gorin, P. D. and E. M. Johnson, Jr. (1980). "Effects of exposure to nerve growth factor antibodies on the developing nervous system of the rat: an experimental autoimmune approach." Dev Biol **80**(2): 313-23.
Gorin, P. D. and E. M. Johnson, Jr. (1980). "Effects of long-term nerve growth factor deprivation on the nervous system of the adult rat: an experimental autoimmune approach." Brain Res **198**(1): 27-42.
Gould, H. J., 3rd, T. N. Gould, et al. (2000). "A possible role for nerve growth factor in the augmentation of sodium channels in models of chronic pain." Brain Res **854**(1-2): 19-29.
Haines, D. E. (2005). Fundamental neuroscience for basic and clinical applications. Philidelphia, Churchill Livingstone.
Hanani, M. (2005). "Satellite glial cells in sensory ganglia: from form to function." Brain Res Brain Res Rev **48**(3): 457-76.
Hargreaves, K., R. Dubner, et al. (1988). "A new and sensitive method for measuring thermal nociception in cutaneous hyperalgesia." Pain **32**(1): 77-88.
Harper, A. A. and S. N. Lawson (1985). "Conduction velocity is related to morphological cell type in rat dorsal root ganglion neurones." J Physiol **359**: 31-46.
Hefti, F. F., A. Rosenthal, et al. (2006). "Novel class of pain drugs based on antagonism of NGF." Trends Pharmacol Sci **27**(2): 85-91.

Hertz, L. (2004). "Intercellular metabolic compartmentation in the brain: past, present and future." Neurochem Int **45**(2-3): 285-96.
Hoffman, E. M., K. M. Edwards, et al. (2007). Glutaminase immunoreactivity in rat dorsal root ganglion neurons during unilateral adjuvant-induced arthritis. Neuroscience, San Diego, CA, USA.
Hoffman, E. M., K. M. Edwards, et al. (2008). Optimization of immunohistochemical methods for primary sensory neuron characterization. World Congress on Pain, Glasgow, Scotland, UK.
Hoffman, E. M. and K. E. Miller (2008). A user-friendly method for immunofluorescence quantitation of protein expression in individual DRG neurons. Society for Neuroscience Annual Meeting, Washington, D.C.
Hoffman, G. E. and W. W. Le (2004). "Just cool it! Cryoprotectant anti-freeze in immunocytochemistry and in situ hybridization." Peptides **25**(3): 425-31.
Honore, P., J. Buritova, et al. (1995). "Carrageenin-evoked c-Fos expression in rat lumbar spinal cord: the effects of indomethacin." Eur J Pharmacol **272**(2-3): 249-59.
Hopwood, D. (2002). Fixation and Fixatives. Theory and Practice of Histological Techniques. J. D. Bancroft and M. Gamble. London, Churchill Livingstone**:** 63-84.
Hu, H. J., B. J. Alter, et al. (2007). "Metabotropic glutamate receptor 5 modulates nociceptive plasticity via extracellular signal-regulated kinase-Kv4.2 signaling in spinal cord dorsal horn neurons." J Neurosci **27**(48): 13181-91.
Hunt, S. P., A. Pini, et al. (1987). "Induction of c-fos-like protein in spinal cord neurons following sensory stimulation." Nature **328**(6131): 632-4.
Indo, Y. (2001). "Molecular basis of congenital insensitivity to pain with anhidrosis (CIPA): mutations and polymorphisms in TRKA (NTRK1) gene encoding the receptor tyrosine kinase for nerve growth factor." Hum Mutat **18**(6): 462-71.
Jackson, D. L., C. B. Graff, et al. (1995). "Glutamate participates in the peripheral modulation of thermal hyperalgesia in rats." Eur J Pharmacol **284**(3): 321-5.
Jancso, G., E. Kiraly, et al. (1977). "Pharmacologically induced selective degeneration of chemosensitive primary sensory neurones." Nature **270**(5639): 741-3.
Ji, R. R., T. A. Samad, et al. (2002). "p38 MAPK activation by NGF in primary sensory neurons after inflammation increases TRPV1 levels and maintains heat hyperalgesia." Neuron **36**(1): 57-68.
Jin, Y. H., H. Nishioka, et al. (2006). "Effect of morphine on the release of excitatory amino acids in the rat hind instep: Pain is modulated by the interaction between the peripheral opioid and glutamate systems." Neuroscience **138**(4): 1329-39.
Johnson, E. M., Jr., P. D. Gorin, et al. (1980). "Dorsal root ganglion neurons are destroyed by exposure in utero to maternal antibody to nerve growth factor." Science **210**(4472): 916-8.
Johnson, E. M., Jr., P. D. Gorin, et al. (1982). "Effects of autoimmune NGF deprivation in the adult rabbit and offspring." Brain Res **240**(1): 131-40.
Kaneko, T., K. Itoh, et al. (1989). "Glutaminase-like immunoreactivity in the lower brainstem and cerebellum of the adult rat." Neuroscience **32**(1): 79-98.
Kashiba, H., Y. Uchida, et al. (2001). "Difference in binding by isolectin B4 to trkA and c-ret mRNA-expressing neurons in rat sensory ganglia." Brain Res Mol Brain Res **95**(1-2): 18-26.

Kinkelin, I., E. B. Brocker, et al. (2000). "Localization of ionotropic glutamate receptors in peripheral axons of human skin." Neurosci Lett **283**(2): 149-52.
Koltzenburg, M., D. L. Bennett, et al. (1999). "Neutralization of endogenous NGF prevents the sensitization of nociceptors supplying inflamed skin." Eur J Neurosci **11**(5): 1698-704.
Kort, M. E., I. Drizin, et al. (2008). "Discovery and biological evaluation of 5-aryl-2-furfuramides, potent and selective blockers of the Nav1.8 sodium channel with efficacy in models of neuropathic and inflammatory pain." J Med Chem **51**(3): 407-16.
Kruger, L., A. M. Kavookjian, et al. (2003). "Nociceptor structural specialization in canine and rodent testicular "free" nerve endings." J Comp Neurol **463**(2): 197-211.
Kuduk, S. D. and M. G. Bock (2008). "Bradykinin B1 receptor antagonists as novel analgesics: a retrospective of selected medicinal chemistry developments." Curr Top Med Chem **8**(16): 1420-30.
Kvamme, E., I. A. Torgner, et al. (2001). "Kinetics and localization of brain phosphate activated glutaminase." J Neurosci Res **66**(5): 951-8.
Lawand, N. B., T. McNearney, et al. (2000). "Amino acid release into the knee joint: key role in nociception and inflammation." Pain **86**(1-2): 69-74.
Lawand, N. B., W. D. Willis, et al. (1997). "Excitatory amino acid receptor involvement in peripheral nociceptive transmission in rats." Eur J Pharmacol **324**(2-3): 169-77.
Lawson, S. N. (2002). "Phenotype and function of somatic primary afferent nociceptive neurones with C-, Adelta- or Aalpha/beta-fibres." Exp Physiol **87**(2): 239-44.
Lawson, S. N., A. A. Harper, et al. (1984). "A monoclonal antibody against neurofilament protein specifically labels a subpopulation of rat sensory neurones." J Comp Neurol **228**(2): 263-72.
Le Bars, D., M. Gozariu, et al. (2001). "Animal models of nociception." Pharmacol Rev **53**(4): 597-652.
Le Botlan, D. J., B. G. Mechin, et al. (1983). "Proton and carbon-13 nuclear magnetic resonance spectrometry of formaldehyde in water." Anal Chem **55**(3): 587-591.
Lee, K. H., K. Chung, et al. (1986). "Correlation of cell body size, axon size, and signal conduction velocity for individually labelled dorsal root ganglion cells in the cat." J Comp Neurol **243**(3): 335-46.
Leem, J. W., J. H. Hwang, et al. (2001). "The role of peripheral N-methyl-D-aspartate receptors in Freund's complete adjuvant induced mechanical hyperalgesia in rats." Neurosci Lett **297**(3): 155-8.
Leslie, T. A., P. C. Emson, et al. (1995). "Nerve growth factor contributes to the up-regulation of growth-associated protein 43 and preprotachykinin A messenger RNAs in primary sensory neurons following peripheral inflammation." Neuroscience **67**(3): 753-61.
Levi-Montalcini, R. and B. Booker (1960). "Destruction of the sympathetic ganglia in mammals by an antiserum to a nerve-growth protein." Proc Natl Acad Sci U S A **46**(3): 384-91.
Lewin, G. R., A. M. Ritter, et al. (1993). "Nerve growth factor-induced hyperalgesia in the neonatal and adult rat." J Neurosci **13**(5): 2136-48.

Li, J. L., F. Fujiyama, et al. (2003). "Expression of vesicular glutamate transporters, VGluT1 and VGluT2, in axon terminals of nociceptive primary afferent fibers in the superficial layers of the medullary and spinal dorsal horns of the rat." J Comp Neurol **457**(3): 236-49.

Li, J. L., H. Ohishi, et al. (1996). "Immunohistochemical localization of a metabotropic glutamate receptor, mGluR7, in ganglion neurons of the rat; with special reference to the presence in glutamatergic ganglion neurons." Neurosci Lett **204**(1-2): 9-12.

Li, J. L., K. H. Xiong, et al. (2003). "Vesicular glutamate transporters, VGluT1 and VGluT2, in the trigeminal ganglion neurons of the rat, with special reference to coexpression." J Comp Neurol **463**(2): 212-20.

Liu, H., H. Wang, et al. (1994). "Evidence for presynaptic N-methyl-D-aspartate autoreceptors in the spinal cord dorsal horn." Proc Natl Acad Sci U S A **91**(18): 8383-7.

Ma, Q. P. and C. J. Woolf (1997). "The progressive tactile hyperalgesia induced by peripheral inflammation is nerve growth factor dependent." Neuroreport **8**(4): 807-10.

Mamet, J., M. Lazdunski, et al. (2003). "How nerve growth factor drives physiological and inflammatory expressions of acid-sensing ion channel 3 in sensory neurons." J Biol Chem **278**(49): 48907-13.

Martin, J. H. (2003). Spinal Somatic Sensory Systems. Neuroanatomy: text and atlas, McGraw Hill**:** 107-133.

McDougal, D. B., Jr., M. J. Yu, et al. (1981). "Transported enzymes in sciatic nerve and sensory ganglia of rats exposed to maternal antibodies against nerve growth factor." J Neurochem **36**(5): 1847-52.

McDougal, D. B., Jr., M. J. Yuan, et al. (1983). "Neonatal capsaicin and guanethidine and axonally transported organelle-specific enzymes in sciatic nerve and in sympathetic and dorsal root ganglia." J Neurosci **3**(1): 124-32.

McKenna, M. C. (2007). "The glutamate-glutamine cycle is not stoichiometric: fates of glutamate in brain." J Neurosci Res **85**(15): 3347-58.

McMahon, S. B. (1996). "NGF as a mediator of inflammatory pain." Philos Trans R Soc Lond B Biol Sci **351**(1338): 431-40.

McMahon, S. B., M. P. Armanini, et al. (1994). "Expression and coexpression of Trk receptors in subpopulations of adult primary sensory neurons projecting to identified peripheral targets." Neuron **12**(5): 1161-71.

McMahon, S. B., D. L. Bennett, et al. (1995). "The biological effects of endogenous nerve growth factor on adult sensory neurons revealed by a trkA-IgG fusion molecule." Nat Med **1**(8): 774-80.

McNearney, T., B. A. Baethge, et al. (2004). "Excitatory amino acids, TNF-alpha, and chemokine levels in synovial fluids of patients with active arthropathies." Clin Exp Immunol **137**(3): 621-7.

McNearney, T., D. Speegle, et al. (2000). "Excitatory amino acid profiles of synovial fluid from patients with arthritis." J Rheumatol **27**(3): 739-45.

McQuay, H. J. and R. A. Moore (2005). NSAIDS and Coxibs: clinical use. Wall and Melzack's Textbook of Pain. S. B. McMahon and M. Koltzenburg. London, Churchill Livingstone**:** 1-10.

Merighi, A., J. M. Polak, et al. (1991). "Ultrastructural visualization of glutamate and aspartate immunoreactivities in the rat dorsal horn, with special reference to the co-localization of glutamate, substance P and calcitonin-gene related peptide." Neuroscience **40**(1): 67-80.

Meyer, R. A., R. M., et al. (2005). Peripheral mechanisms of cutaneous nociception. Wall and Melzack's Textbook of Pain. S. B. McMahon and M. Koltzenburg. London, Churchill Livingstone**:** 3-34.

Miller, K. E., E. Akesson, et al. (1999). "Nerve growth factor-induced stimulation of dorsal root ganglion/spinal cord co-grafts in oculo: enhanced survival and growth of CGRP-immunoreactive sensory neurons." Cell Tissue Res **298**(2): 243-53.

Miller, K. E., S. R. Caire, et al. (2001). Effects of nerve growth factor (NGF) on glutamate metabolism in primary sensory neurons. Neuroscience, San Diego, CA.

Miller, K. E., V. D. Douglas, et al. (1993). "Glutaminase immunoreactive neurons in the rat dorsal root ganglion contain calcitonin gene-related peptide (CGRP)." Neurosci Lett **160**(1): 113-6.

Miller, K. E., B. H. Herzog, et al. (2006). Intraplantar glutaminase inhibition: analgesic dose response of 6-diazo-5-oxo-L-norleucine during adjuvant induced arthritis in rats. Neuroscience, Atlanta, GA.

Miller, K. E. and R. M. Kriebel (2003). Glutamine and glutamine synthetase levels are increased in rat DRG satellite cells following peripheral inflammation. Neuroscience, Washington, D.C.

Miller, K. E., R. M. Kriebel, et al. (2005). Localization of neutral amino acid transporters (SNAT1, ASCT1, ASCT2) in rat DRG and spinal dorsal horn. Neuroscience, Washington, D.C.

Miller, K. E., B. A. Richards, et al. (2002). "Glutamine-, glutamine synthetase-, glutamate dehydrogenase- and pyruvate carboxylase-immunoreactivities in the rat dorsal root ganglion and peripheral nerve." Brain Res **945**(2): 202-11.

Miller, R. D. (2005). Chronic Pain. Miller's Anesthesia. Philadelphia, Elsevier, Churchill Livingstone. **2**.

Moechars, D., M. C. Weston, et al. (2006). "Vesicular glutamate transporter VGLUT2 expression levels control quantal size and neuropathic pain." J Neurosci **26**(46): 12055-66.

Molander, C., Q. Xu, et al. (1984). "The cytoarchitectonic organization of the spinal cord in the rat. I. The lower thoracic and lumbosacral cord." J Comp Neurol **230**(1): 133-41.

Morris, J. L., P. Konig, et al. (2005). "Most peptide-containing sensory neurons lack proteins for exocytotic release and vesicular transport of glutamate." J Comp Neurol **483**(1): 1-16.

Newsholme, E. A., B. Crabtree, et al. (1985). "Glutamine metabolism in lymphocytes: its biochemical, physiological and clinical importance." Q J Exp Physiol **70**(4): 473-89.

Nguyen, D. T. and D. Keast (1991). "Maximal activities of glutaminase, citrate synthase, hexokinase, 6-phosphofructokinase and lactate dehydrogenase in skin of immune-competent Balb/c and immune-deficient Balb/c (nu/nu) mice during wound healing." Int J Biochem **23**(5-6): 589-93.

NIH, N. R. C.-. (2003). Guidelines for the Care and Use of Mammals in Neuroscience and Behavioral Research. Washington, DC, The National Academic Press**:** 223.

Nordlind, K., O. Johansson, et al. (1993). "Glutamate- and aspartate-like immunoreactivities in human normal and inflamed skin." Virchows Arch B Cell Pathol Incl Mol Pathol **64**(2): 75-82.

Nunzi, M. G., A. Pisarek, et al. (2004). "Merkel cells, corpuscular nerve endings and free nerve endings in the mouse palatine mucosa express three subtypes of vesicular glutamate transporters." J Neurocytol **33**(3): 359-76.

Okuse, K., S. R. Chaplan, et al. (1997). "Regulation of expression of the sensory neuron-specific sodium channel SNS in inflammatory and neuropathic pain." Mol Cell Neurosci **10**(3-4): 196-207.

Oliveira, A. L., F. Hydling, et al. (2003). "Cellular localization of three vesicular glutamate transporter mRNAs and proteins in rat spinal cord and dorsal root ganglia." Synapse **50**(2): 117-29.

Omote, K., T. Kawamata, et al. (1998). "Formalin-induced release of excitatory amino acids in the skin of the rat hindpaw." Brain Res **787**(1): 161-4.

Otten, U., M. Goedert, et al. (1979). "Immunization of adult rats against 2.5 S NGF: effects on the peripheral sympathetic nervous system." Brain Res **176**(1): 79-90.

Otten, U., U. T. Ruegg, et al. (1982). "Correlation between substance P content of primary sensory neurones and pain sensitivity in rats exposed to antibodies to nerve growth factor." Eur J Pharmacol **85**(3-4): 351-3.

Owolabi, J. B., G. Rizkalla, et al. (1999). "Characterization of antiallodynic actions of ALE-0540, a novel nerve growth factor receptor antagonist, in the rat." J Pharmacol Exp Ther **289**(3): 1271-6.

Patapoutian, A., S. Tate, et al. (2009). "Transient receptor potential channels: targeting pain at the source." Nat Rev Drug Discov **8**(1): 55-68.

Pezet, S., F. Marchand, et al. (2008). "Phosphatidylinositol 3-kinase is a key mediator of central sensitization in painful inflammatory conditions." J Neurosci **28**(16): 4261-70.

Pezet, S. and S. B. McMahon (2006). "Neurotrophins: Mediators and Modulators of Pain." Annu Rev Neurosci **29**: 507-38.

Phillips, H. S. and M. P. Armanini (1996). "Expression of the trk family of neurotrophin receptors in developing and adult dorsal root ganglion neurons." Philos Trans R Soc Lond B Biol Sci **351**(1338): 413-6.

Polak, J. M. and S. Van Noorden (2003). Introduction to Immunocytochemistry. Oxford, BIOS Scientific Publishers.

Popp, L., A. Haussler, et al. (2008). "Comparison of nociceptive behavior in prostaglandin E, F, D, prostacyclin and thromboxane receptor knockout mice." Eur J Pain.

Priestley, J. V., G. J. Michael, et al. (2002). "Regulation of nociceptive neurons by nerve growth factor and glial cell line derived neurotrophic factor." Can J Physiol Pharmacol **80**(5): 495-505.

Puchtler, H. and S. N. Meloan (1985). "On the chemistry of formaldehyde fixation and its effects on immunohistochemical reactions." Histochemistry **82**(3): 201-4.

Ramer, M. S., E. J. Bradbury, et al. (2001). "Nerve growth factor induces P2X(3) expression in sensory neurons." J Neurochem **77**(3): 864-75.

Rich, K. M., H. K. Yip, et al. (1984). "Role of nerve growth factor in the adult dorsal root ganglia neuron and its response to injury." J Comp Neurol **230**(1): 110-8.
Roberts, P. J. and P. Keen (1974). "(14C)glutamate uptake and compartmentation in glia of rat dorsal sensory ganglion." J Neurochem **23**(1): 201-9.
Robinson, M. M., S. J. McBryant, et al. (2007). "Novel mechanism of inhibition of rat kidney-type glutaminase by bis-2-(5-phenylacetamido-1,2,4-thiadiazol-2-yl)ethyl sulfide (BPTES)." Biochem J **406**(3): 407-14.
Sann, H. and F. K. Pierau (1998). "Efferent functions of C-fiber nociceptors." Z Rheumatol **57 Suppl 2**: 8-13.
Sarantos, P., A. Abouhamze, et al. (1994). "Cytokines decrease glutaminase expression in human fibroblasts." Surgery **116**(2): 276-83; discussion 283-4.
Sato, K., H. Kiyama, et al. (1993). "AMPA, KA and NMDA receptors are expressed in the rat DRG neurones." Neuroreport **4**(11): 1263-5.
Schuligoi, R. and R. Amann (1998). "Differential effects of treatment with nerve growth factor on thermal nociception and on calcitonin gene-related peptide content of primary afferent neurons in the rat." Neurosci Lett **252**(2): 147-9.
Schuligoi, R., R. Ulcar, et al. (2003). "Effect of endotoxin treatment on the expression of cyclooxygenase-2 and prostaglandin synthases in spinal cord, dorsal root ganglia, and skin of rats." Neuroscience **116**(4): 1043-52.
Schwartz, J. P., J. Pearson, et al. (1982). "Effect of exposure to anti-NGF on sensory neurons of adult rats and guinea pigs." Brain Res **244**(2): 378-81.
Sevcik, M. A., J. R. Ghilardi, et al. (2005). "Anti-NGF therapy profoundly reduces bone cancer pain and the accompanying increase in markers of peripheral and central sensitization." Pain **115**(1-2): 128-41.
Shi, S. R., R. J. Cote, et al. (2001). "Antigen retrieval techniques: current perspectives." J Histochem Cytochem **49**(8): 931-7.
Shi, S. R., M. E. Key, et al. (1991). "Antigen retrieval in formalin-fixed, paraffin-embedded tissues: an enhancement method for immunohistochemical staining based on microwave oven heating of tissue sections." J Histochem Cytochem **39**(6): 741-8.
Shi, S. R., C. Liu, et al. (2007). "Standardization of immunohistochemistry for formalin-fixed, paraffin-embedded tissue sections based on the antigen-retrieval technique: from experiments to hypothesis." J Histochem Cytochem **55**(2): 105-9.
Sivilia, S., M. Paradisi, et al. (2008). "Skin homeostasis during inflammation: a role for nerve growth factor." Histol Histopathol **23**(1): 1-10.
Skilling, S. R., D. H. Smullin, et al. (1988). "Extracellular amino acid concentrations in the dorsal spinal cord of freely moving rats following veratridine and nociceptive stimulation." J Neurochem **51**(1): 127-32.
Sompuram, S. R., K. Vani, et al. (2004). "A molecular mechanism of formalin fixation and antigen retrieval." Am J Clin Pathol **121**(2): 190-9.
Sugiura, T., M. Tominaga, et al. (2002). "Bradykinin lowers the threshold temperature for heat activation of vanilloid receptor 1." J Neurophysiol **88**(1): 544-8.
Svensson, P., B. E. Cairns, et al. (2003). "Injection of nerve growth factor into human masseter muscle evokes long-lasting mechanical allodynia and hyperalgesia." Pain **104**(1-2): 241-7.

Tanaka, M., T. R. Cummins, et al. (1998). "SNS Na+ channel expression increases in dorsal root ganglion neurons in the carrageenan inflammatory pain model." Neuroreport **9**(6): 967-72.
Tao, F., W. J. Liaw, et al. (2004). "Evidence of neuronal excitatory amino acid carrier 1 expression in rat dorsal root ganglion neurons and their central terminals." Neuroscience **123**(4): 1045-51.
Taylor, C. R. and R. M. Levenson (2006). "Quantification of immunohistochemistry--issues concerning methods, utility and semiquantitative assessment II." Histopathology **49**(4): 411-24.
Tominaga, M. and M. J. Caterina (2004). "Thermosensation and pain." J Neurobiol **61**(1): 3-12.
Tomita, H., S. Ishiguro, et al. (1999). "Administration of nerve growth factor, brain-derived neurotrophic factor and insulin-like growth factor-II protects phosphate-activated glutaminase in the ischemic and reperfused rat retinas." Tohoku J Exp Med **187**(3): 227-36.
Walker, R. A. (2006). "Quantification of immunohistochemistry--issues concerning methods, utility and semiquantitative assessment I." Histopathology **49**(4): 406-10.
Wang, H., R. J. Liu, et al. (1997). "Peripheral NMDA receptors contribute to activation of nociceptors: a c-fos expression study in rats." Neurosci Lett **221**(2-3): 101-4.
Warncke, T., E. Jorum, et al. (1997). "Local treatment with the N-methyl-D-aspartate receptor antagonist ketamine, inhibit development of secondary hyperalgesia in man by a peripheral action." Neurosci Lett **227**(1): 1-4.
Watson, J. J., S. J. Allen, et al. (2008). "Targeting nerve growth factor in pain: what is the therapeutic potential?" BioDrugs **22**(6): 349-59.
Weick, M., P. S. Cherkas, et al. (2003). "P2 receptors in satellite glial cells in trigeminal ganglia of mice." Neuroscience **120**(4): 969-77.
Westlund, K. N., Y. C. Sun, et al. (1992). "Neural changes in acute arthritis in monkeys. II. Increased glutamate immunoreactivity in the medial articular nerve." Brain Res Brain Res Rev **17**(1): 15-27.
Willis, W. D. and R. E. Coggeshall (1991). Dorsal root ganglion cells and their processes. Sensory Mechanisms of the Spinal Cord. New York, Springer-Verlag**:** 47-78.
Woolf, C. J. and M. Costigan (1999). "Transcriptional and posttranslational plasticity and the generation of inflammatory pain." Proc Natl Acad Sci U S A **96**(14): 7723-30.
Woolf, C. J. and Q. Ma (2007). "Nociceptors--noxious stimulus detectors." Neuron **55**(3): 353-64.
Woolf, C. J., B. Safieh-Garabedian, et al. (1994). "Nerve growth factor contributes to the generation of inflammatory sensory hypersensitivity." Neuroscience **62**(2): 327-31.
Woolf, C. J. and M. W. Salter (2000). "Neuronal plasticity: increasing the gain in pain." Science **288**(5472): 1765-9.
Xue, Q., B. Jong, et al. (2007). "Transcription of rat TRPV1 utilizes a dual promoter system that is positively regulated by nerve growth factor." J Neurochem **101**(1): 212-22.

Yoshida, S. and Y. Matsuda (1979). "Studies on sensory neurons of the mouse with intracellular-recording and horseradish peroxidase-injection techniques." J Neurophysiol **42**(4): 1134-45.

Yu, X. M., B. J. Sessle, et al. (1996). "Involvement of NMDA receptor mechanisms in jaw electromyographic activity and plasma extravasation induced by inflammatory irritant application to temporomandibular joint region of rats." Pain **68**(1): 169-78.

Zahn, P. K., K. A. Sluka, et al. (2002). "Excitatory amino acid release in the spinal cord caused by plantar incision in the rat." Pain **100**(1-2): 65-76.

Zhou, S., L. Bonasera, et al. (1996). "Peripheral administration of NMDA, AMPA or KA results in pain behaviors in rats." Neuroreport **7**(4): 895-900.

Zimmermann, M. (1983). "Ethical guidelines for investigations of experimental pain in conscious animals." Pain **16**(2): 109-10.

Zylka, M. J., F. L. Rice, et al. (2005). "Topographically distinct epidermal nociceptive circuits revealed by axonal tracers targeted to Mrgprd." Neuron **45**(1): 17-25.

APPENDICES

Appendix A

User-friendly method of immunofluorescence quantitation in individual DRG neurons

Neurons regulate their function by altering the activity and expression of proteins. The latter is commonly studied by immunoblotting lysates from the cells of interest and normalizing to a loading control with densitometry. Immunoblotting works well when studying cell populations of high purity such as in culture. However, *in vivo* studies often involve neural tissue of heterogeneous cell types. If a subpopulation of cells in a tissue alters expression of a target protein, the magnitude of the effect detected by immunoblotting will be diluted by the cells that do not alter expression. This dilution effect may go so far as to mask the changes in expression that take place. If neural tissue is subjected to histological sectioning instead of homogenization, immunofluorescence microscopy can be used to label specific proteins. Since immunofluorescence microscopy uses a similar protocol to immunoblotting once the tissue has been processed, it may be used to study protein expression if proper optimization is performed. Although immunofluorescence microscopy is used frequently in both medicine and research, the goal is rarely to study the expression level of proteins on a per cell basis. This is likely due to the variability of labeling intensity under non-optimized conditions and the architecture of many neural tissues, which makes identification of individual cells difficult. The dorsal root ganglion (DRG) is comprised of spherical to ellipsoidal sensory

neurons, each surrounded by a capsule of satellite glial cells. The DRG is very amenable to immunofluorescence microscopy for measurement of protein expression at the level of individual cells because of its architecture and heterogeneous neuron populations that serve different sensory modalities. In this appendix, we demonstrate a streamlined protocol for measuring immunofluorescence of individual cells using free image analysis software (Image J, NIH). We detail the steps involved in tracing neuron profiles, measuring immunofluorescence. This method could be used to elucidate protein expression changes not previously detectable *in vivo* and localize the changes to specific subpopulations of nociceptive DRG neurons based on phenotypic markers that indicate function. Understanding which neurons of the DRG regulate expression of specific proteins during pathological conditions such as inflammatory or neuropathic pain could identify novel targets for the treatment of pain.

1. Go to http://rsb.info.nih.gov/ij/, download and install the newest version of ImageJ.
2. Open Image J. For basic operation of ImageJ, consult the "Documentation" link on their website.
3. Open a grayscale image of the field from the color channel containing the most universal labeling (whichever antibody labels the most cells).
4. Go to Image > Zoom > View 100% and then resize the image window to fill your screen. You can use the "scrolling tool" (looks like a hand) to move the image around so that you can see all of the cells.
5. If you want the output measurements to be in a real unit (like micrometers) and you know the conversion factor for the microscope and objective you used to take the image then go to Analyze > Set Scale.

6. Go to Analyze > Set Measurements and select the measurements you want to obtain from each Region of Interest (ROI).
7. Using the freehand selections tool to trace the outline of a cell against the background.
8. While holding Alt, trace the nucleus. This will remove the nucleus from the ROI, making it into a 'donut' shape.
9. Press 't' to add the cytoplasmic profile to the ROI Manager.
10. Within the ROI Manager window, press the 'Show All' button.
11. Repeat steps 7 through 9 for all nucleated cells on the image. You should now see the outlines overlays on the image for all of the cytoplasmic profiles that you traced.
12. Press the 'Measure' button in the ROI Manager window. This will cause a Results window to appear.
13. Select all of the data in the Results window. Cut and paste them to a spreadsheet.
14. Press the 'Save' button in the ROI Manager window to save the outline overlays as a .zip archive folder.
15. If you have an image from another color channel from the same field of view, open it and close the first image.
16. Make sure your ROI Manager window still has the ROIs listed and press the 'Show All' button, which will put the outline overlays on the second image.
17. Repeat steps 12 and 13.
18. If you have images from additional color channels from the same field of view, repeat steps 15 through 17.

19. Now you have quantitative data for individual cells, which you can use to measure changes in intensity among cells of certain sizes, or, if you had multiple color channels, among cells with specific markers.

Appendix B

CellProfiler pipeline used for identification of Fos labeled nuclei in spinal cord

Saved Pipeline, in file c-fos at 4XPIPE.txt, Saved on 02-Mar-2009

Pixel Size: 1

Pipeline:

LoadImages

IdentifyPrimAutomatic

InvertIntensity

ApplyThreshold

IdentifyPrimAutomatic

MeasureObjectAreaShape

MeasureObjectIntensity

Relate

OverlayOutlines

ConvertToImage

ImageMath

SaveImages

ExportToExcel

Module #1: LoadImages revision - 2

How do you want to load these files? Order

Type the text that one type of image has in common (for TEXT options), or their position in each group (for ORDER option): 1

What do you want to call these images within CellProfiler? Original

Type the text that one type of image has in common (for TEXT options), or their position in each group (for ORDER option). Type "Do not use" to ignore: 2

What do you want to call these images within CellProfiler? (Type "Do not use" to ignore) LaminaeOriginal

Type the text that one type of image has in common (for TEXT options), or their position in each group (for ORDER option): Do not use

What do you want to call these images within CellProfiler? Do not use

Type the text that one type of image has in common (for TEXT options), or their position in each group (for ORDER option): Do not use

What do you want to call these images within CellProfiler? Do not use

If using ORDER, how many images are there in each group (i.e. each field of view)? 2

What type of files are you loading? individual images

Analyze all subfolders within the selected folder? Yes

Enter the path name to the folder where the images to be loaded are located. Type period (.) for default image folder. .

Note - If the movies contain more than just one image type (e.g., brightfield, fluorescent, field-of-view), add the GroupMovieFrames module. n/a

Module #2: IdentifyPrimAutomatic revision - 12

What did you call the images you want to process? LaminaeOriginal

What do you want to call the objects identified by this module? Laminae

Typical diameter of objects, in pixel units (Min,Max): 0,1000

Discard objects outside the diameter range? No

Try to merge too small objects with nearby larger objects? No

Discard objects touching the border of the image? Yes

Select an automatic thresholding method or enter an absolute threshold in the range [0,1]. To choose a binary image, select "Other" and type its name. Choosing "All" will use the Otsu Global method to calculate a single threshold for the entire image group. The other methods calculate a threshold for each image individually. "Set interactively" will allow you to manually adjust the threshold during the first cycle to determine what will work well. .98

Threshold correction factor 1

Lower and upper bounds on threshold, in the range [0,1] 0,1

For MoG thresholding, what is the approximate fraction of image covered by objects? 0.01

Method to distinguish clumped objects (see help for details): None

Method to draw dividing lines between clumped objects (see help for details): None

Size of smoothing filter, in pixel units (if you are distinguishing between clumped objects). Enter 0 for low resolution images with small objects (~< 5 pixel diameter) to prevent any image smoothing. Automatic

Suppress local maxima within this distance, (a positive integer, in pixel units) (if you are distinguishing between clumped objects) Automatic

Speed up by using lower-resolution image to find local maxima? (if you are distinguishing between clumped objects) Yes

Enter the following information, separated by commas, if you would like to use the Laplacian of Gaussian method for identifying objects instead of using the above settings: Size of neighborhood(height,width),Sigma,Minimum Area,Size for Wiener Filter(height,width),Threshold Do not use

What do you want to call the outlines of the identified objects (optional)? LaminaeOutlines

Do you want to fill holes in identified objects? Yes

Do you want to run in test mode where each method for distinguishing clumped objects is compared? No

Module #3: InvertIntensity revision - 1

What did you call the image to be inverted (made negative)? Original

What do you want to call the inverted image? inverted

Module #4: ApplyThreshold revision - 4

What did you call the image to be thresholded? inverted

What do you want to call the thresholded image? thresholded

Pixels below this value (Range = 0-1) will be set to zero (0 will not threshold any pixels) 0.4

If your answer was not 0, do you want to shift the remaining pixels" intensities down by that intensity or retain their original values? Retain

Pixels above this value (Range = 0-1) will be set to zero (1 will not threshold any pixels) 1

If your answer was not 1, you can expand the thresholding around those excluded bright pixels by entering the number of pixels to expand here: 0

Binary option: Enter the threshold to use to make the incoming image binary (black and white) where pixels equal to or below this value will be zero and above this value will be 1. If instead you want to use the settings above to preserve grayscale information, enter 0 here. 0

Module #5: IdentifyPrimAutomatic revision - 12

What did you call the images you want to process? thresholded

What do you want to call the objects identified by this module? FosNuclei

Typical diameter of objects, in pixel units (Min,Max): 5,13

Discard objects outside the diameter range? Yes

Try to merge too small objects with nearby larger objects? No

Discard objects touching the border of the image? Yes

Select an automatic thresholding method or enter an absolute threshold in the range [0,1]. To choose a binary image, select "Other" and type its name. Choosing "All" will use the Otsu Global method to calculate a single threshold for the entire image group. The other methods calculate a threshold for each image individually. "Set interactively" will allow you to manually adjust the threshold during the first cycle to determine what will work well. Otsu Global

Threshold correction factor 1

Lower and upper bounds on threshold, in the range [0,1] 0,1

For MoG thresholding, what is the approximate fraction of image covered by objects? 0.01

Method to distinguish clumped objects (see help for details): Shape

Method to draw dividing lines between clumped objects (see help for details): Intensity

Size of smoothing filter, in pixel units (if you are distinguishing between clumped objects). Enter 0 for low resolution images with small objects (~< 5 pixel diameter) to prevent any image smoothing. Automatic

Suppress local maxima within this distance, (a positive integer, in pixel units) (if you are distinguishing between clumped objects) Automatic

Speed up by using lower-resolution image to find local maxima? (if you are distinguishing between clumped objects) No

Enter the following information, separated by commas, if you would like to use the Laplacian of Gaussian method for identifying objects instead of using the above settings: Size of neighborhood(height,width),Sigma,Minimum Area,Size for Wiener Filter(height,width),Threshold Do not use

What do you want to call the outlines of the identified objects (optional)? FosNucleiOutlines

Do you want to fill holes in identified objects? Yes

Do you want to run in test mode where each method for distinguishing clumped objects is compared? No

Module #6: MeasureObjectAreaShape revision - 3

What did you call the objects that you want to measure? FosNuclei

Do not use

Do not use

Do not use

Do not use

Do not use

Do not use

Would you like to calculate the Zernike features for each object (with lots of objects, this can be very slow)? No

Module #7: MeasureObjectIntensity revision - 2

What did you call the greyscale images you want to measure? Original

What did you call the objects that you want to measure? FosNuclei

Do not use

Do not use

Do not use

Do not use

Do not use

Module #8: Relate revision - 2

What objects are the children objects (subobjects)? FosNuclei

What are the parent objects? Laminae

What other object do you want to find distances to? (Must be one object per parent object, e.g. Nuclei) None

Module #9: OverlayOutlines revision - 2

On which image would you like to display the outlines? inverted

What did you call the outlines that you would like to display? LaminaeOutlines

Would you like to set the intensity (brightness) of the outlines to be the same as the brightest point in the image, or the maximum possible value for this image format? Max possible

What do you want to call the image with the outlines displayed? LaminaeImage

For color images, what do you want the color of the outlines to be? White

Module #10: ConvertToImage revision - 1

What did you call the objects you want to convert to an image? FosNuclei

What do you want to call the resulting image? FosNucleiImage

What colors should the resulting image use? Binary (black & white)

For COLOR, what do you want the colormap to be? Default

Module #11: ImageMath revision - 1

What do you want to call the resulting image? AnalyzedImage

Choose first image: LaminaeImage

Choose second image, or "Other..." and enter a constant. Note: if the operation chosen below is "Complement", this second image will not be used FosNucleiImage

What operation would you like performed? Add

Enter a factor to multiply the first image by (before other operations): 1

Enter a factor to multiply the second image by (before other operations): 1

Do you want negative values in the image to be set to zero? Yes

Do you want values greater than one in the image to be set to one? Yes

Module #12: SaveImages revision - 14

What did you call the images you want to save? If you would like to save an entire figure, enter the module number here AnalyzedImage

Which images" original filenames do you want use as a prefix for these new images" filenames? Your choice MUST be images loaded directly with a Load module. Alternately, type N to use sequential numbers for the file names, or type =DesiredFilename to use the single file name you specify (replace DesiredFilename with the name you actually want) for all files (this is *required* when saving an avi movie). Original

Enter text to append to the image name, type N to use sequential numbers, or leave "Do not use" to not append anything. _analyzed

In what file format do you want to save images (figures must be saved as fig, which is only openable in Matlab)? tif

Enter the pathname to the directory where you want to save the images. Type period (.) for default output directory or ampersand (&) for the directory of the original image.

.

Enter the bit depth at which to save the images (Note: some image formats do not support saving at a bit depth of 12 or 16; see Matlab"s imwrite function for more details.) 8

Do you want to always check whether you will be overwriting a file when saving images? No

At what point in the pipeline do you want to save the image? When saving in avi (movie) format, choose Every cycle. Every cycle

If you are saving in avi (movie) format, do you want to save the movie only after the last cycle is processed (enter "L"), or after every Nth cycle (1,2,3...)? Saving movies is time-consuming. See the help for this module for more details. L

Do you want to rescale the images to use a full 8 bit (256 graylevel) dynamic range (Y or N)? Use the RescaleIntensity module for other rescaling options. Yes

For grayscale images, specify the colormap to use (see help). This is critical for movie (avi) files. Choosing anything other than gray may degrade image quality or result in image stretching. gray

Enter any optional parameters here ("Quality",1 or "Quality",100 etc.) or leave "Do not use" for no optional parameters. Do not use

Update file names within CellProfiler? See help for details. No

Do you want to create subdirectories in the output directory to match the input image directory structure? (Note: This option cannot be used with the "N" or "=DesiredFilename" option above) Yes

Warning! It is possible to overwrite existing files using this module! n/a

Module #13: ExportToExcel revision - 1

Which objects do you want to export? Image

Laminae

FosNuclei

Do not use

Do not use

Do not use

Do not use

Do not use

VITA

Ernest Matthew Hoffman

Candidate for the Degree of

Doctor of Philosophy

Dissertation: THE ROLE OF DORSAL ROOT GANGLION GLUTAMINASE IN NOCICEPTION – A NOVEL THERAPEUTIC TARGET FOR INFLAMMATORY PAIN

Major Field: Biomedical Science

Biographical:

Personal Data: Born in Tulsa, Oklahoma, On March 11th, 1983.

Education: Received Bachelor of Science degree in Biology from The University of Tulsa, Tulsa, Oklahoma in May, 2004. Completed the requirements for the Doctor of Philosophy degree in Biomedical Science at Oklahoma State University Center for Health Sciences, Tulsa, Oklahoma in May, 2009.

Experience: Raised in Broken Arrow, Oklahoma; employed by University of Tulsa and Oklahoma State University Center for Health Sciences as research assistant, 2001 to present. Served as teaching assistant for Neuroanatomy course at Oklahoma State University Center for Health Sciences, 2006 to present. Employed by Tulsa Community College as an adjunct Human Physiology instructor for two semesters in 2008.

Professional Memberships: Society for Neuroscience, American Academy of Neurology, American Pain Society, International Association for the Study of Pain, Oklahoma Microscopy Society, Oklahoma Society of Physiologists

Name: Ernest Matthew Hoffman Date of Degree: May, 2009

Institution: Oklahoma State University Center for Health Sciences

Location: Tulsa, Oklahoma

Title of Study: THE ROLE OF DORSAL ROOT GANGLION GLUTAMINASE IN NOCICEPTION – A NOVEL THERAPEUTIC TARGET FOR INFLAMMATORY PAIN

Pages in Study: 170 Candidate for the Degree of Doctor of Philosophy

Major Field: Biomedical Science

Scope and Method of Study: The purpose of this study was to examine the distribution of the enzyme glutaminase in rat dorsal root ganglion and determine its potential as a target for analgesic development. The study used a combination of behavioral analysis and quantitative microscopy to investigate the distribution of glutaminase in the rat dorsal root ganglion, expression of glutaminase during inflammation, expression of glutaminase under conditions of nerve growth factor depletion, and effect of glutaminase inhibition on inflammation induced Fos expression in spinal cord.

Findings and Conclusions: Glutaminase was found to be distributed ubiquitously in rat dorsal root ganglion neurons. Past discrepancies on its distribution were attributed to tissue fixation methods, and optimization of tissue fixation proved useful in properly identifying distributions of other proteins in the dorsal root ganglion. Glutaminase expression in dorsal root ganglion neurons was increased after four days of hind paw inflammation and remained elevated after eight days in small diameter neurons. Autoimmunization with nerve growth factor was effective at depleting nerve growth factor levels and causing hypoalgesia as had been reported previously. Deprivation of nerve growth factor did not alter basal expression of glutaminase in dorsal root ganglion neurons, but it did decrease expression the voltage-gated sodium channel $Na_v1.8$ in small isolectin B4 negative neurons. Lastly, peripheral inhibition of glutaminase during carrageenan induced inflammation decreased spinal cord Fos expression, which is typically an indicator of nociceptive activity at the spinal level. Clarification of glutaminase distribution, understanding its basal regulation and in response to inflammation, and demonstrating the effectiveness of its inhibition at decreasing activity in pain pathways gave support for nomination of glutaminase as a novel therapeutic target for inflammatory pain.

ADVISER'S APPROVAL: Kenneth E. Miller